Idaho National Engineering and Environmental Laboratory

INEEL/EXT-98-00970
REV. 1

March 1999

The Preparation and Characterization of INTEC HAW Phase 1 Composition Variation Study Glasses

B. A. Staples
D. K. Peeler
J. D. Vienna
B. A. Scholes
C. A. Musick

LOCKHEED MARTIN

INEEL/EXT-98-00970
REV. 1

The Preparation and Characterization of INTEC HAW Phase 1 Composition Variation Study Glasses

B. A. Staples
D. K. Peeler
J. D. Vienna
B. A. Scholes
C. A. Musick

Published March 1999

Idaho National Engineering and Environmental Laboratory
High-Level Waste Operations
Lockheed Martin Idaho Technologies Company
Idaho Falls, Idaho 83415

Prepared for the
U.S. Department of Energy
Office of Science and Technology
Under DOE Idaho Operations Office
Contract DE-AC07-94ID13223

ABSTRACT

A glass composition variation study (CVS) is in progress to define formulations for the vitrification of high activity waste (HAW) proposed to be separated from dissolved calcine stored at the Idaho National Engineering and Environmental Laboratory (INEEL). Estimates of calcine and HAW compositions prepared in FY97 were used to define test matrix glasses. The HAW composition is of particular interest because high aluminum, zirconium, phosphorous and potassium, and low iron and sodium content places it outside the realm of vitrification experience in the Department of Energy (DOE) complex. Through application of statistical techniques, a test matrix was defined for Phase 1 of the CVS. From this matrix, formulations were systematically selected for preparation and characterization with respect to homogeneity, viscosity, liquidus temperature (T_L), and leaching response when subjected to the Product Consistency Test (PCT). Based on the properties determined, certain formulations appear suitable for further development including use in planning Phase 2 of the study. It is recommended that glasses to be investigated in Phase 2 be limited to 3-5 wt % phosphate. The results of characterizing the Phase 1 glasses are presented in this document. A full analysis of the composition-property relationships of glasses being developed for immobilizing HAWs will be performed at the completion of CVS phases. This analysis will be needed for the optimization of the glass formulations for vitrifying HAW. Contributions were made to this document by personnel working at the INEEL, Pacific Northwest National Laboratories (PNNL), and the Savannah River Technology Center (SRTC).

EXECUTIVE SUMMARY

An option for immobilizing and reducing the volume of high level waste (HLW) at the INEEL is to dissolve calcined waste then separate the radionuclides into a smaller fraction. This fraction is known as high activity waste (HAW), and it is proposed to immobilize it by vitrification. The separation process concentrates and separates the radionuclides but retains a significant amount of aluminum and zirconium from the dissolved calcine. The separation process also adds phosphate and potassium to the HAW. The concentrations of these elements in the HAW place its composition outside that of wastes anticipated to be immobilized in the DOE complex. Thus, a cooperative glass CVS conducted at the INEEL, PNNL and SRTC is in progress to define vitrifying formulations for this waste and to observe the composition-product property relationships of the glasses formed.

This CVS has the purpose of investigating how glass properties depend on composition within a region compatible with the expected range of INEEL/Idaho Nuclear Technology and Engineering Center (INTEC) HAW. As currently defined, the multi-year scope of the INEEL glass formulation task resulted in the decision to design and perform the CVS in two or more phases. The first phase (Phase 1a and Phase 1b) began in FY98 and has been completed. The results are given in this document. Phase 1a glasses were prepared at the INEEL, and Phase 1b glasses were prepared at SRTC and PNNL. The second phase (Phase 2) of the CVS will begin in FY99. Glasses prepared and characterized during it will use updated estimates of the HAW composition.

Given the range of the HAW compositions, mixture design techniques were applied at PNNL to derive a formulation matrix for the first phase of the CVS. Formulations for preparation and characterization with respect to homogeneity, viscosity, T_L and leaching response to the PCT were derived from this matrix through systematic selection. These formulations are given in Table 7.

Characterization of these glasses with respect to visual and optical homogeneity are given in Table 8. Table 9 presents the results of the canister centerline cooling experiment conducted on some Phases 1a and 1b glasses. Tables 10, 12, and 13 give T_L, leaching response to the PCT, and viscosity data, respectively.

A number of the glasses prepared appear to be homogeneous and have characteristics that make further efforts to define the development of HAW vitrifying formulations worthy of pursuit. A full analysis of the composition-product property relationships in these glasses is beyond the scope of this report. These analyses will be performed on completion of the CVS phases. Such analyses will be needed for the optimization of the glass formulations for vitrifying HAW.

As a result of the observations made in this study, it is apparent that phosphate content in the INTEC HAW has an impact on the tendency of the resulting glasses to phase separate (i.e., amorphous glass separation or

glass-in-glass separation) and a major influence on crystalline formation in the glass products. Through the results of canister centerline cooling (CCC) experiments performed on some of the glasses produced in this study, it is revealed that phase separation and crystallization in the HAW glasses of significant phosphate content also depends on the cooling rate.

The phosphate content of the HAW glasses investigated ranges from 0.00 to amounts known to cause phase separation in borosilicate glasses. Other major components changing within the glass region probably have some impact on viscosity, phase separation, and on silicate and alkali phosphate crystallization. The evidence for composition effects in these glasses comes from T_L investigations and from homogeneity observations on the glasses formed by air quenching and at CCC rates. Inhomogeneous HAW glass products formed in these tests have as little as 2.5 wt % phosphate. All HAW glasses in this CVS were formed under the same processing conditions (four hours at 1150°C and immediate air quenching onto a stainless steel surface to form a pour patty).

Because of the observations of phosphate impact on the properties of glasses formed in this study, it is recommended that in Phase 2, the amount of phosphate in the glass products should be limited to 3-5 wt %. This recommendation assumes that INTEC will convert HAW into homogeneous glass products. The 3-5 wt % phosphate constraint provides opportunity for observing the limits of phase separation and the formation of alkali phosphate, silicates or other crystalline phases in glasses cooled at near quench conditions. Refinement of this limit will come after more information is obtained on the relationship of phosphate content to product characteristics.

Cooling rate influences phase separation and crystalline phase formation in the Phase 1a and 1b glasses. Therefore Phase 2 studies of HAW glass, must also include observations of the effects of cooling rates down to those expected at the centerline of full scale canisters. More thorough use of TEM analysis should be applied during homogeneity characterization of glasses formed in this phase of the CVS. Information on the effect of cooling rate is required for the development and optimization of processable HAW glasses with good potential for repository storage. This also provides data for the development of generalized models for defining the tendency of a glass to phase separate as a function of cooling rate and composition.

The information provided in Section 6 of this report reveals that more accurate estimates of HAW compositions have been made since the initial estimates were provided in FY97 at the beginning of this CVS. Current estimates given in Section 6 include information on major and minor components not included in the FY97 estimate. It is vital that all components identified as present in the HAWs be included in the surrogates made up for use in future phases of this CVS. Each of these components by themselves, or in combination with others present, could have significant effects on the processability and acceptability for repository storage of the glasses being developed.

Recommendations for other important areas of attention with respect to the four product properties investigated in Phases 1a and 1b of the CVS for INTEC HAW glasses include:

1. Obtaining more data for the definition of primary phase fields of the crystalline species that determine T_L of glasses investigated.

   Much of the information obtained from T_L investigations performed in this study is new and therefore incompletely defines the conditions that result in a given T_L. Lithium phosphate appears to be the most common phase to crystallize below 1150°C from glasses containing phosphate. Certain silicate phases appear frequently at T_L in glasses not containing phosphate. It was outside the scope of this study to define the primary phase fields for these species, but obtaining such information will be required for optimizing glasses for vitrifying INTEC HAW. In some glasses, it appears that more than one primary phase field for crystalline species is encountered near T_L. The determination of the extent of these fields and the number of fields encompassed by the glass composition envelope will also require more data.

2. Studying the effects of composition changes on durability.

   The leaching data obtained in this study suggest some relationship between glass composition and leachability. Several composition-durability relationships may be present in the component ranges of the glasses investigated, but more data is required to define these. Defining these relationships will also be needed for optimization of glasses for vitrifying INTEC HAW.

3. Defining the influence of composition on the ability to accommodate phosphate and retain a homogeneous product.

   Information obtained in this CVS suggests a relationship between product homogeneity and phosphate content in the glasses. The results of this study to date have produced indications that other significant component-homogeneity relationships exist in these glasses. Those component-homogeneity relationships which are significant must be defined before INTEC HAW glasses can be optimized.

4. Defining the influence of composition on glass viscosity.

   Information obtained to date in this CVS reveals that phosphate composition impacts viscosity to the point that high amounts can interfere with profile continuity at lower temperatures. Lithium appears to have the dominant compositional effect on glass viscosity, and its dominance may mask other compositional effects that could be significant. As with the other characteristics investigated to date, the effects of composition on viscosity must be defined before formulation optimization can be performed.

ACKNOWLEDGMENTS

The authors acknowledge the guidance and funding provided for this multi-institutional task by the Department of Energy's (DOE) Tanks Focus Area (TFA). The following personnel from the indicated institutions made significant technical contributions towards the completion of this task:

Tommy Edwards, SRTC

Bill Holtzscheiter, SRTC

Carol Jantzen, SRTC

Irene Reamer, SRTC

Jarrod Crum, PNNL

Pavel Hrma, PNNL

Greg Piepel, PNNL

Mike Schweiger, PNNL

Arlin Olson, INEEL

Rich Tillotson, INEEL

Natasha Wheatley, INEEL

The following individuals made significant contributions toward the issue of this report:

Sharla Mickelsen, INEEL

Ina Moore, INEEL

SRTC Mobile Laboratory (David Best, Eric Frickey and Sherry Vissage)

Also acknowledged are the contributions of Jim Rindfleisch (INEEL), Krishna Vinjamuri (INEEL), Jim Herzog (INEEL), Tony Watson (INEEL), Brenda Boyle (INEEL), and Lucy Torres (INEEL).

Funding to perform this task, Technical Task Plan ID-77WT-31, Subtask B, was provided by the U.S. Department of Energy's Office of Science and Technology.

CONTENTS

FIGURES

TABLES

ACRONYMS

CCC	Canister centerline cooling
CVS	Composition variation study
DOE	Department of Energy
DWPF	Defense Waste Processing Facility
EGCR	Experimental glass composition region
HAW	High activity waste
HLW	High level waste
ICP	Inductively coupled plasma emission spectroscopy
INEEL	Idaho National Environmental and Engineering Laboratory
INTEC	Idaho Nuclear Technology and Engineering Center, formerly Idaho Chemical Processing Plant (ICPP)
LMITCO	Lockheed Martin Idaho Technologies Company
NBS	National Bureau of Standards
PCT	Product Consistency Test
PNNL	Pacific Northwest National Laboratory
RCRA	Resource Conservation and Recovery Act
SBW	Sodium bearing waste
SEM	Scanning Electron Microscopy
SRS	Savannah River Site
SRTC	Savannah River Technology Center
TEM	Transmission Electron Microscopy
TFA	Tanks Focus Area
T_A	Lowest observed temperature where glass remains amorphous
T_C	Highest observed temperature where glass and crystals coexist
T_L	Liquidus temperature
T_M	Melter operating temperature
USDOE	United States Department of Energy
VTF	Vogel-Tamman-Fulcher model
WAPS	Waste Acceptance Product Specifications
WCUR	Waste composition uncertainty region
WVDP	West Valley Demonstration Project
XRD	X-ray diffraction analysis

The Preparation and Characterization of INTEC HAW Phase 1 Composition Variation Study Glasses

1. INTRODUCTION

As a result of four decades of nuclear fuels reprocessing at the Idaho Nuclear Technology and Engineering Center (INTEC), large amounts of radioactive wastes have been collected. Since 1963 these wastes have been converted to a granular form through fluidized bed calcination. These calcined wastes, also called high level waste (HLW), total about 4,000 m^3 in volume and are currently stored onsite in stainless steel bin sets. Figure 1 provides a view of a typical INTEC calcine storage bin set. Over the four-decade reprocessing time span, secondary radioactive wastes high in alkali oxide content have also been collected and stored as liquid. These wastes originate from decontamination, laboratory activities and fuels storage activities, and they cannot be directly calcined because of their high sodium content. Historically they have been blended as a minor component with reprocessing wastes or nonradioactive aluminum nitrate prior to calcination. Collectively, these liquid wastes are known as "sodium bearing wastes (SBW)" and because fuel reprocessing is no longer being performed at INTEC, the option of waste blending to deplete their inventory is eliminated. Consequently, about 5.7 million liters of these wastes are temporarily stored in stainless steel tanks at INTEC.

The Batt Settlement Agreement was established in August, 1995, between the U.S. Navy, the State of Idaho and the U.S. Department of Energy (DOE). Section E.6 of the Agreement states that all HLW stored at the Idaho National Engineering and Environmental Laboratory (INEEL) will be rendered ready (immobilized) for transport to a suitable repository by the end of year 2035. More immediately, the technology must be applied to provide information for the year 2007 beginning of design of the HLW treatment facility. This design supports the Settlement Agreement milestone of submitting a Resource Conservation and Recovery Act (RCRA) Part B permit application in year 2012 and the Site Treatment Plan operational date of September 30, 2019. Vitrification is considered the "Best Demonstrated Available Technology" for immobilizing HLW.[1] Therefore vitrification is being studied for the purpose of immobilizing INTEC HLW. Precedents for the vitrification of INTEC HLW into borosilicate glass are established by the production scale operation of the Defense Waste Processing Facility (DWPF) at the Savannah River Site (SRS), the West Valley Demonstration Project (WVDP) at the West Valley, New York, site and certain European facilities.

Efforts are in progress at the INEEL to investigate processes and formulations for vitrifying HLW stored as calcines or as liquid. The INEEL Spent Nuclear Fuel and Environmental Restoration and Waste Management Program's Environmental Impact Statement identifies radionuclide partitioning as a treatment option for HLW.[2] This option is attractive because it has the potential to significantly reduce the volume of HLW to be sent from INTEC to a federal repository. Thus, the separation and vitrification of the radioactive component, also called high activity waste (HAW), from the dissolved calcine is being investigated. Such an approach results in the potential reduction of about an order of magnitude in the volume of resulting vitrified waste. The HAWs will be of unique chemical composition by containing high concentrations of aluminum, phosphate, potassium and zirconium, and low concentrations of iron and sodium. The concentration of these components makes INTEC HAWs significantly different from those wastes being vitrified at the DWPF at the WVDP and planned for vitrification at Hanford. Production scale operations at DWPF and WVDP use vitrifying formulations developed specifically for their waste compositions. However, it is uncertain that the frit formulations developed for vitrifying waste compositions at these sites could vitrify the INTEC HAW to homogeneous products in a cost-effective manner.

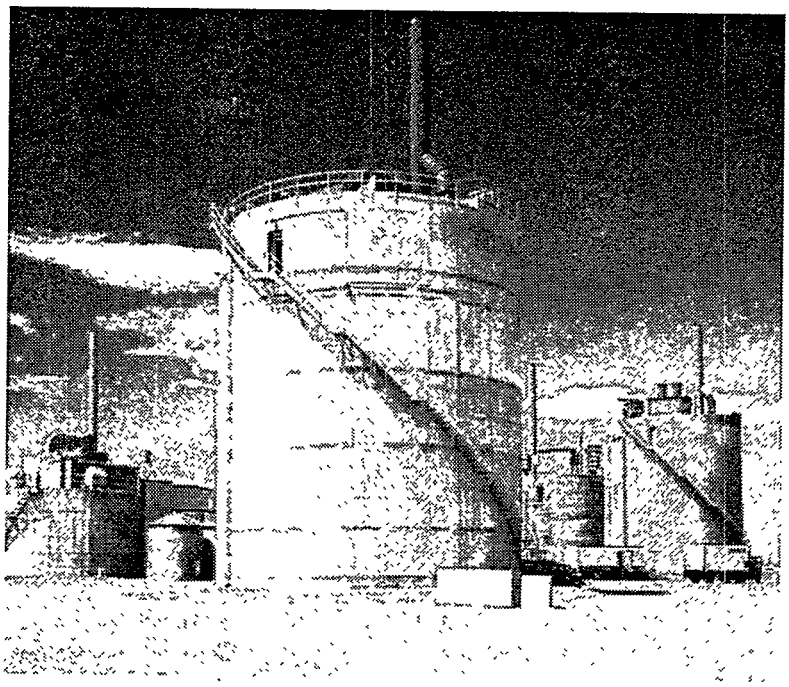

Figure 1. Typical calcined solids storage bin set at INTEC.

In the development of the HAW vitrification process, direct evidence is needed to demonstrate that the separated HAW product can be rendered to a processable vitrified form. Thus, the initial goal of this program is to provide feedback into the developing separations process for altering compositions for suitability for cost-effective vitrification. Next, this goal evolves into establishing the extensive database required for developing formulations for use in glass composition optimization, pretreatment and staging plans, plant design, plant operation and waste form acceptance. Another goal of this program is to collect data that indicates the suitability of the borosilicate glass system for immobilizing INEEL HAW in a manner that is acceptable for repository storage.

A capability for small scale glass formulation development has been in progress through years of active HLW management programs at the INTEC. At the Savannah River Technology Center (SRTC) and at Pacific Northwest National Laboratory (PNNL), expertise exists by applying vitrification technology on a production and engineering scale, respectively. These technologies have established glass formulation refinement through the entire scale-up process. They have also established an extensive database and operating experience on vitrification in joule-heated ceramic brick melters.

In FY97, the DOE Tanks Focus Area-Immobilization Area (TFA-Immobilization) sponsored a task at PNNL and SRTC to investigate the effects of INTEC glass composition on product properties and process variables on the corrosion of melter materials. Also in 1997, the TFA brought experts from the INEEL, PNNL and SRTC together to define a path forward for developing vitrifying formulations for the INTEC HAWs. These persons collaborated in FY98 to:

1. Provide the best estimate of the HAW compositions,
2. Define an approach to develop vitrifying formulations for the HAWs, and
3. Prepare and characterize initial glasses to begin database development.

Existing databases, although extensive, support only the processability and acceptability for repository disposal of the glasses produced at DWPF, Hanford and WVDP. A benefit of the activity performed in this task is the acquisition of data that can display the capability of models already established at PNNL and SRTC for assessing the acceptability and processing characteristics of vitrified wastes. Displaying the capabilities of these models away from specific waste compositions demonstrates their suitability to address the immobilization of radioactive wastes existing throughout the DOE complex.

Results in this study obtained before September, 1998, were presented in the initial release of this report.[3] This revision contains all testing data on Phase 1 CVS glasses including data generated after September, 1998.

2. BASIS

2.1 INTEC Waste Streams

The INTEC separations flowsheets are preliminary in nature. Thus, the HAW compositions are not well defined. Likewise, only partial information is available on the compositions of HLWs. As the separations process develops, and as assumptions with respect to it are verified, modified or rejected, the estimates of HAW compositions will improve. During FY98 and FY99 more information became available about the composition of INTEC calcines and SBW. This information revises the composition estimate of these wastes and therefore of the HAW fraction separated from them. The estimates from FY98 and FY99 information will be used in formulating Phase 2 CVS study glasses for INTEC HAW.

2.2 Approach

In initial stages lasting into FY99, this CVS acquired glass property and waste composition data that can be applied to defining preliminary glass formulations capable of vitrifying INTEC HAW. The HAWs and the glasses for vitrifying them will have compositions based on current separations flowsheet assumptions. Characteristics of resulting glasses will provide information to the developing separations and pretreatment processes about the HAWs suitability for vitrification.

Glasses produced in this study therefore are not optimized to meet processing and acceptance/qualification related criteria. Optimization of glass compositions with respect to processing and acceptance/qualification related criteria will be performed in future testing.

Phase 1 of this CVS was conducted as described in Piepel, et al (1999).[4,5] Steps given by Piepel, et al (1999), to define an experimental glass composition region addressed in this document are:

1. Identify a waste composition uncertainty region (WCUR) expected to include the range of HAW compositions.

   Because of the preliminary nature of the separations flowsheets, and incomplete knowledge of calcine compositions, INTEC personnel used current assumptions to define projected HAW composition ranges expected from the various INTEC calcine types. Thus, the glass compositions for this effort were modified to include anticipated changes resulting from future flowsheet development. The HAW compositions provided for this task are baseline mass balances with ranges of high and low compositions that capture the results of contemporary assumptions. These compositions, which were estimated in FY97, and their low and high limits are given in Table 1. They were transferred to PNNL personnel during the first INEEL HAW immobilization workshop held during October 22-23, 1997, in Idaho Falls, Idaho. The formulations of glass to be derived through the CVS would therefore address the range of all possible HAW compositions.

2. Specify the acceptability constraints on glass composition, glass quality properties, and glass processing qualities.

   During the initial INEEL HAW immobilization workshop, INEEL, PNNL, and SRTC researchers agreed to use similar processing and product performance constraints that are imposed at the DWPF on the Savannah River Site (SRS). These constraints focus primarily on viscosity, liquidus temperature (T_L), homogeneity, and durability as defined the Product Consistency Test (PCT).[6]

Table 1. Compositions of wastes used to derive glass formulations prepared and characterized in this task.

Component	High, wt %	Mass Balance, wt %	Low, wt %
A. Denitrated liquid HAW for zirconia calcine, no resin or solids			
ZrO_2	94.10	94.92	90.21
K_3PO_4	3.99	4.16	6.55
Fe_2O_3	0.44	0.02	0.06
Gd_2O_3	0.23	0.45	1.51
Al_2O_3	0.16	0.00001	0.02
$NaAlO_2$	0.11	0.00001	0.01
CaO	0.71	0.00004	0.07
Cs_2O	0.15	0.27	0.93
SrO	0.02	0.05	0.16
TRU Oxides	0.08	0.14	0.48
	100.00	100.00	100.00
B. Denitrated liquid HAW for alumina calcine, no resin or solids			
K_3PO_4	47.68	75.49	71.97
Fe_2O_3	4.07	0.16	0.18
Al_2O_3	33.86	1.045	1.20
$NaAlO_2$	2.35	0.0726	0.08
Cs_2O	8.01	15.46	17.68
SrO	1.28	2.48	2.83
TRU Oxides	2.74	5.30	6.06
	100.00	100.00	100.00
C. Denitrated liquid HAW for sodium bearing waste, no resin or solids			
ZrO_2	1.84	2.96	1.28
K_3PO_4	90.09	85.45	60.21
K_2O	0.00	6.63	30.77
Na_2O	0.92	0.04	0.07
PbO	0.18	0.25	0.16
MoO_3	0.66	0.93	1.52
Fe_2O_3	1.46	0.15	0.13
BaO	0.11	0.31	0.51
Al_2O_3	3.42	0.15	0.25
CaO	0.23	0.01	0.02
Cs_2O	0.16	0.45	0.74
SrO	0.00	0.01	0.02
TRU Oxides	0.93	2.63	4.31
	100.00	100.00	100.00

Table 1. (continued).

D. Undissolved solids and resin					
Undissolved Solids	Stream	SBW Calcine	Total Calcine	Zr Calcine	Al Calcine
Separated UDS, kg	203	12,929	116,720	1.2911	0.8760
SiO_2, wt %		50.0			
$ZrSiO_4$-H_2O, wt %		48.4			
$BaSO_4$, wt %		1.3			
AgCl, wt %		0.3			
Al_2O_3, wt %			68.3	38.0	100
$Ca_{0.15}Zr_{0.85}O_{1.85}$, wt %			31.7	62.0	
Name			Quantity	Units	Composition
Spent IX Resin			1583.9	kg	40% SiO_2, 60% $KCu_{1.5}[Fe(CN)_6]$
Spent IX Resin from SBW Processing			140.6	kg	40% SiO_2, 60% $KCu_{1.5}[Fe(CN)_6]$
Total Spent IX Resin			1724.4	kg	40% SiO_2, 60% $KCu_{1.5}[Fe(CN)_6]$

3. Define an experimental glass composition region (EGCR) containing glass compositions that are candidates for immobilizing HAWs within the WCUR.

   Using the information from steps one and two above, an EGCR was generated through application of first order mixture models. In these models, glass composition-property relationships refined during the Hanford CVS for HLW were used. Where components of the INTEC HAW were not present in Hanford HLW, other data sets were used for the derivation of ad hoc coefficients. The result was an EGCR which contains systematic glass compositions with acceptable PCT durability and good potential for processability.[6] Further details of the development of the EGCR are given in Piepel, et al (1999).[5]

4. Construct a statistical experimental design that augments any relevant existing composition-product property data with new compositions to adequately cover the EGCR.

   For Phase 1, a layered design approach provided an experimental matrix of potential glass compositions taken from the EGCR. The as-targeted glass compositions in the design and their preparation order are given in Tables 2 and 3. Tables 2 and 3 are given in mass fraction are equivalent to corresponding tables in Piepel, et al (1999), except weight % is used in this report to describe compositions. Table 3 provides the composition of the minor components given under the column "Others" in Table 2. Both tables are equivalent to the preparation order and mass fractions for glass components as given in Tables 4a and 4b of Piepel, et al (1999). The matrix contains the EGCR centroid (IG1-1), twelve outer boundary compositions (IG1-2 through IG1-13), and twelve internal compositions within the EGCR (IG1-14 through IG1-25). Three compositions, IG1-26 through IG1-28, are replicates of IG1-1, IG1-8 and IG1-9, respectively. Two PNNL/Hanford glasses, designated IG1-29 and IG1-30, completed the design. These glasses were chosen to be batched, melted and characterized before preparing the other 28 glasses to compare results with the previous PNNL results.

Table 2. Preparation order and formulation (mass fraction) of glass compositions for the Phase 1 CVS experimental design.

Glass	Run Order	Al_2O_3	B_2O_3	K_2O	Li_2O	Na_2O	P_2O_5	SiO_2	ZrO_2	Others
IGI-1	21	0.0591	0.1015	0.0455	0.0585	0.1316	0.0251	0.5044	0.0695	0.0048
IGI-2	5	0.0750	0.1500	0.1000	0.0816	0.0500	0.0500	0.4886	0.0000	0.0048
IGI-3	17	0.0000	0.0500	0.1000	0.0011	0.2000	0.0500	0.4541	0.1400	0.0048
IGI-4	29	0.0000	0.0500	0.0000	0.0900	0.0653	0.0499	0.6000	0.1400	0.0048
IGI-5	23	0.0750	0.1500	0.0000	0.0016	0.2000	0.0500	0.5186	0.0000	0.0048
IGI-6	12	0.0000	0.1500	0.1000	0.0482	0.0500	0.0000	0.5720	0.0750	0.0048
IGI-7	18	0.1500	0.1500	0.0000	0.0845	0.0500	0.0000	0.5307	0.0300	0.0048
IGI-8	9	0.1500	0.0500	0.1000	0.0825	0.0500	0.0500	0.4827	0.0300	0.0048
IGI-9	25	0.0411	0.1500	0.0000	0.0380	0.1872	0.0500	0.3900	0.1389	0.0048
IGI-10	13	0.0000	0.0653	0.0000	0.0900	0.1560	0.0000	0.5439	0.1400	0.0048
IGI-11	26	0.1463	0.0500	0.0000	0.0511	0.2000	0.0000	0.5478	0.0000	0.0048
IGI-12	8	0.0317	0.1500	0.1000	0.0000	0.1530	0.0000	0.4205	0.1400	0.0048
IGI-13	28	0.0759	0.0500	0.1000	0.0709	0.1720	0.0000	0.5264	0.0000	0.0048
IGI-14	14	0.1125	0.0750	0.0250	0.0525	0.1625	0.0125	0.5202	0.0350	0.0048
IGI-15	20	0.0713	0.0750	0.0750	0.0664	0.0875	0.0375	0.5475	0.0350	0.0048
IGI-16	7	0.0750	0.0750	0.0250	0.0480	0.1625	0.0125	0.4922	0.1050	0.0048
IGI-17	10	0.0750	0.0750	0.0250	0.0427	0.1625	0.0375	0.4725	0.1050	0.0048
IGI-18	27	0.0757	0.1250	0.0250	0.0623	0.0875	0.0375	0.5472	0.0350	0.0048
IGI-19	4	0.0756	0.1247	0.0250	0.0624	0.0875	0.0375	0.5475	0.0350	0.0048
IGI-20	22	0.0497	0.1250	0.0250	0.0585	0.0875	0.0375	0.5070	0.1050	0.0048
IGI-21	30	0.0922	0.1250	0.0750	0.0675	0.0875	0.0125	0.4477	0.0878	0.0048
IGI-22	15	0.1120	0.1250	0.0250	0.0675	0.1128	0.0375	0.4474	0.0680	0.0048
IGI-23	19	0.1084	0.0750	0.0734	0.0675	0.0875	0.0375	0.4743	0.0716	0.0048
IGI-24	6	0.0893	0.1250	0.0750	0.0675	0.0896	0.0125	0.4456	0.0907	0.0048
IGI-25	11	0.0750	0.0750	0.0750	0.0510	0.1273	0.0125	0.4744	0.1050	0.0048
IGI-26	24	0.0591	0.1015	0.0455	0.0585	0.1316	0.0251	0.5044	0.0695	0.0048
IGI-27	3	0.1500	0.0500	0.1000	0.0825	0.0500	0.0500	0.4827	0.0300	0.0048
IGI-28	16	0.0411	0.1500	0.0000	0.0380	0.1872	0.0500	0.3900	0.1389	0.0048
IGI-29	1	0.1400	0.0839	0.0000	0.0700	0.1061	0.0002	0.5700	0.0000	0.0298
IGI-30	2	0.0200	0.0600	0.0000	0.0700	0.1800	0.0016	0.4550	0.1100	0.1034

Table 3. Minor components (mass fraction) in formulations of the Phase 1 CVS experimental design.

Component	IG1-1 to IG1-28	IG1-29	IG1-30
BaO	0.00003	0.00018	0.000161
CaO	0.00090	—	0.005
CdO[(a)]	—	0.00134	0.01209
CeO_2	—	0.00027	0.00242
Cr_2O_3	—	0.00022	0.00202
Cs_2O	0.00099	0.00027	0.00242
CuO	0.00071	0.00027	0.00242
F	—	0.00054	0.00483
Fe_2O_3	0.00052	0.02	0.005
Gd_2O_3	0.00072	—	—
La_2O_3	—	0.00112	0.01007
MgO	—	—	0.005
MnO_2	—	0.00027	0.00242
Nd_2O_3	—	0.00221	0.01988
NiO	—	0.00103	0.00927
PbO	0.00002	—	—
PdO	—	0.00009	0.00081
Pr_6O_{11}	—	0.00018	0.00161
Rb_2O	—	0.00009	0.00081
Rh_2O_3	—	0.00009	0.00081
RuO_2	—	0.00027	0.00242
SO_3	—	0.00049	0.00444
Sm_2O_3	—	0.00009	0.00081
SrO	0.00016	0.00018	0.00161
$TruO_2$[(b)]	0.00066	—	—
Y_2O_3	—	0.00009	0.00081
SUM	0.00480	0.02983	0.10341

(a) NiO was used as a surrogate for CdO.

(b) CeO_2 was used as surrogate for divalent transuranic oxides.

5. Prepare the new glass compositions from the statistical experimental design and measure their properties. Glasses were formed according to the random manner suggested in Piepel, et al (1999). Properties having a major influence on glass processability and acceptability for repository disposal were determined on each. The resulting actions have goals of:

    a. Producing a database from which to establish composition–glass property relationships [Step 6 of the CVS strategy described in Piepel, et al (1999)].

    b. Providing information to develop the maturing separations process with respect to producing HAWs of a vitrifiable nature.

    c. Validating existing product property-glass composition models with independent data.

    d. Provide the basis for a consistent data base which would ultimately be used for producing optimal formulations for the vitrification of INTEC HAW.

The remainder of this document describes the preparation and characterization of thirty Phase 1 glasses within the HAW CVS as described in Piepel, et al (1999), and of fourteen Phase 1b glasses, the necessity of which is described in Section 4 below.

3. PERFORMANCE AND PROCESSING CRITERIA

Certain properties are of major significance in determining the suitability of a glass as a waste form. These properties influence glass processability and its acceptability as a waste form. Processing properties have operational constraints. Those properties affecting the suitability of a waste form for repository disposal have regulatory constraints. Properties investigated during the characterization of glasses prepared in this study are given below.

3.1 Properties Influencing Glass Processability

3.1.1 Liquidus Temperature

Liquidus temperature (T_L), the highest temperature at which a glass melt is in equilibrium with its primary crystalline phase, greatly influences melter operating temperature.[7] To avoid crystal formation, the T_L should be lower than the lowest temperature that glass is expected to achieve in the melter. Such formation has the potential to clog the melter pour spout, short its electrodes and alter the heat/mass flow in the melter. The primary crystalline phase at equilibrium with the melt at T_L is dependent on the melt composition. Primary phases form reversibly with respect to temperature, and the rate at which a primary phase will crystallize from a glass is dependent on component concentration and temperature. It is a matter of practice to apply a 100°C differential between the nominal production scale melter operating temperature (T_M), and glass melt liquidus temperature, T_L (i.e., $T_M > T_L + 100°C$).[8] The 100°C differential provides an adequate buffer to avoid crystallization while considering variations or uncertainties in melter temperature, composition and T_L measurement.

Secondary crystalline phases can also form below the T_L of a primary phase. These are also dependent on melter feed composition. They may be of minor importance with respect to melter operations, but as with the primary crystalline phase, their identity and quantification could be important in the qualification of a glass product for repository acceptance.

3.1.2 Viscosity

Molten glass viscosity is strongly dependent on melter operating temperature and melter feed composition. Glass viscosity influences cold cap formation, which inversely affects vaporization from the melt. Glass viscosity also inversely affects melt reactivity, melt corrosion, devitrification rate on cooling, and pouring properties. Glass viscosity can also influence the rate of primary phase crystallization at T_L, and it can influence the annealing properties of a glass product poured into a can for storage.[9]

Through the DWPF and WVDP operating experience, a glass viscosity range of between 20 and 100 Poise (2-10 pascal-seconds) has been recommended for joule heated, ceramic brick lined glass melters operating at 1150°C.[5] Maintaining the glass viscosity within this range minimizes processing problems associated with this property. Thus, it is necessary to characterize the viscosity as a function of temperature of a glass before melter processing.

3.2 Properties Influencing Glass Waste Form Acceptability

3.2.1 Durability

Durability of a waste form primarily refers to its ability to resist degradation by aqueous processes. Degradation by these processes over geologic time is the most likely mechanism to cause subsequent loss to the environment of the hosted radionuclides and hazardous species. Therefore, a waste form must display certain durability properties in order to qualify for repository storage. In support of DWPF product qualification, product specifications on the glass waste form require extensive characterization to meet the Waste Acceptance Preliminary Specifications (WAPS).[10] To aid in this characterization process, the PCT was developed to evaluate the durability of homogeneous and devitrified glasses by measuring the concentrations of the chemical species released from a representative crushed glass sample to a test solution. Thus, the PCT is applied to obtain information about the durability of the candidate waste form and its suitability for disposal in a federal geologic repository.[6] The WAPS specify upper acceptability limits for normalized releases of boron, lithium, silicon and sodium from DWPF glasses as determined by application of the PCT. Because of this precedent, and in order to enhance the database of responses of glasses of various compositions, the PCT was applied to the glasses formed in this study.

3.2.2 Homogeneity

A homogeneous glass consists of a single vitreous phase. Thus, a glass that is devitrified or phase separated is not homogeneous. The WAPS does not exclude an inhomogeneous glass from acceptance for storage if all other criteria are met. For example, spinel formation is not prohibitive in HLW glasses as long as durability, as determined by the PCT, meets the criteria with adequate certainty. However, qualifying an inhomogeneous glass for storage is expensive and time consuming because each phase present in a significant volume fraction must be characterized. This requires first determining if the phase is present in a significant amount. Then, for such a phase, characterization must be performed with respect to composition, hosted radionuclides (if any), structural properties, and thermal properties.

All glasses formed in this study were air quenched onto a steel plate. Some of these glasses were also formed at anticipated canister centerline cooling (CCC) rates. All were inspected visually and by optical microscopy in order to observe product homogeneity. All glasses formed at CCC rates were analyzed for crystallinity by x-ray diffraction analysis (XRD). Certain inhomogeneous glasses were characterized in response to the PCT, T_L and viscosity profile in order to obtain bounding information. In addition, transmission electron microscopy (TEM) was performed at SRTC on selected glasses.

4. GLASS IDENTIFICATION AND OBSERVATIONS DURING PREPARATION

Phase 1a CVS matrix glasses were prepared in INTEC laboratories. During this preparation a batching upset occurred in which excessive phosphate (2.6-2.9X) was added to the targeted Phase 1a glass compositions. Thus, some of the Phase 1a glasses contained as much as 0.1312 mass fraction of phosphate. These glasses were subjected only to the PCT and not further characterized. "As-batched" Phase 1a CVS matrix glasses without phosphate and those prepared with phosphate content adjacent to limits of the matrix (< 7 wt %) were retained for full characterization. These Phase 1a glasses are given in Table 4. Those Phase 1a glasses rejected from further analysis because of extreme phosphate content are given in Table 5.

It is possible that wastes containing phosphate to the extremes contained in these glasses could be encountered in future immobilization actions within the DOE-Complex. Thus, the preparation of these glasses, and their leaching properties, as measured by the PCT test, are included in this report. These observations provide information on the effects of extending phosphate content beyond the EGCR and add to information existing on the impacts of high phosphate content on borosilicate glass systems.

To adequately develop property/composition relationships for the Phase 1a test matrix, additional glasses with phosphate contents slightly greater than in the original design were defined. Using the available data from the Phase 1a glasses, and applying the development strategy at PNNL (as discussed in Section 2.2), 14 additional glasses were developed to augment the Phase 1a test matrix.[5] These 14 glasses, known as Phase 1b formulations, replace the rejected Phase 1a extreme phosphate glasses. Included are formulations at 6 new outer points (IG1-31 to IG1-36), a replicate of IG1-34 (IG1-44), 6 new inner layer points (IG1-38 to IG1-43) and the Phase 1b centroid, IG1-37. The compositions of these 14 glasses, given in Table 6, were designed at PNNL and prepared at SRTC and PNNL using standard procedures.[11, 12] The final array of Phase 1a and 1b glasses fabricated, characterized with respect to homogeneity, T_L, viscosity, and response to the PCT, are given in Table 7.

Table 4. Compositions (wt %) of "as-batched" high phosphate glasses retained for total characterization and designated Phase 1a glasses.

Glass	Al_2O_3	B_2O_3	K_2O	Li_2O	Na_2O	P_2O_5	SiO_2	ZrO_2	Others
IG1-1	5.52	9.47	4.25	5.46	14.32	7.03	47.06	6.48	0.41
IG1-6	0.00	15.01	10.00	4.82	5.00	0.00	57.22	7.51	0.44
IG1-7	15.01	15.01	0.00	8.45	5.00	0.00	53.08	3.00	0.45
IG1-10	0.00	6.54	0.00	9.00	15.60	0.00	54.41	14.01	0.44
IG1-11	14.64	5.01	0.00	5.11	20.00	0.00	54.79	0.00	0.45
IG1-12	3.17	15.01	10.01	0.00	15.30	0.00	42.06	14.01	0.44
IG1-13	7.59	5.01	10.01	7.09	17.20	0.00	52.66	0.00	0.44
IG1-14	10.87	7.24	2.42	5.07	16.74	3.62	50.23	3.38	0.43
IG1-16	7.25	7.25	2.42	4.63	16.74	3.62	47.52	10.14	0.43
IG1-21	8.91	12.07	7.24	6.52	9.50	3.62	43.23	8.48	0.43
IG1-24	8.63	12.07	7.24	6.52	9.71	3.62	43.02	8.76	0.43
IG1-25	7.24	7.24	7.24	4.93	13.35	3.63	45.80	10.14	0.43
IG1-26	5.52	9.47	4.25	5.46	14.32	7.03	47.06	6.48	0.41
IG1-29	14.00	8.39	0.00	7.00	10.62	0.06	57.00	0.00	2.93
IG1-30	2.02	6.07	0.00	7.07	18.32	0.49	45.97	11.12	8.94

Table 5. Compositions (wt %) of "as-batched" Phase 1 glasses not retained for total characterization.

Glass	Al_2O_3	B_2O_3	K_2O	Li_2O	Na_2O	P_2O_5	SiO_2	ZrO_2	Others
IG1-2	6.56	13.12	8.74	7.14	8.19	13.12	42.73	0.00	0.40
IG1-3	0.00	4.38	8.75	0.10	21.30	13.12	39.71	12.24	0.40
IG1-4	0.00	4.37	0.00	7.87	9.53	13.10	52.48	12.25	0.40
IG1-5	6.56	13.13	0.00	0.14	21.31	13.10	45.37	0.00	0.39
IG1-8	13.12	4.37	8.75	7.22	8.19	13.12	42.21	2.62	0.40
IG1-9	3.60	13.12	0.00	3.32	20.18	13.12	34.11	12.15	0.40
IG1-15	6.44	6.77	6.77	6.00	10.86	10.16	49.43	3.16	0.41
IG1-17	6.77	6.78	2.26	3.86	17.63	10.16	42.66	9.48	0.40
IG1-18	6.84	11.29	2.26	5.62	10.86	10.16	49.41	3.16	0.40
IG1-19	6.83	11.26	2.26	5.64	10.86	10.16	49.43	3.16	0.40
IG1-20	4.49	11.29	2.26	5.28	10.86	10.16	45.78	9.48	0.40
IG1-22	10.13	11.18	2.26	6.10	13.16	10.17	40.44	6.15	0.41
IG1-23	9.79	6.77	6.63	6.10	10.86	10.16	42.82	6.46	0.41
IG1-27	13.12	4.37	8.75	7.21	8.19	13.12	42.21	2.63	0.40
IG1-28	13.12	4.37	8.75	7.21	8.19	13.12	42.21	2.63	0.40

Table 6. Compositions (wt %) of Phase 1b glasses defined to replace Phase 1 extreme phosphate glasses.

Glass	Al_2O_3	B_2O_3	K_2O	Li_2O	Na_2O	P_2O_5	SiO_2	ZrO_2	Others
IG1-31	15.00	15.00	0.00	9.00	11.97	0.00	45.65	3.00	0.48
IG1-32	15.00	5.00	10.00	8.36	5.00	5.00	51.16	0.00	0.48
IG1-33	0.00	5.00	10.00	1.16	20.00	0.00	49.36	14.00	0.48
IG1-34	0.00	7.01	0.00	9.00	5.00	5.00	59.51	14.00	0.48
IG1-35	7.50	15.00	0.00	0.16	20.00	5.00	51.86	0.00	0.48
IG1-36	7.50	5.00	10.00	9.00	11.74	0.00	56.28	0.00	0.48
IG1-37	7.62	10.13	4.97	5.68	11.91	2.60	49.02	7.59	0.48
IG1-38	3.75	12.50	2.50	6.31	8.75	1.25	53.96	10.50	0.48
IG1-39	7.51	12.50	7.50	6.75	8.83	1.25	44.69	10.49	0.48
IG1-40	5.46	10.22	7.50	5.59	8.75	3.75	54.75	3.50	0.48
IG1-41	5.13	7.50	7.50	4.71	12.68	3.75	54.75	3.50	0.48
IG1-42	10.84	7.50	7.34	6.75	8.75	3.75	47.43	7.16	0.48
IG1-43	7.04	12.50	2.50	2.49	16.25	3.75	44.49	10.50	0.48
IG1-44	0.00	7.01	0.00	9.00	5.00	5.00	59.51	14.00	0.48

Table 7. As-targeted composition of glasses (wt %) prepared and characterized in this study.

Glass	Al_2O_3	B_2O_3	K_2O	Li_2O	Na_2O	P_2O_5	SiO_2	ZrO_2	Others
Phase 1a glasses									
IG1-1	5.52	9.47	4.25	5.46	14.32	7.03	47.06	6.48	0.41
IG1-6	0.00	15.01	10.00	4.82	5.00	0.00	57.22	7.51	0.44
IG1-7	15.01	15.01	0.00	8.45	5.00	0.00	53.08	3.00	0.45
IG1-10	0.00	6.54	0.00	9.00	15.60	0.00	54.41	14.01	0.44
IG1-11	14.64	5.01	0.00	5.11	20.00	0.00	54.79	0.00	0.45
IG1-12	3.17	15.01	10.01	0.00	15.30	0.00	42.06	14.01	0.44
IG1-14	10.87	7.24	2.42	5.07	16.74	3.62	50.23	3.38	0.43
IG1-16	7.25	7.25	2.42	4.63	16.74	3.62	47.52	10.14	0.43
IG1-21	8.91	12.07	7.24	6.52	9.50	3.62	43.23	8.48	0.43
IG1-24	8.63	12.07	7.24	6.52	9.71	3.62	43.02	8.76	0.43
IG1-25	7.24	7.24	7.24	4.93	13.35	3.63	45.80	10.14	0.43
IG1-26	5.52	9.47	4.25	5.46	14.32	7.03	47.06	6.48	0.41
IG1-29	14.00	8.39	0.00	7.00	10.62	0.06	57.00	0.00	2.93
IG1-30	2.02	6.07	0.00	7.07	18.32	0.49	45.97	11.12	8.94
Phase 1b glasses									
IG1-31	15.00	15.00	0.00	9.00	11.97	0.00	45.65	3.00	0.48
IG1-32	15.00	5.00	10.00	8.36	5.00	5.00	51.16	0.00	0.48
IG1-33	0.00	5.00	10.00	1.16	20.00	0.00	49.36	14.00	0.48
IG1-34	0.00	7.01	0.00	9.00	5.00	5.00	59.51	14.00	0.48
IG1-35	7.50	15.00	0.00	0.16	20.00	5.00	51.86	0.00	0.48
IG1-36	7.50	5.00	10.00	9.00	11.74	0.00	56.28	0.00	0.48
IG1-37	7.62	10.13	4.97	5.68	11.91	2.60	49.02	7.59	0.48
IG1-38	3.75	12.50	2.50	6.31	8.75	1.25	53.96	10.50	0.48
IG1-39	7.51	12.50	7.50	6.75	8.83	1.25	44.69	10.49	0.48
IG1-40	5.46	10.22	7.50	5.59	8.75	3.75	54.75	3.50	0.48
IG1-41	5.13	7.50	7.50	4.71	12.68	3.75	54.75	3.50	0.48
IG1-42	10.84	7.50	7.34	6.75	8.75	3.75	47.43	7.16	0.48
IG1-43	7.04	12.50	2.50	2.49	16.25	3.75	44.49	10.50	0.48
IG1-44	0.00	7.01	0.00	9.00	5.00	5.00	59.51	14.00	0.48

4.1 Preparation Sequence

IG1-29 and IG1-30 were prepared first and characterized with respect to viscosity and homogeneity at INTEC. When it was observed that their compositions, viscosity and homogeneity compared well with versions of these prepared at PNNL, all remaining glasses in the original Phase 1 matrix (Table 2) were prepared in the random order given under the "Run Order" column, then characterized. The Phase 1b (see Table 6) glasses, defined to supplement the Phase 1a glasses remaining for characterization, were also prepared in random order.

4.2 Physical Conditions of Preparation

Each of these glasses was prepared in a 250-gram oxide equivalent batch, mixed, then placed in a 250-ml high form 90% Pt/10% Rh crucible and covered with a 90% Pt/10% Rh cover. Batches were melted for four hours at 1150°C, then were poured onto a stainless steel quench block to form a "pour patty" used as a sampling stock for characterization. Pour patties were typically about three inches (7.62 cm) in diameter and about 1/4-inch (0.6 cm) thick.

4.3 Observations and Melting

Foaming occurred from most Phase 1a glasses because of the release of CO_2 from the conversion of carbonate components (Cs_2CO_3, K_2CO_3, Li_2CO_3, Na_2CO_3) to oxides. Glassy residue collection was observed on the inside surface of crucible lids during heating of these glasses because of the release of glass particles as aerosols from the molten state. No other systematically occurring phenomena were observed during melting of these glasses. Foaming from carbonate decomposition and subsequent deposition on inside cover surfaces did not occur during the formation of Phase 1b glasses because a slower heating rate was used than in melting the Phase 1a glasses.

4.4 Observations after Melting

Glasses that appeared opalescent, presumably from glass-in-glass separation, were noted for the purpose of observing limits of single-phase glass compositions. Beyond being subjected to the PCT phase, separated Phase 1a glasses were only inspected visually and optically to detect the presence of crystalline phases. A particular and significant phenomenon observed optically was that the initially poured mass of some glasses appeared not to phase separate, while their later masses did separate on continued pouring. This phenomena suggests that the rapidly quenched glass on the steel plate did not visually separate, while the slower cooled glass poured on top of it did. If so, the critical temperature for phase separation is below the processing temperature and the time constant for phase separation kinetics is of the same order as cooling time for steel plate quenching. This observation is important because it reveals that the rate of phase separation of a glass depends on the temperature of its surroundings (i.e., a kinetic effect).

Of the Phase 1b glasses, only IG1-32 appeared phase separated through optical means. Phases 1a and 1b glasses visually appeared free of undissolved residues after the initial melt at 1150°C with the exception of three glasses. After rebatching, glass IG1-33 required melting at 1450°C for four hours to dissolve solid particles and form a homogeneous product. Glasses IG1-34 and IG1-44, which are duplicate compositions, contained undissolved solids after being melted at 1150°C for four hours. After grinding each product to sub-micron particle size, and remelting at 1150°C for one hour, homogeneous products of each were formed. No investigation was made in FY98 of the kinetic effect on homogeneity from cooling glasses down at the rate anticipated in the full-scale canister centerline.

4.5 Homogeneity Characterization

All glasses formed in this study were air quenched onto a steel plate after vitrification for four hours at 1150°C. Visual observations and transmitted light optical microscopy (up to 70X) were used to detect phase separation and crystallinity in each of these. Twenty-five of the forty-four glasses characterized were analyzed by TEM for homogeneity. Crushed "as fabricated" glass was submitted for TEM analysis. Magnification up to 100000X was used in this analysis. All Phase 1a and 1b glasses retained for analysis were subjected to XRD analysis in order to observe crystallinity.

Borosilicate glasses containing phosphate tend to phase separate on cooling. All Phase 1a glasses were formed by quenching, and phase separation was observed in many of them. At INTEC in FY99, selected visually homogeneous Phases 1a and 1b glasses were subjected to a CCC test to observe their tendency to remain homogeneous under practical cooling conditions. Thus some of the homogenous Phase 1a and 1b glasses containing less than 5 wt % phosphate were rebatched in 60-gram amounts, added to alumina crucibles, and vitrified at 1150°C for four hours. The rebatched products were cooled from 1150°C at the rate observed in a full-scale canister centerline. Figure 2 is a plot of the cooling curve applied in the programmable furnace used in this experiment. This curve is based on the CCC observed in the prototype DWPF canister formed during the eighth campaign of the scaled glass melter.[13] The effects of conducting this test in alumina crucibles is not known, but the extent of these effects depends in part on glass composition.

X-ray diffraction patterns for air quenched glasses and for those cooled at the CCC are given in Appendix A.

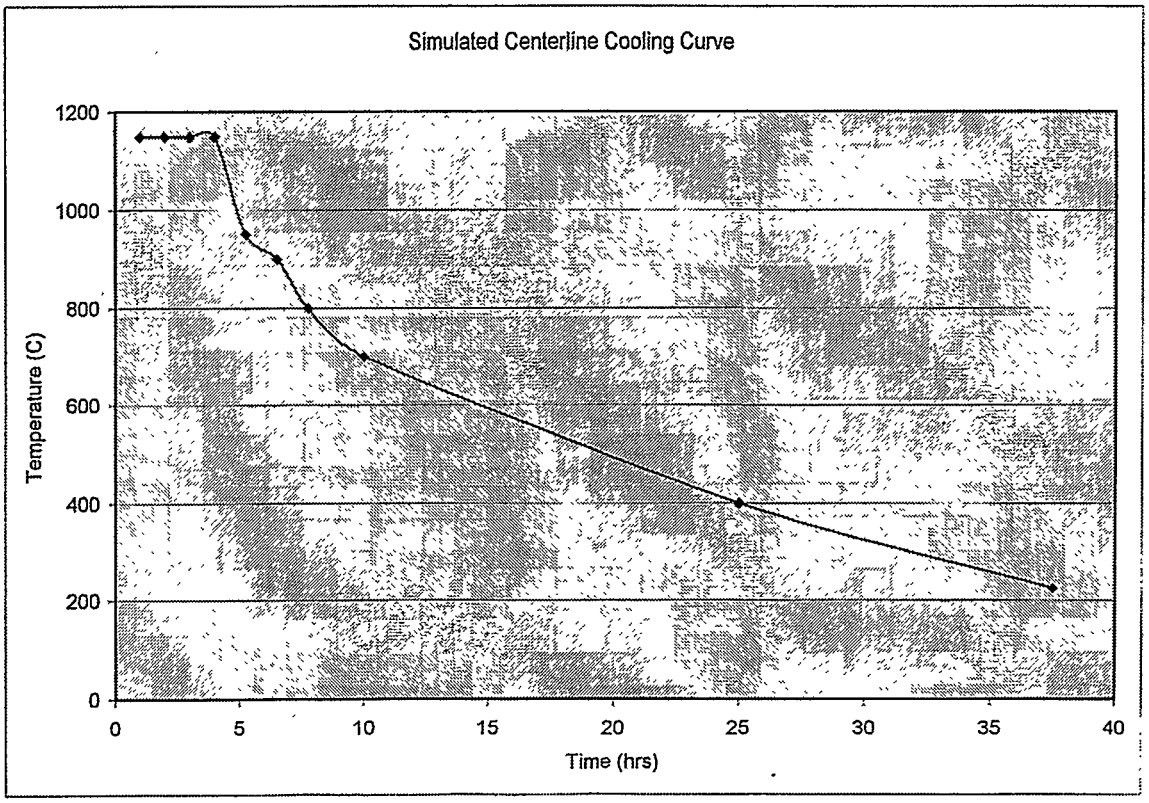

Figure 2. Plot of cooling curve applied to simulate CCC conditions for Phases 1a and 1b glasses.

4.6 Liquidus Temperature Characterization

The T_L was measured at PNNL on Phases 1a and 1b glasses using the gradient temperature method described by Vienna, et al. (1998).[14] In this method, glass samples are placed in 90% Pt/10% Rh boats then subjected to a linear temperature gradient for about 24 hours. After cooling to ambient conditions, the sample was analyzed by transmitted light optical microscopy up to 70X magnification. The temperature (or temperature range) of the crystallization front was identified. This procedure differs from ASTM C-829-81 in the sample preparation step.[7,14] ASTM C-829-81 requires a water wash of the glass before testing. This wash was omitted in the T_L determinations on INTEC CVS glasses because the lithium phosphate crystals present in some test glasses would have dissolved. Dissolution of these crystals would consequently result in an alteration of the glass structure and composition that would influence succeeding measurements.

Further refinements of the T_L values were made on the glass via the uniform temperature method described by Vienna, et al (1998).[14] In this method, glass samples were placed in 90% Pt/10% Rh boxes with tight lids and heat treated at constant temperature for no less than 22 hours. The samples were quenched and analyzed using transmitted light optical microscopy up to 30X magnification to determine if crystals were present. New samples of each glass were heat treated to progressively narrow the temperature difference between the highest temperature where glass and crystals coexist (T_C), and the lowest temperature where the glass remains amorphous (T_A). Higher magnification optical microscopy (up to 70X), SEM, and XRD were applied to various glasses formed in this phase of the CVS. The T_L measurement furnaces used were calibrated using the National Bureau of Standards (NBS) T_L standard glass No. 773.

XRD analyses were made on selected samples with the greatest density of crystals in order to identify the primary crystalline phase at T_L. Generally, too few crystals were present near T_L to detect with certainty where the primary crystalline phase formed. Also at these lower temperatures, additional crystalline phases sometimes formed. Scanning electron microscopy (SEM) was performed on selected glasses heat treated at T_A, T_C, and below to help refine the identity of the primary phase.

4.7 Durability Characterization

The PCT Method A, as described in ASTM C-1285-94, was performed in triplicate on each of the Phase 1a and Phase 1b glasses.[6] The PCT was developed to evaluate the chemical durability of homogeneous and devitrified glasses by measuring the concentrations of the chemical species released from a crushed glass to a test solution. The procedure establishes a strict set of test conditions.

The PCT Method A is a seven-day crushed glass durability test performed at 90 ± 2°C in a leachant of ASTM Type I water. The test is performed under static conditions and is conducted in 304L stainless steel test vessels. Method A requires crushed glass of a particle size between 75 and 150 μm (-100, +200 mesh) using U.S. Standard ASTM screens. After particles are cleaned of adhered fines, crushed glass (a minimum of 1 gram) is placed in a Type 304L stainless steel vessel into which an amount of ASTM Type I water equal to 10 cc per gram of glass is added. For the Phase 1a and 1b glasses, 15 ml of ASTM Type I water was added to 1.5 grams of glass.

The vessels were seated, weighed and placed with blanks and standards into a constant temperature oven at 90 ± 2°C. After the 7-day test, the vessels were allowed to cool to room temperature. The final weight of each vessel and the solution pH were recorded on a data sheet. The leachates were then filtered through a 0.45 μm port filter. Six ml of each solution was acidified with 4 ml of 0.4 M HNO_3 to ensure that cations would remain in solution. Solutions, standards and blanks were then analyzed for various

elemental concentrations by the Savannah River Laboratory Mobile Laboratory using inductively coupled plasma emission spectroscopy (ICP). Analytical plans for measuring the aluminum, boron, lithium, silicon, silicon, phosphorous, and zirconium content in parts per million of the leachate resulting from subjecting the glasses to the PCT are given in References 15 and 16. The concentrations of dissolved glass components are used to calculate the amount of glass reacted and its dissolution rate.

The analytical plans describe the experimental set-up and the submission of solution aliquots to the SRTC Mobile Laboratory. In each phase, PCTs were conducted in triplicate for each glass as well as for samples of the Environmental Assessment (EA) glass (two for Phase 1a and one for Phase 1b), the ARM glass standard (two for Phase 1a and one for Phase 1b), and a blank (B) standard (two for Phase 1a and one for Phase 1b). For each glass sample in each phase, one of its triplicates was randomly placed on each of the three available oven levels. The glass sample identifier was augmented with a suffix of 1 (top), 2 (middle), or 3 (bottom) to indicate oven level. Each of the resulting solution samples was assigned an identifier for use in the laboratory, and were grouped along with samples of a multi-element solution standard for analysis by ICP. An analytical plan of seven ICP blocks (each block representing a new calibration of the instrument) was required to process all of the Phase 1a solution samples, and a plan with three blocks was required for the Phase 1b samples. Tables B.1-B.9 in Appendix B provide the solution analyses (in ppm) for Phase 1a and Phase 1b glasses.

Elemental leaching results determined by the PCT were normalized with respect to the amount of that element "as batched" in the waste form. This allows that result to be reported as a portion of the weight fraction of that element in the waste form. The compositions for the Phase 1a and 1b glasses have been measured at SRTC. "As-measured" compositions will be used to normalize the PCT releases. The results of this normalization will be the subject of a future report.

4.8 Viscosity Characterization

Viscosity (η) profiles with respect to temperature were obtained on the HAW CVS glasses through applying a method based on the ASTM standard procedure.[17] In this procedure, viscosity is systematically taken at equidistant points around a central temperature which can represent the operating temperature of a glass melter. For vitrifying INTEC HAW, this temperature is assumed to be 1150°C, and viscosity readings were taken at 50°C increments first going below this temperature (to 950°C), then up to and beyond it to 1250°C. Temperatures for this calculation were read from the viscometer furnace thermocouple positioned adjacent to the sample crucible. The viscosity measurement reported at a temperature setpoint was based on the arithmetic mean of torque readings taken every fifteen seconds on the spindle rotating in the glass melt. At each setpoint, the glass was held at temperature for 15 minutes. The readings were taken over the last five minutes of the 15-minute hold. Mean viscosities were recorded at each increment of temperature.

Decreasing the temperature incrementally from 1150 to 1050°C also provides an observation of any tendency of phases to crystallize from the glass on cooling and the resulting effect on viscosity. Observations of tendency to devitrify during this part of the procedure provides information useful in determining T_L of the glass. Similarly, systematically heating up the glass from 1150 to 1250°C and cooling back down to 1150°C can be used to observe if volatilization occurs from the glass above melter operating temperatures and the resulting effect on viscosity.

5. CHARACTERIZATION RESULTS AND DISCUSSION

The glasses investigated in this study were characterized with respect to:

1. Visual homogeneity
2. Liquidus temperature (T_L)
3. Durability as measured by the leaching response to the PCT
4. Viscosity profile.

5.1 Homogeneity Results

5.1.1 Data from Air Quenched Glasses

Information with respect to crystalline phase content has been obtained through the completion of XRD analysis on Phases 1a and 1b glasses appearing to be homogeneous. This analysis reveals that alkali phosphate crystallinity is present in many and that this phenomena appears to be primarily a function of phosphate content. Glasses in which the formation of alkali phosphate crystallinity appears to take place during quenching (visually phase separated) are given in Table 8. Table 8 also gives visual and transmitted light microscopy (70X magnification) observations of air quenched Phases 1a and 1b glasses. Also given in the table are the results of XRD analysis for crystallinity in the optically homogeneous glasses and TEM analysis of twenty-five of the glasses. Inspection of the results presented in this table reveals that some glasses contain both glass-in-glass separation and crystallinity. Also, it is observed that glass-in-glass separation in some glasses can only be detected through the application of TEM analysis. Phase separation is illustrated in Figure 3 which is a TEM micrograph (100kX, 200 KV) of IG1-44, a glass appearing optically and visually homogeneous. Through XRD analysis, this glass was also shown to host lithium phosphate. In contrast, Figure 4, a micrograph (100 KX, 200 KV) displays that glass IG1-38 is homogeneous as determined by TEM. This determination supports the optical and visual observation that the glass appears homogeneous and the XRD analysis results which determine the glass to be amorphous. Crystallinity detected in these glasses containing phosphate is mostly from the formation of alkali phosphates. The occurrence of alkali phosphate crystallinity in these products provides information that will eventually be useful in understanding the homogeneity-composition relationship in these glasses.

Table 8. Homogeneity properties of air quenched glasses formed in this study.

Sample ID	Visual/Optical	XRD	TEM
IG1-01	Homogeneous	Li_3PO_4	Phase separated
IG1-02	Phase Separated	Li_3PO_4	—
IG1-03	Phase Separated	Na_3PO_4	—
IG1-04	Phase Separated	—	Phase separated
IG1-05	Phase Separated	—	Phase separated
IG1-06	Homogeneous	Amorphous	—
IG1-07	Homogeneous	Amorphous	—
IG1-08	Phase Separated	—	Phase separated
IG1-09	Homogeneous	Li_2NaPO_4	Phase separated
IG1-10	Homogeneous	Amorphous	—
IG1-11	Homogeneous	Amorphous	—
IG1-12	Homogeneous	Amorphous	Homogeneous
IG1-13	Homogeneous	Amorphous	Homogeneous
IG1-14	Homogeneous	Li_3PO_4	Phase separated
IG1-15	Phase Separated	—	—
IG1-16	Homogeneous	Amorphous	Homogeneous
IG1-17	Homogeneous	Li_2NaPO_4	Phase separated
IG1-18	Phase Separated	—	—
IG1-19	Phase Separated	—	—
IG1-20	Phase Separated	—	Phase separated
IG1-21	Homogeneous	Li_3PO_4	Phase separated
IG1-22	Phase Separated	—	—
IG1-23	Phase Separated	—	—
IG1-24	Homogeneous	Li_3PO_4, Na_2ZrSiO_5	Phase separated
IG1-25	Homogeneous	Li_3PO_4	Questionable
IG1-26	Homogeneous	Li_3PO_4	Phase separated
IG1-27	Phase Separated	—	—
IG1-28	Phase Separated	—	—
IG1-29	Homogeneous	—	—
IG1-30	Homogeneous	—	—
IG1-31	Homogeneous	Li_2SiO_3,ZrO_2	—

Table 8. (continued).

Sample ID		Visual/Optical		XRD		TEM
IG1-32		Phase Separated		Li_3PO_4		—
IG1-33		Homogeneous		Amorphous		—
IG1-34		Homogeneous		Li_3PO_4		Phase separated
IG1-35		Homogeneous		Amorphous		Homogeneous
IG1-36		Homogeneous		Li_2SiO_3		—
IG1-37		Homogeneous		Amorphous		Homogeneous
IG1-38		Homogeneous		Amorphous		Homogeneous
IG1-39		Homogeneous		Amorphous		Homogeneous
IG1-40		Homogeneous		Li_3PO_4		Homogeneous
IG1-41		Homogeneous		Li_3PO_4		Questionable
IG1-42		Homogeneous		Li_3PO_4		Phase separated
IG1-43		Homogeneous		Amorphous		Homogeneous
IG1-44		Homogeneous		Li_3PO_4		Phase separated

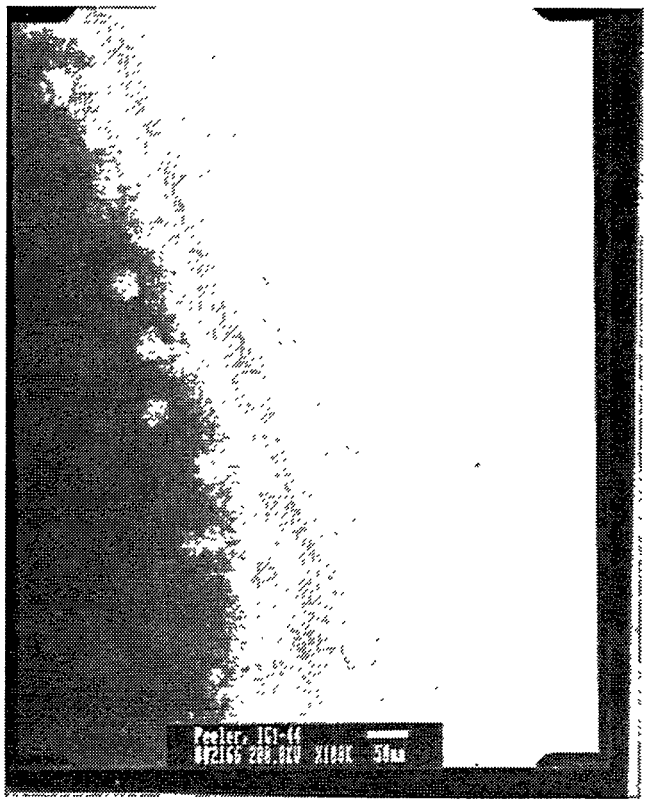

Figure 3. TEM micrograph (100 KX, 200 KV) of glass IG1-44 showing phase separation.

Figure 4. TEM micrograph (100 KX, 200 KV) of glass IG1-38 showing homogeneity.

5.1.2 Data from Glasses Cooled at Full-Scale CCC Rate

Glasses being investigated to immobilize radioactive wastes should be cooled from the proposed melter operating temperature at CCC rates. This is the slowest practical cooling rate encountered in waste vitrification, and applying it allows the formation of any phases with a tendency to crystallize or to separate as a glass. Glasses formed in this study during FY98 were air quenched. Quenching does not allow all kinetic conditions for the formation of phase separation or crystallization. Only glasses observed at INTEC not to have crystallinity as detected by XRD or phase separation as detected by optical or visual means were subjected to CCC tests. The results of these glasses being cooled at CCC rates are given in Table 9. Only visual and optical inspection was used to observe glass-in-glass separation and XRD analysis was used to observe crystallinity in glasses subjected to this test. The results in Table 9 indicate that all except IG1-38 and IG1-39 contained either or both crystallinity, as determined by XRD analysis, or appeared phase separated using optical means. These results indicate that cooling rate influences product homogeneity.

Table 9. Homogeneity and phase formation in glasses subjected to canister centerline cooling experiment.

Glass	Homogeneity by optical microscopy (50X) after test	Major phase formed during test as determined by XRD
IG1-14	Phase separated, opaque, not devitrified has stress cracks and small bubbles	Li_3PO_4
IG1-16	Amorphous and transparent, not devitrified has stress cracks and small bubbles in upper portion of melt	Li_3PO_4
IG1-35	Amorphous and translucent, not devitrified has stress cracks and very few small bubbles	Na_3PO_4
IG1-37	Amorphous and translucent, not devitrified has stress cracks and no bubbles	Li_3PO_4
IG1-38	Amorphous and transparent, not devitrified has minor stress cracks and very small bubbles	None detectable by 2- and 8-hour scans
IG1-39	Amorphous and mainly transparent, small white particles in glass could be reaction products with alumina crucible or separated amorphous phase, no stress cracks or bubbles	None detectable by 2- and 8-hour scans
IG1-41	Phase separated, opaque with stress cracks and bubbles	Li_3PO_4
IG1-43	Amorphous and translucent, not devitrified has stress cracks and no bubbles	Li_3PO_4

5.2 Liquidus Temperature Results

The T_L obtained for Phases 1a and 1b HAW glasses are given in Table 10. Also given are the crystalline phases identified in each glass through the application of XRD. The value T_A gives for each glass investigated the lowest temperature at which that glass remained amorphous as determined by optical microscopy. Likewise, the value T_c gives for each glass investigated the highest temperature at which that glass contains crystallinity as determined by optical microscopy. Subsequent to completing

the first version of this report, XRD analysis has been completed on the visually and optically homogeneous air quenched glasses formed at 1150°C for four hours (see Table 8). Many of these glasses were determined by XRD to contain alkali phosphate crystallinity. Because those glasses containing crystallinity were melted for only four hours at 1150°C, they did not achieve the equilibrium conditions required for determining T_L. In some glasses, two crystalline phases were detected during the analysis for T_L. The phase known to be minor in presence in each of these glasses is enclosed in parentheses. For some of the glasses containing two crystalline phases, the data in Table 10 should be considered preliminary. This is because electronic analysis techniques should be applied to samples heat treated in a uniform temperature furnace in order to determine which phase forms first with decreasing temperature. The T_L information given in Table 10 is significant because it is the first obtained on glasses within the experimental glass composition region for INTEC HAW glasses.

Analysis by XRD was performed on products of all glasses heat treated in the uniform temperature furnace at levels below T_L of each glass. The results are given in Table 10. Analysis by SEM was used on some samples to observe the presence of crystallinity in better detail.

As an example of the analytical approach used, a sample of CVS glass IG1-1 subjected to the gradient furnace technique has been shown by optical microscopy (30X-70X) to contain lithium phosphate when formed at temperatures up to about 897°C. The SEM used in the T_L investigation at INTEC (RJ Lee Group Personal SEM) does not have the capability of detecting lithium. However, a sample of IG1-1 formed in the gradient furnace was subjected to SEM analysis to observe in more detail the presence of phosphorous associated with crystallinity. Figures 5 and 6 show SEM micrographs (3600X) of phases believed to be lithium phosphate and the glass matrix adjacent to it. The area analyzed is within a sample formed at a temperature below but near T_L. The spectra on each figure shows the relative amounts of oxygen, aluminum, silicon, phosphorous, and potassium in the glass matrix and crystalline phase. Figure 7 is an area elemental map of the phosphorous containing crystal identified in Figures 5 and 6. The distribution of aluminum oxygen, phosphorous, potassium, silicon, and sodium within and outside the crystal are shown. Figure 8 is a SEM micrograph (2400X) of the glass matrix formed at a temperature nearer T_L. The micrograph indicates a diminishing amount of crystallinity containing phosphorous in the glass sample.

Another example of using the INTEC SEM is in the T_L analysis applied to IG1-10, a glass not containing phosphate. Through the application of XRD, parakeldyshite ($Na_2ZrSi_2O_7$) appears to be the major crystalline phase present. Figures 9 and 10 show micrographs (1000X) of the parakeldyshite crystals and the adjacent glass taken in the area of the glass formed at about 975°C. Spectra on each micrograph show respective relative amounts of Al, Si, Na, P, and Zr. Figure 11 shows an area elemental map of the vicinity of the parakeldyshite crystal. The distribution of calcium, oxygen, phosphorous, silicon, and zirconium between the glass matrix and the crystalline phase are shown. The map provides further indications of the relative differences in the elements analyzed within and adjacent to the crystal. Figure 12 is a SEM micrograph (1000X) taken in an area of the sample where the amount of parakeldyshite appears to be diminishing.

At least two separate phases were identified in the T_L investigation of several glasses. Such was the case for IG1-6, IG1-9, IG1-10, IG1-11, IG1-16, IG1-25, IG1-31, IG1-34, IG1-37, and IG1-44 (see Table 10). The presence of zirconia in the XRD spectra suggests the possibility of incomplete vitrification of glass IG1-37. This may also be the case in IG1-6 where SiO_2 is identified as a phase present in the product.

Glasses IG1-1, IG1-2, IG1-14, IG1-21, IG1-24, IG1-26, IG1-40, IG1-41, IG1-42, and IG1-43 appear to be in the lithium phosphate primary phase stability field with T_L values ranging from a low of 811°C for IG1-43 to a high of 954°C for IG1-42. In general, glasses from which an alkali phosphate is

the primary crystalline phase formed on cooling meet the T_L <1050°C condition. Only those glasses with zirconium containing primary phases had measured T_L values above 1050°C (IG1-12, -33, -34, and -44).

Table 10. Results of liquidus temperature measurements (°C) on glasses formed in this study.

Sample ID	Gradient T_L °C	Uniform T_L °C	Primary Phase
IG1-01	897	902	Li_3PO_4
IG1-02	—		Li_3PO_4
IG1-03	—		Na_3PO_4
IG1-04	—		—
IG1-05	—		—
IG1-06	883-855	887	$SiO_2(LiB_2O_4)$
IG1-07	915-897	885	$LiA_1Si_3O_8$
IG1-08	—	—	—
IG1-09	N/A	861	$Li_2NaPO_4(Na_2Si_3O_7)$
IG1-10	985-965	981	$Na_2ZrSi_2O_7(Li_2SiO_3)$
IG1-11	848-743	827	$NaAlSiO_4(Li_2SiO_3)$
IG1-12	N/A	1075	$K_2ZrSi_3O_9$
IG1-13	775-770	765	Li_2SiO_3
IG1-14	850-840	862	Li_3PO_4
IG1-15	—	—	—
IG1-16	908-882	917	$Li_3PO_4(Zr_2P_2O_7)$
IG1-17	930-925	—	$(Li,Na_3)PO_4(Li_2NaPO_4)$
IG1-18	—	—	—
IG1-19	—	—	—
IG1-20	—	—	—
IG1-21	918-898	927	Li_3PO_4
IG1-22	—	—	—
IG1-23	—	—	—
IG1-24	918	905	Li_3PO_4
IG1-25	990-980	991	$K_2ZrSi_3O_9(Li_3PO_4)$
IG1-26	888	875	Li_3PO_4
IG1-27	—	—	—
IG1-28	—	—	—

Table 10. (continued).

Sample ID	Gradient T_L °C	Uniform T_L °C	Primary Phase
IG1-29	1090-1080	—	—
IG1-30	1135-1125	—	—
IG1-31	785	791	$Li_2SiO_3(ZrO_2)$
IG1-32	—	—	—
IG1-33	N/A	1310	$Na_2ZrSi_2O_7$
IG1-34	N/A	1142	$LiNaZrSi_6O_{15}(Li_3PO_4)$
IG1-35	863	850	Na_3PO_4
IG1-36	865	855	Li_2SiO_3
IG1-37	871	887	Li_3PO_4,ZrO_2
IG1-38	900-885	922	$LiNaZrSi_6O_{15}$
IG1-39	875-840	855	$K_2ZrSi_3O_9$
IG1-40	927	927	Li_3PO_4
IG1-41	835-827	847	Li_3PO_4
IG1-42	960-953	954	Li_3PO_4
IG1-43	815	811	Li_3PO_4
IG1-44	N/A	1142	$LiNaZrSi_6O_{15}(Li_3PO_4)$

Note: Gradient furnace T_Ls are estimated.

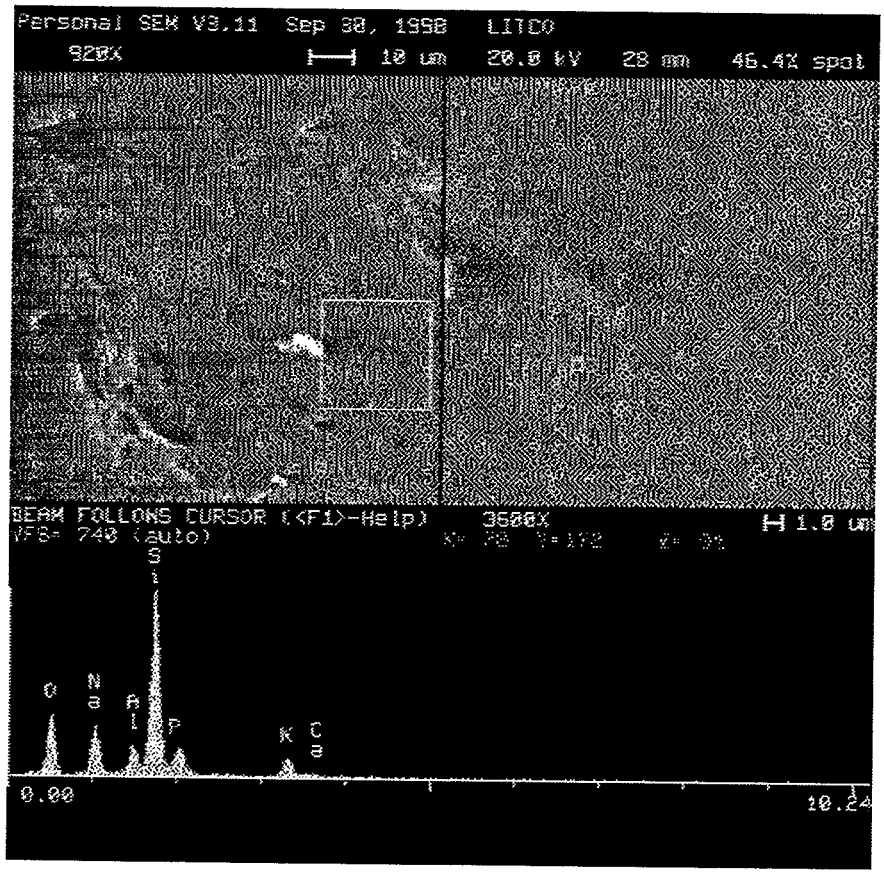

Figure 6. SEM micrograph (3600X) of IG1-1 sample containing lithium phosphate crystal and adjacent glass with spectra taken from adjacent glass.

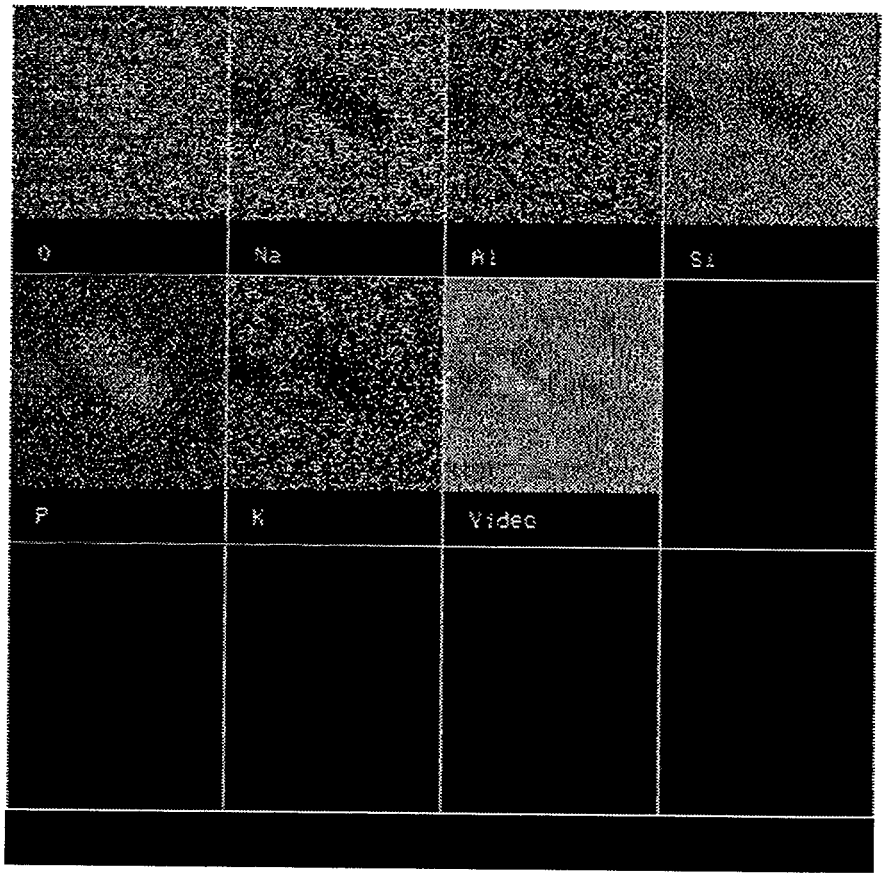

Figure 7. Elemental map of lithium phosphate crystal identified in Figures 2 and 3 showing distribution of aluminum, oxygen, phosphorous, potassium, silicon, and sodium in an IG1-1 sample.

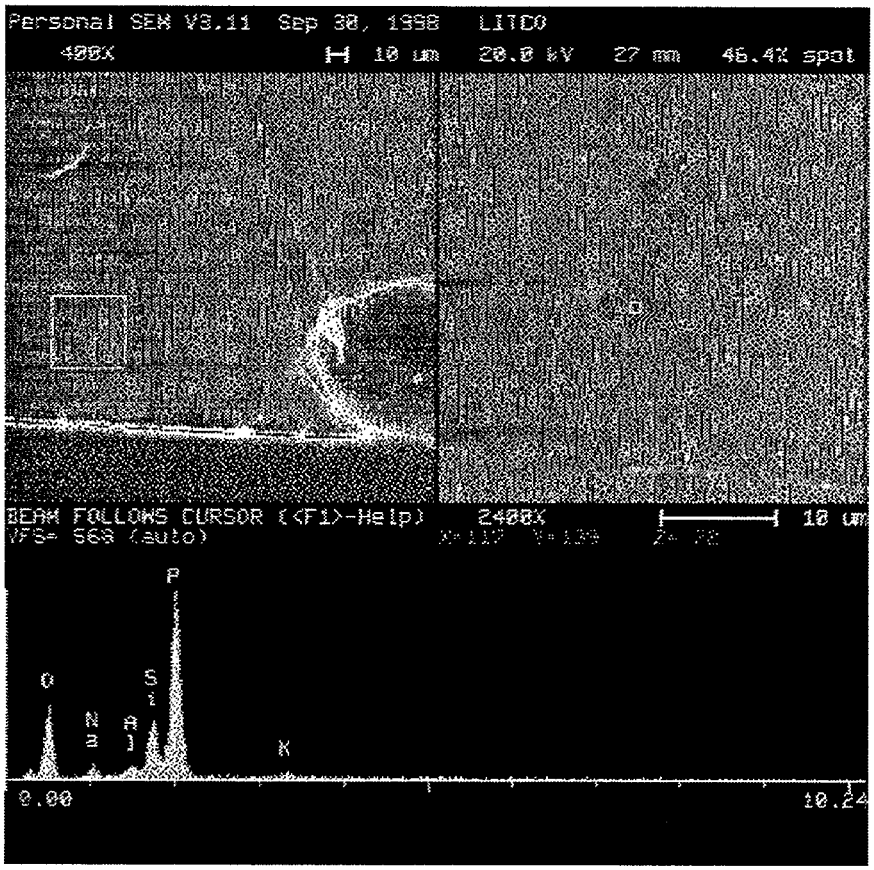

Figure 8. SEM micrograph (2400X) of IG1-1 sample with glass matrix in area expected to hold T_L.

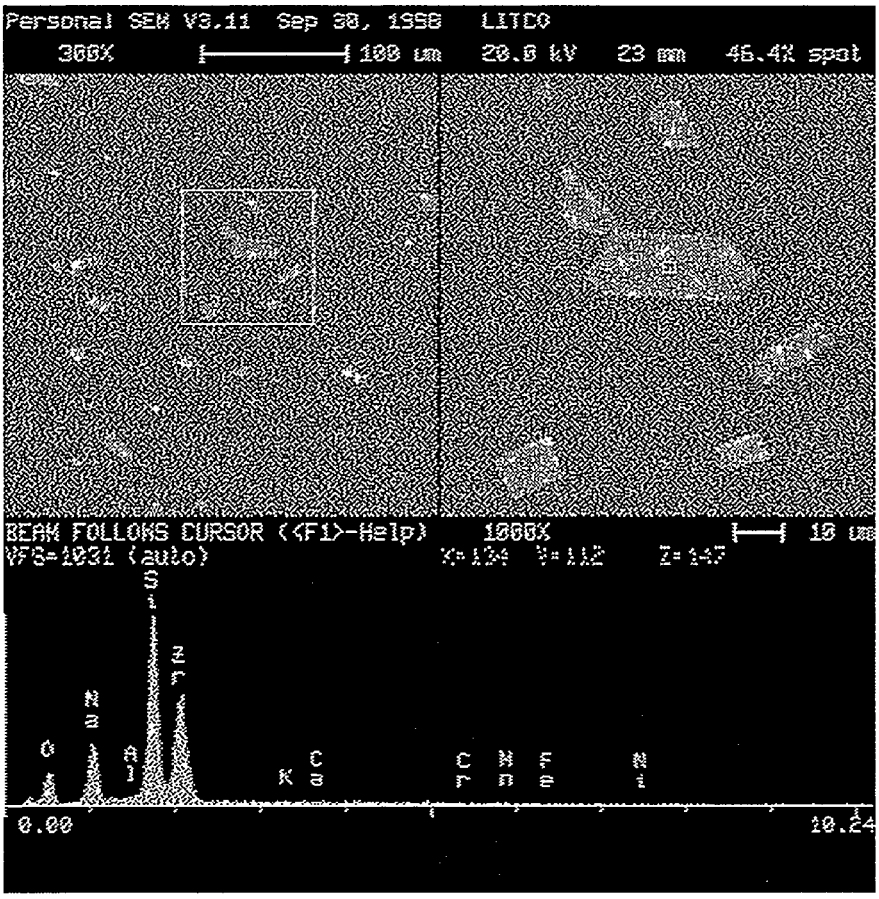

Figure 9. SEM micrograph (1000X) of IG1-10 sample containing sodium zirconium silicate crystal and adjacent glass matrix area with spectra taken from crystal.

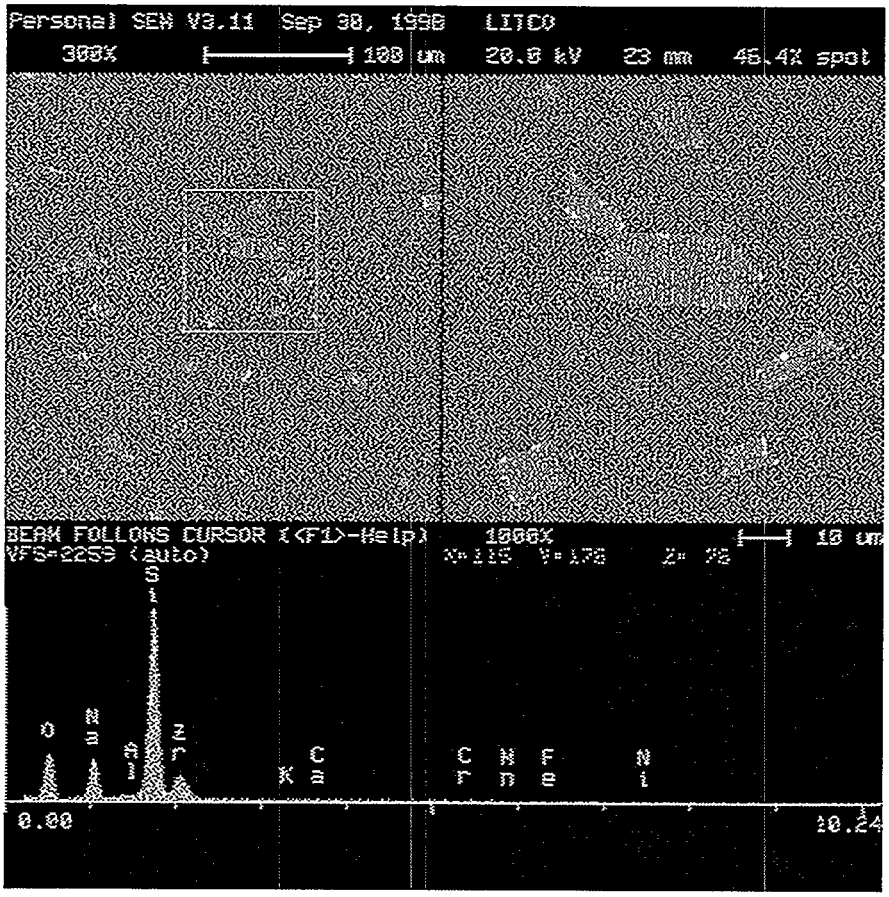

Figure 10. SEM micrograph (1000X) of IG1-10 sample containing sodium zirconium silicate crystal and adjacent glass matrix with spectra taken from glass matrix.

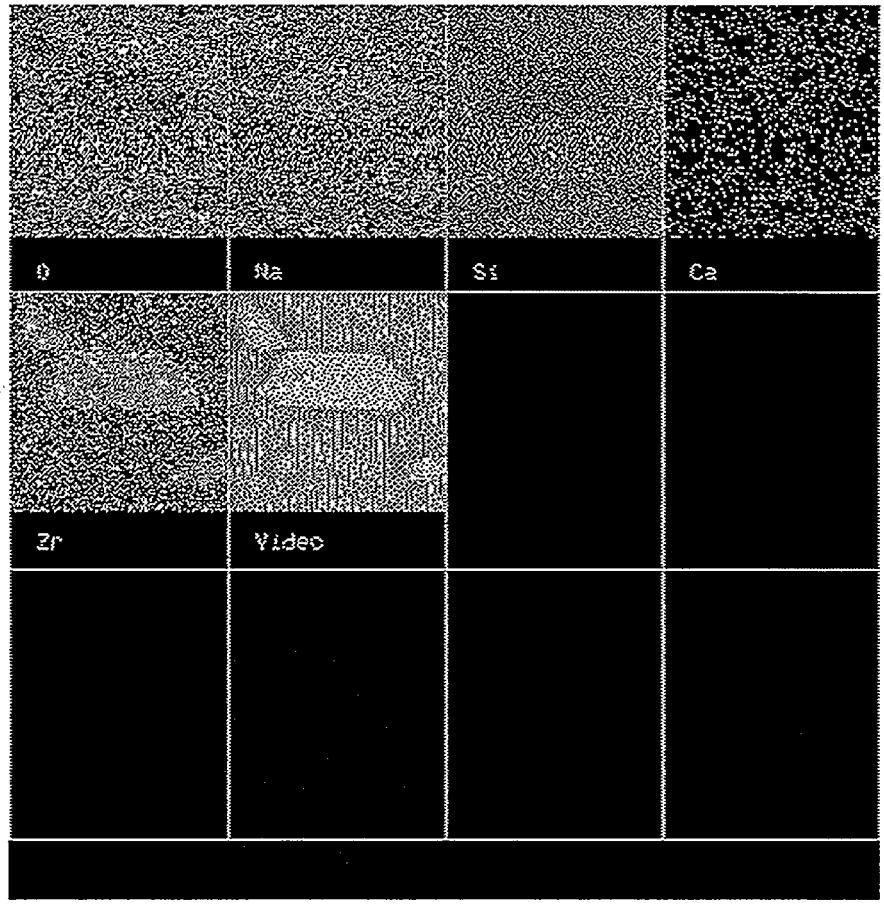

Figure 11. Elemental map of IG1-10 sample containing sodium zirconium silicate crystal identified in Figures 9 and 10 showing distribution of calcium, oxygen, phosphorous, silicon, and zirconium.

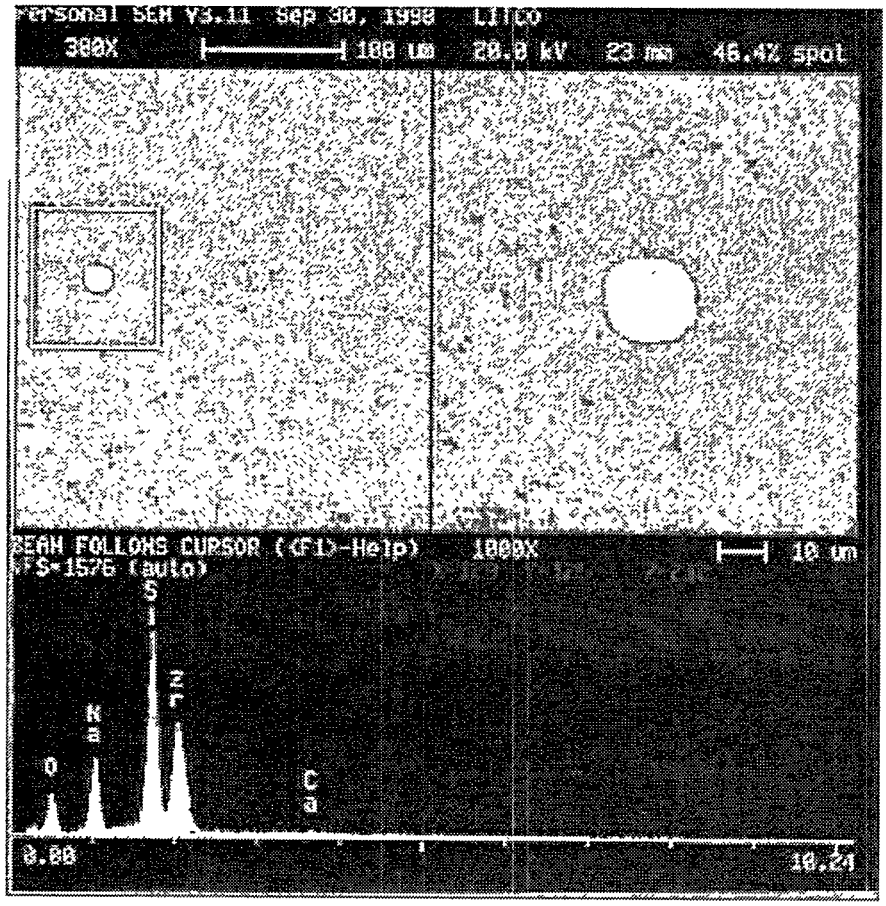

Figure 12. SEM micrograph (1000X) of IG1-10 sample formed in gradient furnace with glass matrix in area expected to hold T_L.

5.3 Durability Results

5.3.1 Results from the Multi-Element Solution Standard

A multi-element solution standard was included for measurement three times in every ICP calibration block, for both the Phase 1a and Phase 1b studies. The multi-element solution standard[a] is a 2% HNO_3 solution containing B, Si, Li, Al, Fe Na, and K.

The elemental concentrations of the multi-element solution standard are summarized in Table 11. Also summarized in Table 11 are the average values for all standards run for Phase 1a and Phase 1b. Very good agreement between the targeted elemental values and those determined experimentally was observed throughout this study. These results reveal that bias-correction based upon these results does not appear helpful. Therefore, this option was not pursued in the discussion that follows. A more detailed analysis of these results is provided by Edwards.[18]

Table 11. Analytical results from multi-element solution standard.

Element	Standard Values (ppm ± 0.5%)	Average Phase 1a and Phase 1b Values (ppm)
Al	4	4.002
B	20	20.724
Li	10	10.182
Na	81	85.748
P	—	0.320
Si	50	52.010
Zr	—	0.073

5.3.2 Normalized PCTs Using As-Batched Glass Compositions

For the glasses discussed in Section 3 (see Table 7), each of the elemental leaching concentrations can be normalized to obtain grams per liter (g/L) leached by relating it to the amount of the element in the glass. This is usually accomplished using the measured concentrations of the elements making up the glass composition. Measured concentrations in leachates from glasses subjected to the PCT are given in Appendix B. As-batched compositions were used for the normalization of results obtained in this study.

The common logarithm of the normalized PCT is frequently used to represent elemental leaching concentrations. To accomplish this calculation,

1. The common logarithm of the ppm leachate concentration is determined for each of three triplicates for an element of interest (see Appendix A),

2. The common logarithms are averaged over the three triplicates, and

a. Prepared by High Purity Standards, Charleston, SC.

3. Then a quantity equal to 1 plus the common logarithm of the as-batched cation weight percent of this element in the glass is subtracted from the average of step 2.

Using the "as-batched" compositions for the Phase 1a glasses and the "as-targeted" compositions for the Phase 1b glasses, the PCT results for these glasses were normalized. The normalized PCTs for these glasses are presented in Table 12.

Two entries appear in Table 12 for IG1-4 and IG1-40. An outlying lithium concentration value for one of the triplicates was excluded from the calculations presented in the starred row for IG1-4, while the calculations for the first entry for this glass included all of the data. Similarly, the outlying phosphate leachate concentration for IG1-40 was excluded from the calculations presented in the starred entry for this glass.

Table 12. Normalized PCT results from Phase 1a and Phase 1b glasses.

Test	Short ID	ID	Log NL [Al (g/L)]	Log NL [B (g/L)]	Log NL [Li (g/L)]	Log NL [Na (g/L)]	Log NL [P (g/L)]	Log NL [Si (g/L)]	Log NL [Zr (g/L)]
Phase 1a	ARM	ARM-A	-0.7533	-0.2807	-0.2049	-0.2643	-0.3312	-0.5403	-2.0428
Phase 1a	ARM	ARM-B	-0.7758	-0.2493	-0.2096	-0.2672	-0.3260	-0.5061	-2.1478
Phase 1a	EA	EA-A	-0.9553	1.1989	0.9851	1.1143	—	0.6186	-0.4543
Phase 1a	EA	EA-B	-0.9422	1.3014	1.0281	1.1722	—	0.6470	-0.7082
Phase 1a	1	IG1-01	-1.2439	0.7420	0.5152	0.6588	0.5085	0.1270	-1.8577
Phase 1a	2	IG1-02	-1.3188	0.8462	0.2438	0.7765	0.2477	-0.0729	—
Phase 1a	3	IG1-03	—	1.6317	1.0835	1.5186	1.6297	0.7108	-2.1332
Phase 1a	4	IG1-04	—	-0.1199	0.2942	0.0783	0.0790	-0.3983	-2.5524
Phase 1a	4*	IG1-04	—	-0.1199	-0.0156	0.0783	0.0790	-0.3983	-2.5524
Phase 1a	5	IG1-05	-1.3195	0.9101	-0.5914	0.6507	0.4277	-0.0959	—
Phase 1a	6	IG1-06	—	1.2842	1.2803	1.2524	—	0.5005	-1.6594
Phase 1a	7	IG1-07	-0.2920	-0.2492	-0.1421	-0.9390	—	-0.2885	-0.3296
Phase 1a	8	IG1-08	-0.6384	-0.4507	-0.2473	-0.1687	-0.1609	-0.5976	-1.9110
Phase 1a	9	IG1-09	-0.5701	0.7580	0.3470	0.6613	0.5013	-0.3021	-1.8751
Phase 1a	10	IG1-10	—	1.4676	1.3286	1.2793	—	1.0519	-2.1919
Phase 1a	11	IG1-11	-0.2846	-0.2365	-0.1198	0.2728	—	-0.2476	—
Phase 1a	12	IG1-12	-1.0030	0.9642	—	0.9037	—	-0.5081	-1.9313
Phase 1a	13	IG1-13	-0.1531	1.7737	1.6672	1.7687	—	1.6036	—
Phase 1a	14	IG1-14	-0.4438	-0.0025	-0.2452	0.1146	-0.6377	-0.4100	-1.9123
Phase 1a	15	IG1-15	-0.8582	-0.0066	-0.1019	0.0672	-0.0780	-0.3912	-1.9223
Phase 1a	16	IG1-16	-0.5430	-0.1518	-0.3653	0.0753	-0.3762	-0.5042	-2.4391
Phase 1a	17	IG1-17	-0.6563	-0.3935	-0.8839	-0.1741	-0.5190	-0.6253	-2.2830
Phase 1a	18	IG1-18	-0.6686	-0.2002	-0.2415	-0.1517	-0.2036	-0.5671	-1.7613
Phase 1a	19	IG1-19	-0.6762	-0.2530	-0.2999	-0.1897	-0.2360	-0.6032	-1.5535
Phase 1a	20	IG1-20	-0.7020	-0.2978	-0.3573	-0.2491	-0.2986	-0.6595	-2.2707

Table 12. (continued).

Test	Short ID	ID	Log NL [Al (g/L)]	Log NL [B (g/L)]	Log NL [Li (g/L)]	Log NL [Na (g/L)]	Log NL [P (g/L)]	Log NL [Si (g/L)]	Log NL [Zr (g/L)]
Phase 1a	21	IG1-21	-0.5408	0.2491	0.1680	0.1695	-0.3778	-0.5859	-2.0794
Phase 1a	22	IG1-22	-0.6085	-0.1035	-0.3519	-0.1017	-0.2958	-0.5893	-1.5841
Phase 1a	23	IG1-23	-0.6778	-0.4555	-0.3834	-0.1829	-0.2665	-0.6488	-1.6510
Phase 1a	24	IG1-24	-0.5837	0.3183	0.1597	0.1766	-0.2750	-0.5754	-2.0648
Phase 1a	25	IG1-25	-0.5463	-0.0463	-0.0955	0.1015	-0.3742	-0.5391	-2.4989
Phase 1a	26	IG1-26	-1.1392	0.7945	0.5595	0.6978	0.5516	0.1574	-1.8577
Phase 1a	27	IG1-27	-0.6485	-0.5208	-0.2315	-0.1715	-0.1737	-0.6269	-1.3039
Phase 1a	28	IG1-28	-0.6442	-0.4508	-0.2021	-0.1470	-0.1172	-0.5873	-2.4405
Phase 1a	29	IG1-29	-0.3686	-0.3450	-0.1471	-0.4574	0.4341	-0.3876	—
Phase 1a	30	IG1-30	-0.4547	1.3853	1.2125	1.2541	0.7917	0.8360	-2.0915
Phase 1b	ARM	ARM	-0.7314	-0.2106	-0.1716	-0.2285	-0.4849	-0.4886	-2.3007
Phase 1b	ARM	ARM	-0.7828	-0.2839	-0.1556	-0.2075	-0.3918	-0.5036	-2.3007
Phase 1b	EA	EA1	-0.8375	1.1054	0.8704	1.0063	—	0.5352	-0.7082
Phase 1b	EA	EA2	-1.0701	1.1776	0.9768	1.1197	—	0.5805	-0.7082
Phase 1b	31	IG1-31	-0.2913	0.4810	0.4054	0.1955	—	-0.2764	-0.3800
Phase 1b	32	IG1-32	-0.5438	-0.4123	-0.2390	-0.2708	-0.1956	-0.5228	—
Phase 1b	33	IG1-33	—	1.0668	1.2866	1.3275	—	0.9330	-2.1916
Phase 1b	34	IG1-34	—	0.0348	0.0348	-0.6239	-0.0382	-0.2893	-2.6502
Phase 1b	35	IG1-35	-0.5371	-0.0572	1.5658	-0.1468	-0.7303	-0.5183	—
Phase 1b	36	IG1-36	-0.4517	1.2484	1.2546	1.2523	—	0.9670	—
Phase 1b	37	IG1-37	-1.1926	1.1932	-0.9790	1.1052	0.8784	-0.0147	-1.9257
Phase 1b	38	IG1-38	-1.4745	0.3888	0.3459	0.1690	0.3665	-0.2011	-3.0666
Phase 1b	39	IG1-39	-0.4857	0.5305	0.4462	0.3344	-0.3947	-0.4695	-2.6711
Phase 1b	40	IG1-40	-1.2391	0.9161	0.7542	0.8607	-0.0368	0.3326	-1.5895
Phase 1b	40*	IG1-40	-1.2391	0.9161	0.7542	0.8607	-0.0368	0.5184	-1.5895
Phase 1b	41	IG1-41	-1.2120	1.6065	1.2140	1.5267	0.7300	1.1028	-1.5895
Phase 1b	42	IG1-42	-0.5959	-0.3952	-0.2777	-0.2125	-0.3774	-0.5986	-2.1897
Phase 1b	43	IG1-43	-0.6487	0.1607	-0.1497	0.0431	-0.5038	-0.6217	-2.7523
Phase 1b	44	IG1-44	—	0.0646	0.0586	-0.6007	-0.0220	-0.2608	-2.4003

4* Outlying Li concentration of one triplicate excluded from calculation.
40* Outlying phosphate concentration of one triplicate excluded from calculation.

5.4 Viscosity Profile Determinations

Viscosity measurements were made on glasses over the range of 950°C to 1250°C according to the procedure described in Section 4. Table 13 contains the raw η data for the test glasses. Glass η – T data were fitted to the Vogel-Tamman-Fulcher (VTF) model (1), although it was observed that the coefficients A, B, and T_0 could not be uniquely determined for most glasses tested. The data was also fitted to the Arrhenius model (2):

$$\ln\eta = A + \frac{B}{T - T_0}, \tag{1}$$

$$\ln\eta = E + \frac{F}{T}, \tag{2}$$

where A, B, E, F, and T_0 are temperature independent coefficients and T is temperature (absolute temperature in Equation 2). Occasionally data points were omitted from the VTF and Arrhenius fits in-order to obtain lower standard error on the coefficients (A, B, E, F, and T_0). The omitted points are listed in Table 13 with a line draw through them. These data were influenced by crystallization, phase separation, or volatility in each of the glasses during measurement. In fact glasses IG1-8, -19, -27, -28, and-33 were inhomogeneous because of phase separation and/or crystallinity which formed on air quenching. Glass IG1-33 required melting at 1450°C to yield an optically homogeneous product on air quenching, and its T_L was determined to be 1310°C. The impact of data point removal is best described with an example. Figure 13 shows the η-T data from IG1-27 fitted to a VTF model with all data. Figure 14 shows the η-T data from IG1-27 fitted to a VTF model with four data points removed. It is clear by comparing the two figures that the latter fit yields a model that better estimates actual η-T behavior of the glass. The errors associated with each coefficient are far lower in the latter fit. For glasses IG1-08, -19, -27, -28, and –33, the Arrhenius and VTF fits are poor and should not be considered reliable glass viscosity data. These glasses are marked in Table 13 with an asterisk on the glass number.

Table 14 shows the fitted coefficients (A, B, F, and T_0). It is assumed that the melter of the proposed INTEC vitrification plant will operate at 1150°C. Therefore, the viscosity at 1150°C (η_{1150}) was calculated for each test glass using the VTF model. This value is within the viscosity range of 2 to 10 Pa s which appears most suitable based on waste glass melter operating experience. In addition, the temperature at a glass viscosity of 5 Pa s, (T_0) was calculated using the VTF model. The η_{1150} and T_0 values for Phase 1 test glasses are also listed in Table 14.

Table 13. Viscosities calculated from temperatures (°C) measured by viscometer furnace thermocouple.

Sample No.	Measured Viscosity (Pa s) at Sample Temperature (°C)									
IG1-01										
Temp (C)	1160.0	1105.8	1055.1	1108.0	1158.7	1206.5	1255.2	1153.4	1005.5	956.0
η (Pa s)	3.8.	6.22	10.32	6.42	3.99	2.69	1.87	4.23	19.20	36.53
IG1-02*										
Temp (C)	1162.2	1109.3	1058.4	1109.5	1158.7	1207.9	1255.9	1156.3	1008.0	—
η (Pa s)	1.70	2.6.	4.23	2.68.	1.85	1.32	0.96	1.92	8.10	—
IG1-06										
Temp (C)	1156.1	1105.9	1056.0	1107.9	1157.5	1206.1	1255.3	1155.2	1006.7	957.2
η (Pa s)	6.66	11.21	20.00	10.93	6.60	4.27	2.89	6.98	39.19	83.12
IG1-07										
Temp (C)	1159.5	1106.6	1055.6	1107.6	1158.0	1206.1	1254.9	1154.4	1005.9	955.9
η (Pa s)	8.76	13.83	22.59	13.61	8.86	6.10	4.31	9.22	39.25	72.99
IG1-08*										
Temp (C)	1159.0	1107.9	—	—	1158.6	1207.2	1256.0	1156.2	—	—
η (Pa s)	13.18	27.35	—	—	12.48	8.14	5.31	13.76	—	—
IG1-09*										
Temp (C)	1155.9	1105.5	1055.6	1105.9	1155.2	1204.1	1252.9	1154.6	1006.0	956.9
η (Pa s)	1.64	2.70	4.77	2.71	1.65	1.06	.0.72	1.69	9.31	19.38
IG1-10										
Temp (C)	1159.1	1106.4	1055.8	1107.3	1157.0	1206.1	1256.0	1155.0	1006.1	956.8
η (Pa s)	2.68	4.47	7.70	4.38	2.71	1.75	1.17	2.77	14.07	27.35
IG1-11										
Temp (C)	1158.6	1105.4	1055.4	1107.2	1156.6	1205.8	1254.7	1154.0	1006.1	956.6
η (Pa s)	11.19	17.35	27.25	16.99	11.34	7.83	5.54	11.80	45.23	78.54
IG1-12										
Temp (C)	1158.7	1108.0	1057.9	1109.5	1158.8	1207.6	1255.8	1156.2	1007.9	958.6
η (Pa s)	5.67	10.80	21.25	10.59	5.77	3.29	1.97	6.58	50.70	120.84

Table 13. (continued).

Sample No.	Measured Viscosity (Pa s) at Sample Temperature (°C)									
IG1-13										
Temp (C)	1156.0	1105.1	1055.0	1105.3	1154.8	1204.0	1253.1	1154.1	1005.2	956.1
η (Pa s)	2.33	3.35	4.94	3.36	2.37	1.72	1.27	2.42	7.69	12.12
IG1-14										
Temp (C)	1157.6	1106.6	1056.3	1106.7	1156.2	1205.2	1254.2	1155.4	1006.4	957.0
η (Pa s)	7.18	11.30	18.29	11.30	7.34	4.99	3.49	7.51	31.97	57.77
IG1-16										
Temp (C)	1162.1	1109.0	1058.4	1109.5	1158.8	1207.7	1256.4	1156.6	1008.1	958.9
η (Pa s)	7.05	12.03	21.33	11.97	7.28	4.67	3.14	7.48	40.40	80.74
IG1-17*										
Temp (C)	1159.9	1107.4	1056.5	1107.6	1157.1	1206.2	1255.2	1155.4	1006.5	957.2
η (Pa s)	7.25	12.77	23.31	12.61	7.63	4.75	3.10	7.76	47.37	100.39
IG1-19*										
Temp (C)	1160.8	1108.5	1057.6	1108.9	1158.3	1207.1	1255.8	1156.1	—	—
η (Pa s)	7.23	11.95	21.06	11.94	7.42	4.93	3.43	7.74	—	—
IG1-21										
Temp (C)	1158.0	1105.8	1055.4	1107.9	1157.3	1206.1	1255.0	1154.8	1005.9	956.7
η (Pa s)	3.24	5.20	8.62	5.06	3.26	2.20	1.54	3.37	15.16	28.39
IG1-23*										
Temp (C)	1158.0	1107.0	1056.8	1107.2	1156.5	1205.5	1254.4	1155.7	—	—
η (Pa s)	6.88	11.53	20.36	11.55	7.01	4.52	3.00	7.19	—	—
IG1-24										
Temp (C)	1162.4	1109.8	1059.0	1110.2	1159.5	1208.3	1256.9	1157.3	1008.7	959.6
η (Pa s)	3.06	4.78	7.79	4.76	3.14	2.17	1.57	3.29	14.23	26.37
IG1-25										
Temp (C)	1159.6	1107.2	1056.5	1107.9	1157.4	1206.3	1255.1	1155.3	1006.5	957.3
η (Pa s)	5.92	10.09	17.80	10.00	6.12	3.92	2.60	6.33	34.28	68.32

Table 13. (continued).

Sample No.	Measured Viscosity (Pa s) at Sample Temperature (°C)									
IG1-26										
Temp (C)	1158.0	1107.0	1057.1	1107.1	1156.9	1206.0	1255.0	1156.2	1007.0	957.6
η (Pa s)	3.78	6.03	10.01	6.06	3.86	2.59	1.79	3.94	18.25	34.67
IG1-27*										
Temp (C)	1159.9	1109.0	1158.5	1107.6	—	—	1158.8	1207.5	1256.2	1156.3
η (Pa s)	12.38	25.34	12.54	27.00	—	—	11.91	7.60	5.11	13.36
IG1-28*										
Temp (C)	1158.1	1107.0	—	1106.2	1156.4	1205.4	1254.3	1155.5	—	—
η (Pa s)	12.17	26.29	—	27.59	12.02	7.27	4.92	12.76	—	—
IG1-29										
Temp (C)	1163.2	1110.333	1059.5	1110.9	1160.0	1208.9	1258.0	1158.1	1009.4	960.2
η (Pa s)	11.74	18.22	29.02	18.24	12.13	8.38	6.02	12.45	49.44	86.88
IG1-30										
Temp (C)	1155.3	1104.1	1055.8	1107.4	1157.0	1206.1	1255.2	1155.6	1006.9	957.1
η (Pa s)	1.71	2.55	4.05	2.53	1.72	1.20	0.87	1.73	7.25	13.49
IG1-31										
Temp (C)	1157.3	1106.6	1056.2	1106.7	1156.1	1205.4	1254.2	1155.4	1006.2	956.9
η (Pa s)	1.87	2.70	4.05	2.71	1.89	1.36	1.00	1.90	6.43	10.65
IG1-32*										
Temp (C)	1157.1	1106.1	1055.9	1106.4	1155.8	1204.8	1253.8	1155.0	1006.1	—
η (Pa s)	13.75	21.69	35.77	21.65	13.83	9.23	6.35	14.05	63.75	—
IG1-33*										
Temp (C)	—	—	—	—	—	—	—	—	—	—
η (Pa s)	—	—	—	—	—	—	—	—	—	—
IG1-34*										
Temp (C)	1158.0	1106.9	1056.5	1106.7	1156.1	1205.1	1254.1	1155.2	1006.1	—
η (Pa s)	15.95	29.34	57.34	29.46	16.34	9.70	6.06	16.67	124.10	—

Table 13. (continued).

Sample No.	Measured Viscosity (Pa s) at Sample Temperature (°C)									
IG1-35										
Temp (C)	1158.5	1107.4	1057.1	1107.4	1156.9	1205.8	1254.7	1155.8	1006.8	957.5
η (Pa s)	8.25	13.59	23.86	13.66	8.54	5.66	3.94	8.86	48.16	101.63
IG1-36										
Temp (C)	1155.9	1106.0	1056.1	1106.7	1156.1	1205.3	1254.2	1155.4	1006.4	957.1
η (Pa s)	3.25	4.66	6.98	4.64	3.23	2.31	1.68	3.27	10.99	17.74
IG1-37										
Temp (C)	1157.5	1106.8	1056.7	1107.0	1156.5	1205.5	1254.4	1155.6	1006.7	957.6
η (Pa s)	5.45	8.81	14.75	8.80	5.58	3.68	2.51	5.70	26.90	51.17
IG1-38										
Temp (C)	1157.5	1106.7	1056.4	1106.6	1156.1	1205.2	1254.2	1155.3	1006.3	956.9
η (Pa s)	6.74	11.31	20.03	11.34	6.89	4.42	2.96	7.03	38.39	78.91
IG1-39										
Temp (C)	1159.2	1107.7	1057.1	1107.4	1156.7	1205.6	1254.4	1155.5	1006.6	957.3
η (Pa s)	2.62	4.17	6.92	4.20	2.70	1.81	1.25	2.73	12.48	23.35
IG1-40										
Temp (C)	1157.9	1106.7	1056.5	1107.0	1156.5	1205.5	1254.4	1155.6	1006.8	957.4
η (Pa s)	6.92	1109	18.48	11.12	7.17	4.83	3.36	7.31	34.26	65.23
IG1-41										
Temp (C)	1158.0	1106.9	1056.5	1106.9	1156.2	1205.3	1254.1	1155.2	1006.3	956.9
η (Pa s)	7.16	11.32	18.64	11.39	7.34	4.95	3.45	7.57	33.42	62.31
IG1-42										
Temp (C)	1158.6	1107.2	1056.7	1107.2	1156.6	1205.5	1254.5	1155.5	1006.7	957.5
η (Pa s)	7.60	12.51	21.47	12.57	7.80	5.11	3.45	7.97	39.82	76.91
IG1-43										
Temp (C)	1159.7	1107.2	1057.1	1107.8	1157.7	1206.2	1255.2	1155.5	1006.3	958.8
η (Pa s)	6.82	11.98	21.86	11.89	7.08	4.47	2.94	7.39	43.86	92.76

Table 13. (continued).

Sample No.	Measured Viscosity (Pa s) at Sample Temperature (°C)									
IG1-44*										
Temp (C)	1158.9	1107.5	1057.0	1107.3	1156.6	1205.5	1254.4	1155.5	1006.5	—
η (Pa s)	15.43	28.44	55.43	28.61	15.92	9.42	5.88	16.16	119.96	—

* Glass is phase separated and data fitted model poorly.

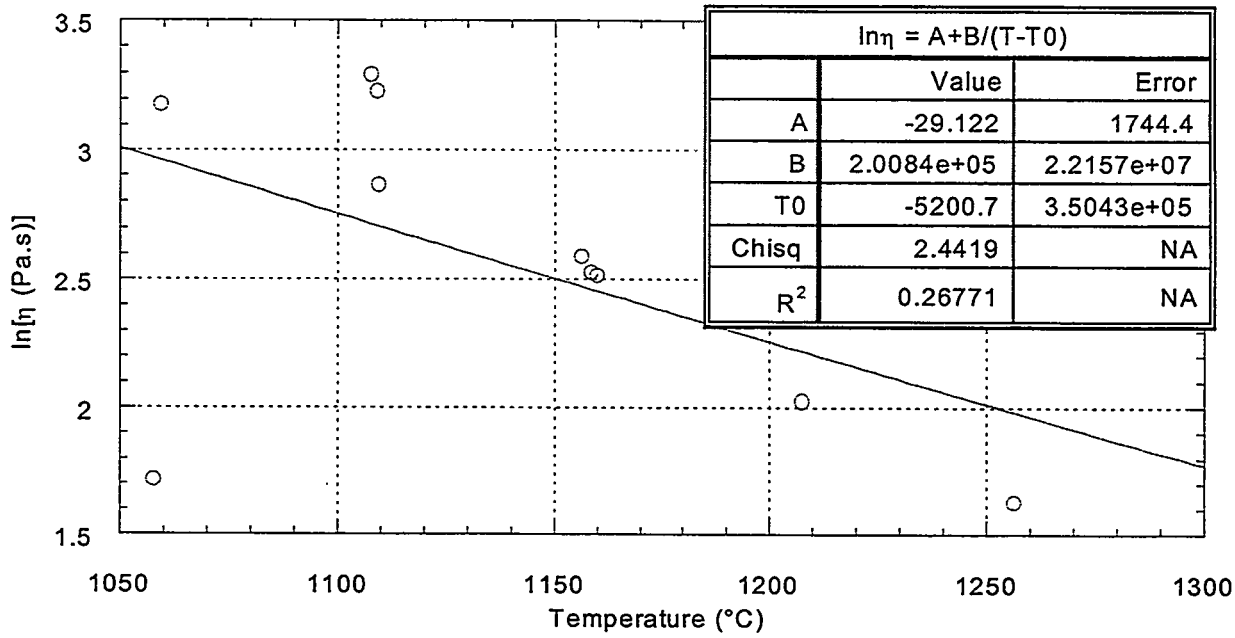

Figure 13. VTF equation fit to IG1-27 glass with all data.

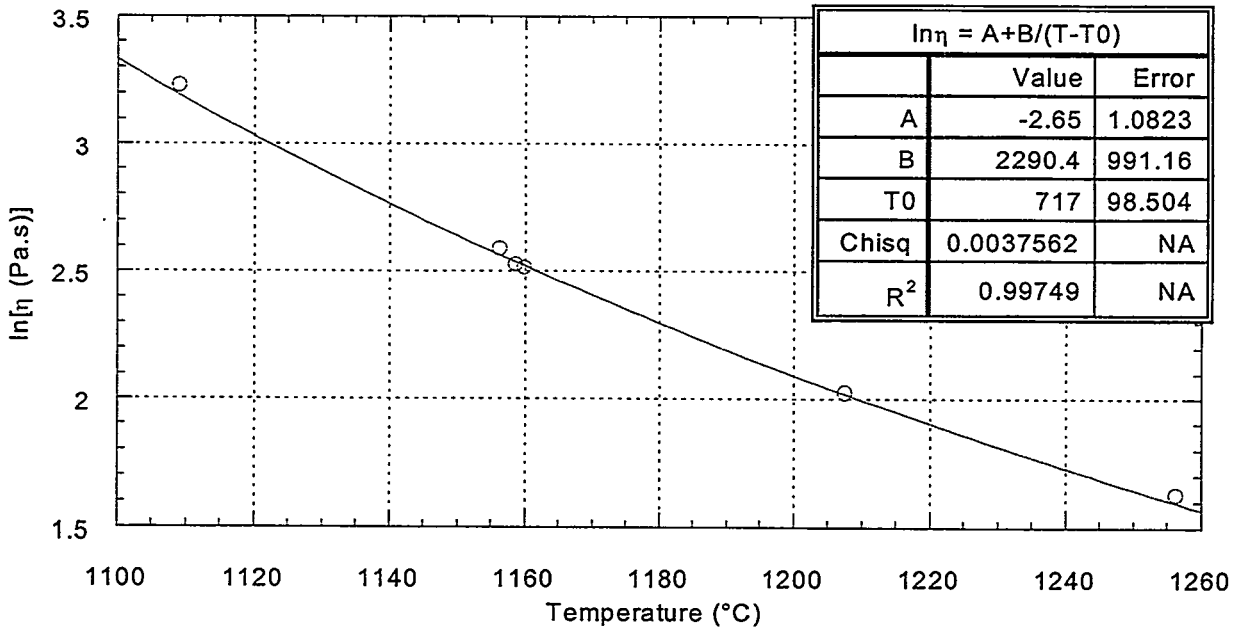

Figure 14. VTF equation fit to IG1-27 glass with four data points removed.

Table 14. Viscosity at 1150°C using Fulcher equation model.

Sample ID	A	B (K)	T_0 (°C)	Pa-sec	Poise
IG1-01	-5.8791	6252.6	296.52	4.25	42.5
IG1-02	-3.5888	2400.8	584.24	1.92	19.2
IG1-03	—	—	—	—	—
IG1-04	—	—	—	—	—
IG1-05	—	—	—	—	—
IG1-06	-5.9344	6419	337.53	7.14	71.4
IG1-07	-5.061	6470.2	264.42	9.44	94.4
IG1-08	-1.1538	1153.3	849.2	14.59	145.9
IG1-09	-7.0245	6030	353.72	1.73	17.3
IG1-10	-7.3343	7607.1	242.89	2.86	28.6
IG1-11	-4.8207	6807	216.48	11.83	118.3
IG1-12	-9.6209	10796	209.54	6.41	64.1
IG1-13	-5.5947	6261.9	183.91	2.43	24.3
IG1-14	-5.3455	6601.5	255.8	7.67	76.7
IG1-15	—	—	—	—	—
IG1-16	-5.9717	6781.3	305.43	7.83	78.3
IG1-17	-6.0772	6626.8	338.08	8.04	80.4
IG1-18	—	—	—	—	—
IG1-19	-5.4745	6233.2	325.58	8.05	80.5
IG1-20	—	—	—	—	—
IG1-21	-6.1136	6360	285.07	3.45	34.5
IG1-22	—	—	—	—	—
IG1-23	-5.8418	6380.9	337.04	7.44	74.4
IG1-24	-5.7323	5834.4	311.32	3.40	34.0
IG1-25	-6.1325	6734.2	307.96	6.46	64.6
IG1-26	-5.9698	6285.1	297.72	4.07	40.7
IG1-27	-1.2374	1166.9	848.61	13.93	139.3
IG1-28	-1.8747	1522.3	811.08	13.69	136.9
IG1-29	-4.6669	6594.3	238.87	13.07	130.7
IG1-30	-5.0111	4049.1	425.74	1.79	17.9
IG1-31	-5.816	6034.3	220.07	1.96	19.6

Table 14. (continued).

Sample ID	A	B (K)	T_0 (°C)	Pa-sec	Poise
IG1-32	-4.9198	6656.4	273.09	14.45	144.5
IG1-33	—	—	—	—	—
IG1-34	-5.8934	6799.9	373.14	17.46	174.6
IG1-35	-5.1402	5750.5	366.4	9.01	90.1
IG1-36	-5.5219	6460.8	189.34	3.33	33.3
IG1-37	-5.849	6571.6	286.65	5.83	58.3
IG1-38	-5.9294	6569.3	319.64	7.26	72.6
IG1-39	-6.3307	6346.2	288.7	2.82	28.2
IG1-40	-5.2199	6054.7	313.58	7.53	75.3
IG1-41	-5.3757	6490.9	274.82	7.70	77.0
IG1-42	-5.7084	6720.2	289.77	8.20	82.0
IG1-43	-6.0533	6513.7	343.86	7.59	75.9
IG1-44	-5.9383	6830.5	371.37	17.02	170.2

6. INEEL HIGH LEVEL WASTE COMPOSITIONS

In FY98, the CVS Phase 1 test matrix was designed and tested utilizing the April, 1997, HAW composition estimates (see Table 15). These estimates were at that time (October 1997), the most accurate estimates available. Development of the pretreatment processes and characterization of INEEL wastes continued while laboratory tests were being performed for completing Phase 1 of the CVS. The results from these development and characterization activities have been collected, analyzed, and entered in FY99 into an integrated flowsheet database. The result is improved composition estimates for calcine, SBW, and HAWs.

Table 15. April 1997 HAW—mass balance compositions.

	Al-HAW (wt %)	Al-Solids (wt %)	Zr-HAW (wt %)	Zr-Solids (wt %)	SBW-HAW (wt %)	SBW-Solids (wt %)	IEX Resins (wt %)	All-Blend (wt %)
Al_2O_3	1.09	100.00	0.01	38.00	0.16	100.00	0.00	8.9
BaO	0.00	0.00	0.00	0.00	0.31	0.00	0.00	0.02
CaO	0.00	0.00	0.02	9.30	0.01	0.00	0.00	0.45
Cs_2O	15.46	0.00	0.28	0.00	0.45	0.00	0.00	0.5
CuO	0.00	0.00	0.00	0.00	0.00	0.00	31.98	0.36
Fe_2O_3	0.16	0.00	0.02	0.00	0.16	0.00	21.40	0.26
Gd_2O_3	0.00	0.00	0.45	0.00	0.00	0.00	0.00	0.36
K_2O	50.25	0.00	2.76	0.00	63.55	0.00	12.62	6.29
MoO_3	0.00	0.00	0.00	0.00	0.92	0.00	0.00	0.05
Na_2O	0.03	0.00	0.00	0.00	0.00	0.00	0.00	0
P_2O_5	25.24	0.00	1.39	0.00	28.59	0.00	0.00	2.93
PbO	0.00	0.00	0.00	0.00	0.25	0.00	0.00	0.01
SiO_2	0.00	0.00	0.00	0.00	0.00	0.00	34.00	0.38
SrO	2.48	0.00	0.05	0.00	0.01	0.00	0.00	0.08
$TRUO_2$	5.29	0.00	0.14	0.00	2.63	0.00	0.00	0.33
ZrO_2	0.00	0.00	94.89	52.70	2.96	0.00	0.00	79.09
Total	100.00	100.00	100.01	100.00	100.00	100.00	100.00	100.00
Total KG	2933.00	0.876	146,761.00	8483.00	8889.00	12,929.00	1724.40	181,720.00
wt %	1.61%	0.001%	80.76%	4.67%	4.89%	7.11%	0.95%	—

Table 16 includes the high, medium, and low range compositions of the 1999 estimates for the HAWs. These fractions are the SBW-HAW, Zr-HAW, Al-HAW, and Total HAW. They result from the dissolution of calcine and separation of radioactive elements from dissolved calcine and liquid sodium bearing waste. The HAW fraction consists of radioactive elements, undissolved solids, and ion exchange resins used in the pretreatment processes. Comparison of the 1999 HAW composition estimates to those calculated in 1997 indicates an increase of phosphorous and fluorine. The results of the CCC test suggest that about 1.25 wt % may be the upper phosphate content limit for a homogeneous HAW glass. This phosphate content limit results in a 2.5 wt % waste loading in glasses formulated with the FY99 HAW composition estimates. This waste loading would produce about 4000 m^3 of HAW glass, nearly six times the 700 m^3 volume projected from the FY97 HAW composition estimates. Per review of these glass volumes and the 1999 HAW compositions, pretreatment personnel are currently identifying modifications to the separations flow sheet that significantly reduce the amounts of fluorine and phosphate. The goal of these modifications is to decrease the total high level waste volume to the targeted 700 cubic meters. However, the current pretreatment flowsheet is not considered feasible at this time, therefore INEEL management recommends that glass formulation and process development activities be redirected to direct vitrification of the calcine and liquid SBW.

Table 16. 1999 Estimates of the high activity waste fraction.

	Low Kg	Expected Kg	High Kg	Low wt %	Expected wt %	High wt %
			Range of Compositions for Sodium Bearing Waste			
Al	234.4	234.9	241.5	1.68	1.17	0.95
B	388.2	388.2	388.2	2.79	1.94	1.53
Ba	7.3	10.6	14.6	0.05	0.05	0.06
Ca	118.4	118.4	119.1	0.85	0.59	0.47
Cd + Ni	211.1	211.1	211.1	1.52	1.05	0.83
Ce + TRU	19.0	19.0	19.0	0.14	0.09	0.08
Cl	361.8	361.8	361.8	2.60	1.81	1.43
Cr	29.9	29.9	29.9	0.21	0.15	0.12
Cs	13.5	13.5	13.5	0.10	0.07	0.05
Cu	21.0	21.0	21.0	0.15	0.10	0.08
F	346.1	346.1	346.1	2.49	1.73	1.37
Fe	326.7	334.2	490.3	2.35	1.67	1.94
K	914.9	2475.1	3741.3	6.57	12.36	14.78
Li	21.0	21.0	21.0	0.15	0.10	0.08
Mg	210.0	210.0	210.0	1.51	1.05	0.83
Mn	50.6	50.6	50.6	0.36	0.25	0.20
Mo	738.7	768.3	768.4	5.31	3.84	3.04
Na	925.5	2220.8	3397.8	6.65	11.09	13.43
Nb	20.1	20.1	20.1	0.14	0.10	0.08

Table 16. (continued).

	Low Kg	Expected Kg	High Kg	Low wt %	Expected wt %	High wt %
Nd	21.9	21.9	21.9	0.16	0.11	0.09
Pb	51.5	82.5	83.2	0.37	0.41	0.33
Pd	12.6	12.6	12.6	0.09	0.06	0.05
Pr	6.0	6.0	6.0	0.04	0.03	0.02
PO_4	4946.6	4946.6	4946.6	35.52	24.70	19.55
Rh	21.0	21.0	21.0	0.15	0.10	0.08
Ru	210.0	210.0	210.0	1.51	1.05	0.83
Si	531.3	531.3	531.3	3.82	2.65	2.10
Sm	3.9	3.9	3.9	0.03	0.02	0.02
Sn	105.0	105.0	105.0	0.75	0.52	0.41
Sr	6.6	6.6	6.6	0.05	0.03	0.03
SO_4	1919.6	1919.6	1919.6	13.79	9.59	7.59
Tc	1.1	1.1	1.1	0.01	0.01	0.00
Ti	21.0	21.0	21.0	0.15	0.10	0.08
Zn	21.0	21.0	21.0	0.15	0.10	0.08
Zr	1087.8	4258.9	6930.8	7.81	21.27	27.39
Total	13,925	20,023	25,307	100.00	100.00	200.00
			Range of Compositions for Alumina Calcine – Binset 1			
Al	1,903.3	1,903.3	1,912.9	24.54	24.45	24.30
B	10.0	10.0	10.0	0.13	0.13	0.13
Ba	1.5	1.5	1.5	0.02	0.02	0.02
Ce + TRU	80.9	80.9	80.9	1.04	1.04	1.03
Cl	25.2	25.2	25.2	0.32	0.32	0.32
Cs	82.3	82.3	82.3	1.06	1.06	1.05
Eu	2.0	2.0	2.0	0.03	0.03	0.03
Fe	34.9	34.9	85.1	0.45	0.45	1.08
Mo	826.9	838.0	838.0	10.66	10.77	10.65
Na	288.9	288.9	315.5	3.73	3.71	4.01
Nd	137.5	137.5	137.5	1.77	1.77	1.75
Pr	38.1	38.1	38.1	0.49	0.49	0.48
PO_4	4,225.4	4,225.4	4,225.4	54.48	54.28	53.68
Ru	1.1	1.1	1.1	0.01	0.01	0.01
Sm	26.7	26.7	26.7	0.34	0.34	0.34
SO_4	17.0	17.0	17.0	0.22	0.22	0.22
Sr	47.3	47.3	47.3	0.61	0.61	0.60

Table 16. (continued).

	Low Kg	Expected Kg	High Kg	Low wt %	Expected wt %	High wt %
Tc	5.0	5.0	5.0	0.06	0.06	0.06
Zr	1.5	19.0	19.7	0.02	0.24	0.25
Total	7,756	7,784	7,871	100.00	100.00	100.00
			Range of Compositions for Zirconia Calcine			
Al	1351.0	1351.3	1357.0	3.85	3.67	3.52
B	124.7	124.7	124.7	0.36	0.34	0.32
Ba	17.1	59.2	60.4	0.05	0.16	0.16
Ca	3905.1	3906.1	3922.7	11.12	10.61	10.18
Ce+TRU	90.5	90.5	90.5	0.26	0.25	0.23
Cl	13.9	13.9	13.9	0.04	0.04	0.04
Cr	33.8	33.8	33.8	0.10	0.09	0.09
Cs	113.6	113.6	113.6	0.32	0.31	0.29
F	8156.1	8156.1	8156.1	23.23	22.15	21.16
Fe	75.1	110.4	183.3	0.21	0.30	0.48
Gd	1.7	1.9	1.9	0.00	0.01	0.00
K	119.6	247.7	358.7	0.34	0.67	0.93
Mg	36.4	36.4	36.4	0.10	0.10	0.09
Mo	1778.2	1781.1	1781.1	5.06	4.84	4.62
Na	810.2	2301.8	932.8	2.31	6.25	2.42
Nd	142.5	142.5	142.5	0.41	0.39	0.37
Ni	11.4	11.4	11.4	0.03	0.03	0.03
Pb	5.2	5.7	5.8	0.01	0.02	0.02
PO_4	14231.0	14231.0	14231.0	40.52	38.65	36.92
Pr	38.2	38.2	38.2	0.11	0.10	0.10
Sm	17.1	17.1	17.1	0.05	0.05	0.04
Sn	30.7	30.7	30.7	0.09	0.08	0.08
Sr	2055.8	2055.8	2055.8	5.85	5.58	5.33
SO_4	16.1	16.1	16.1	0.05	0.04	0.04
Tc	6.3	6.3	6.3	0.02	0.02	0.02
Zr	1936.1	1936.1	4821.6	5.51	5.26	12.51
Total kg	35,118	36,819	38,543	100.00	100.00	100.00

Table 16. (continued).

	Low Kg	Expected Kg	High Kg	Low wt %	Expected wt %	High wt %
			Range of Composition for the total calcine case			
Al	19422.7	19427.7	19510.0	6.92	6.60	6.44
B	840.8	840.8	840.8	0.30	0.29	0.28
Ba	143.4	495.0	504.8	0.05	0.17	0.17
Ca	23904.6	23910.8	24012.1	8.52	8.12	7.92
Ce+TRU	717.3	717.3	717.3	0.26	0.24	0.24
Cl	117.3	117.3	117.3	0.04	0.04	0.04
Cr	185.1	185.1	185.1	0.07	0.06	0.06
Cs	825.5	825.5	825.5	0.29	0.28	0.27
F	62282.6	62282.6	62282.6	22.20	21.14	20.55
Fe	467.5	686.8	1140.2	0.17	0.23	0.38
K	1069.6	2216.0	3208.8	0.38	0.75	1.06
Mg	562.0	562.0	562.0	0.20	0.19	0.19
Mo	16108.0	16160.1	16160.1	5.74	5.49	5.33
Na	7453.7	19753.4	8668.7	2.66	6.71	2.86
Nb	63.2	63.2	63.2	0.02	0.02	0.02
Nd	1066.1	1066.1	1066.1	0.38	0.36	0.35
Ni+Cd	1047.9	1047.9	1047.9	0.37	0.36	0.35
Pb	32.5	35.3	36.0	0.01	0.01	0.01
PO_4	117868.5	117868.5	117868.5	42.02	40.01	38.90
Pr	290.7	290.7	290.7	0.10	0.10	0.10
Sm	143.0	143.0	143.0	0.05	0.05	0.05
Sn	190.1	190.1	190.1	0.07	0.06	0.06
Sr	12542.2	12542.2	12542.2	4.47	4.26	4.14
SO_4	1099.5	1099.5	1099.5	0.39	0.37	0.36
Tc	41.8	41.8	41.8	0.01	0.01	0.01
Zr	12004.3	12004.3	29895.1	4.28	4.08	9.87
Total kg	280,490	294,573	303,019	100.00	100.00	100.00

Table 17 includes the estimates of the calcine compositions per binset and liquid SBW compositions after evaporation. Binset 1 can be defined as alumina calcine, binset 4 as zirconia calcine, and binsets 2, 3, 5, and 6 as total calcine. The SBW compositions given do not include newly generated liquid wastes. These compositions are being used in Phase 2a and Phase 2b of the CVS for generating glasses for the direct vitrification of calcines and SBW. Phase 2a is a small test matrix (6-10 glasses) that was designed and tested to provide data for the integration of the Phase 1 and Phase 2 test matrices.

Table 17. 1999 Composition estimates of the calcine and liquid sodium bearing waste.

Element	Binset #1	Binset #2	Binset #3	Binset #4	Binset #5	Binset #6	SBW
Al	89.56	35.17	14.56	12.69	14.84	51.65	20.20
B	0.47	0.80	1.06	1.17	1.20	0.92	0.28
Ba	0.07	0.02	0.01	0.01	0.01	0.01	0.00
Ca	0.00	24.45	32.83	36.67	33.19	15.84	2.22
Ce	0.08	0.02	0.01	0.02	0.02	0.01	0.00
Cl	0.00	0.00	0.05	0.13	0.19	0.28	1.45
Cr	0.00	0.20	0.27	0.32	0.17	0.27	0.24
Cs	0.06	0.02	0.01	0.02	0.01	0.01	0.00
F	0.00	21.28	26.81	25.86	21.97	7.43	1.36
Fe	1.58	0.17	0.30	0.69	0.70	1.31	1.51
I	0.00	0.00	0.00	0.00	0.00	0.01	0.02
K	0.00	0.18	0.25	0.56	0.90	2.50	9.17
La	0.04	0.01	0.01	0.01	0.01	0.01	0.00
Mg	0.00	0.71	0.83	0.34	0.62	1.12	0.05
Mn	0.00	0.00	0.03	0.00	0.03	0.10	0.84
Mo	0.10	0.03	0.01	0.01	0.01	0.01	0.12
Na	2.48	0.86	1.27	2.30	4.47	9.53	51.84
Nb	0.00	0.00	0.01	0.01	0.28	0.01	0.00
Nd	0.13	0.04	0.02	0.03	0.03	0.02	0.00
Ni	0.00	0.06	0.08	0.11	4.00	1.75	0.60
Pb	0.00	0.00	0.00	0.00	0.00	0.00	0.40
Pd	0.01	0.00	0.00	0.00	0.00	0.00	0.00
PO_4	2.02	0.43	1.25	0.09	0.24	0.54	2.23
Pr	0.04	0.01	0.01	0.01	0.01	0.01	0.00
Rb	0.01	0.00	0.00	0.00	0.00	0.00	0.00
Rh	0.01	0.00	0.00	0.00	0.00	0.00	0.00
Ru	0.05	0.01	0.00	0.00	0.01	0.01	0.05

Table 17. (continued).

Element	Binset #1	Binset #2	Binset #3	Binset #4	Binset #5	Binset #6	SBW
Si	0.00	0.00	0.00	0.00	0.00	0.00	0.12
Sm	0.03	0.01	0.00	0.00	0.00	0.00	0.00
Sn	0.00	0.23	0.30	0.29	0.21	0.07	0.02
SO_4	3.03	0.68	0.65	0.15	2.72	2.19	6.24
Sr	0.04	0.26	0.34	0.39	0.35	0.13	0.00
Tc	0.03	0.01	0.00	0.00	0.01	0.00	0.00
Te	0.01	0.00	0.00	0.00	0.00	0.00	0.00
U	0.02	0.01	0.01	0.01	0.02	0.16	0.00
Y	0.00	0.00	0.01	0.01	0.01	0.00	0.00
Zr	0.14	14.34	19.01	18.12	13.79	4.10	1.03
Total	100.00	100.00	100.00	100.00	100.00	100.00	100.00
Total (kg)	9.71E+04	7.58E+05	1.08E+06	5.02E+05	1.03E+06	3.57E+05	2.76E+05

Estimates of INEEL waste compositions are continuously being improved. Thus a CVS approach is most suitable for addressing vitrification formulation development as the waste compositions change within the bounds of the WCUR. In the near future, the USDOE will release a Record of Decision which will select the treatment option for immobilizing INEEL HLW. After this selection, the CVS will be applied to a waste composition estimate specific to either direct vitrification or HAW separation in order to define glasses for the option chosen.

7. RECOMMENDATIONS

As a result of the observations made in this study, it is apparent that phosphate content in the INTEC HAW has a dominant impact on the tendency of Phases 1a and 1b glasses to phase separate. When phosphate is present in these glasses it also combines with alkali metals to form the major crystalline phases present. Through the formation of the glasses of this study under air quenched and canister centerline cooling rates, it is displayed that phase separation and crystallization in the HAW glasses of significant phosphate content depends also on cooling rate.

All HAW glasses in this CVS were formed under the same processing conditions (four hours at 1150°C and immediate air quenching to form a pour patty). Thus under equivalent conditions of formation, composition appears to determine the tendency of these glasses to phase separate. The phosphate content of the HAW glasses investigated ranges from 0.00% to amounts known to cause phase separation in borosilicate glasses. Other major components changing within the bounds established by the "all blend" HAW composition probably have impacts on T_L, viscosity, phase separation, and on silicate and alkali phosphate crystallization. The evidence for compositional impacts comes from the homogeneity and viscosity observations and T_L investigations of air quenched glasses. Separation and crystallization are visually observed using optical microscopy in some of these glasses having as little as 2.5 wt % phosphate. It was outside the scope of this investigation to quantify or define the limits of compositional interactions, but an investigation of these is of great importance in defining suitable formulations for vitrifying INTEC HAW. The mechanism for effects of phosphate content and the possibility of similar relationships from other major elements on durability, viscosity and T_L must be completed before optimized glasses are defined for vitrifying INTEC HAW.

In a production scenario, glass poured into a disposal canister will be cooled to ambient temperature at a rate as slow as the CCC. Glasses remaining homogeneous when cooled at these slow rates should more easily qualify for repository storage than those that phase separate or devitrify. It is currently assumed that INTEC will submit only homogeneous glasses for repository storage. In order to observe the effects of slower cooling, some homogeneous Phases 1a and 1b glasses containing less than 5 wt % phosphate were cooled at the rate observed at the centerline in a full- scale canister. The major observation of this test was that slower cooling rates significantly promote phase separation and crystallization in the Phases 1a and 1b glasses that appeared homogeneous, through optical and XRD analyses, when air quenched to ambient conditions. Only two of the eight Phases 1a and 1b glasses cooled at canister centerline rates remained homogeneous when subjected to this cooling rate. This observation suggests that a much lower phosphate content may be the upper practical limit than 3-5 wt % for homogeneous INTEC HAW glasses. These results also indicate that a study of the onset of phase separation and alkali oxide phosphate or silicate crystallization in the HAW glasses should also be made as a function of composition (i.e., relative amounts of glass components). The data generated from conducting such studies will provide information for modeling the progress of devitrification as a function of both cooling rate and composition.

Because of the observations of phosphate impact on the properties of glasses formed to date in this study, it is recommended that in Phase 2, the amount of phosphate in the glass products should be in the range of 3-5 wt %. This recommendation assumes that INTEC will convert HAW into homogeneous glass products. The 3-5 wt % phosphate constraint provides opportunity for observing the phase separation boundary limits and the formation of alkali phosphate, silicates or other crystalline phases in glasses cooled at near quench conditions. Refinement of these limits will come after more information is obtained on the relationship of phosphate content to -product characteristics.

Cooling rate influences phase separation and crystalline phase formation in the Phases 1a and 1b glasses. Therefore Phase 2 studies of HAW glasses, must also include observations of the effects of

cooling rates down to the CCC rate on the tendency in HAW glasses for phase separation and crystalline phase formation. More thorough use of TEM analysis should be applied during homogeneity characterization of glasses formed in this phase of the CVS. Information on the effect of cooling rate is required for the development and optimization of processable HAW glasses with good potential for repository storage. It also provides data for the development of generalized models for defining the tendency of a glass to phase separate as functions of cooling rate and composition.

The information provided in Section 6 of this report reveals that more accurate estimates of HAW compositions have been made since the initial estimates were provided in FY97 at the beginning of this CVS. Current estimates given in Section 6 include information on major and minor components not included in the FY97 estimate. It is vital that all components identified as present in the HAWs be included in the surrogates made up for use in future phases of this CVS. Each of these components by themselves, or in combination with others present, could have significant effects on the processability and acceptability for repository storage of the glasses being developed.

Recommendations for other important areas of attention with respect to the four product properties investigated in Phases 1a and 1b of the CVS for INTEC HAW glasses include:

1. Obtaining more data for the definition of primary phase fields of the crystalline species that determine T_L of glasses investigated.

   Much of the information obtained from T_L investigations performed in this study is new and therefore incompletely defines the conditions that result in a given T_L. Lithium phosphate appears to be the most common phase to crystallize below 1150°C from phosphate containing glasses. Certain silicate phases appear frequently at T_L in glasses not containing phosphate. It was outside the scope of this study to define the primary phase fields for these species, but obtaining such information will be required for optimizing glasses for vitrifying INTEC HAW. In some glasses, it appears that more than one primary phase field for crystalline species is encountered near T_L. The determination of the extent of these fields and the number of fields will also require more data.

2. Studying the effects of composition changes on durability.

   The leaching data obtained in this study suggest a relationship between glass composition and leachability. Several composition-durability relationships may be present in the component ranges of the glasses investigated, but more data is required to define these. Defining these relationships will also be needed for optimization of glasses for vitrifying INTEC HAW.

3. Defining the influence of composition on the ability to accommodate phosphate and retain a homogeneous product.

   Information obtained in this CVS suggests a relationship between product homogeneity and phosphate content in the glasses. The results of this study to date have produced indications that other significant component-homogeneity relationships exist in these glasses. Those component-homogeneity relationships which are significant must be defined before INTEC HAW glasses can be optimized.

4. Defining the influence of composition on glass viscosity profile.

Information obtained to date in this CVS reveals that phosphate composition impacts viscosity to the point that high amounts can interfere with profile continuity at lower temperatures. Lithium appears to have the dominant compositional effect on glass viscosity, and its' dominance may mask other compositional effects that could be significant. As with the other characteristics investigated to date, the effects of composition on viscosity profile must be defined before formulation optimization can be performed.

8. REFERENCES

1. 40CFR268, Federal Registrar, Vol. 57, pgs. 22046-22047, May 26, 1992.

2. The INEEL Spent Nuclear Fuel and Environmental Restoration and Waste Management Programs Environmental Impact Statement, DOE\EIS-0203-F, April, 1995.

3. B. A. Staples, et al, "The Preparation and Characterization of INTEC HAW Phase 1 Composition Variation Study Glasses," INEEL/EXT-98-00970, September 1998.

4. G. F. Piepel, J. D. Vienna and P. Hrma, "Phase 1 Experimental Design for the INEEL HLW Glass Composition Variation Study," PNNL-SA-29594, Rev. 1, January, 1998.

5. G. F. Piepel, J. D. Vienna and P. Hrma, "Phase 1 Experimental Design for the INEEL HLW Glass Composition Variation Study," PNNL-SA-29594, Rev. 2, January, 1999.

6. American Society for Testing and Materials, "Standard Test Method for Determining Chemical Durability of Nuclear Waste Glasses, The Product Consistency Test (PCT)," ASTM-C-1285-94, 1994.

7. American Society for Testing and Materials, "Standard Practices for Measurement of Liquidus Temperature of Glass by the Gradient Furnace Method," ASTM C-829-81, 1998.

8. D. K. Peeler, I. A. Reamer, J. D. Vienna and J. V. Crum, "Technical Status Report: Preliminary Glass Formulation Report for the INEEL HAW," WSRC-TR-98-0012, Rev. 1, March, 1998.

9. R. H. Doremus, "Glass Science," John Wiley & Sons, New York, 1973.

10. Waste Acceptance Product Specifications for Vitrified High-Level Waste Forms, Office of Environmental Restoration and Waste Management, U.S. Department of Energy, Washington, DC, February, 1993.

11. "Glass Melting Procedure," GTOP-3-004, Westinghouse Savannah River Company, Savannah River Technology Center, Aiken, SC, 1996.

12. "Laboratory-Scale Glass Preparation Procedure," GTOP-3-016, Westinghouse Savannah River Company, Savannah River Technology Center, Aiken, SC, 1998.

13. S. L. Marra and C. M. Jantzen, "Characterization of Projected DWPF Glasses Heat Treated to Simulate Canister Centerline Cooling (U)," WSRC-TR-92-142, Rev. 1, June, 1993

14. J. D. Vienna, D. K. Peeler, C. M. Jantzen, J. V. Crum and Larry Bruckner, "Standard Test Methods for Determining the Liquidus Temperature (T_L) of Waste and Simulated Waste Glasses," Submitted to ASTM C26.13 for Committee Ballot, 1998.

15. T. B. Edwards, "A Plan for the SRTC Mobile Laboratory to Follow in Analyzing INEEL PCT Solutions," SRT-SCS-98-031, July 6, 1998.

16. T. B. Edwards, "A Plan for the SRTC Mobile Laboratory to Follow in Analyzing INEEL Phase 1b PCT Solutions," SRT-SCS-98-041, August 25, 1998.

17. American Society for Testing and Materials, "Standard Practice for Measuring Viscosity of Glass Above the Softening Point," ASTM C-965-95, 1995.

18. T. B. Edwards, "A Statistical Analysis of the INEEL Phase 1a and 1b PCT Results Based Upon As-Batched Compositions," SRT-SCS-98-0045, August 1998.

Appendix A

X-ray Diffraction Patterns for Air Quenched Glasses and for those Cooled at Canister Centerline Rate

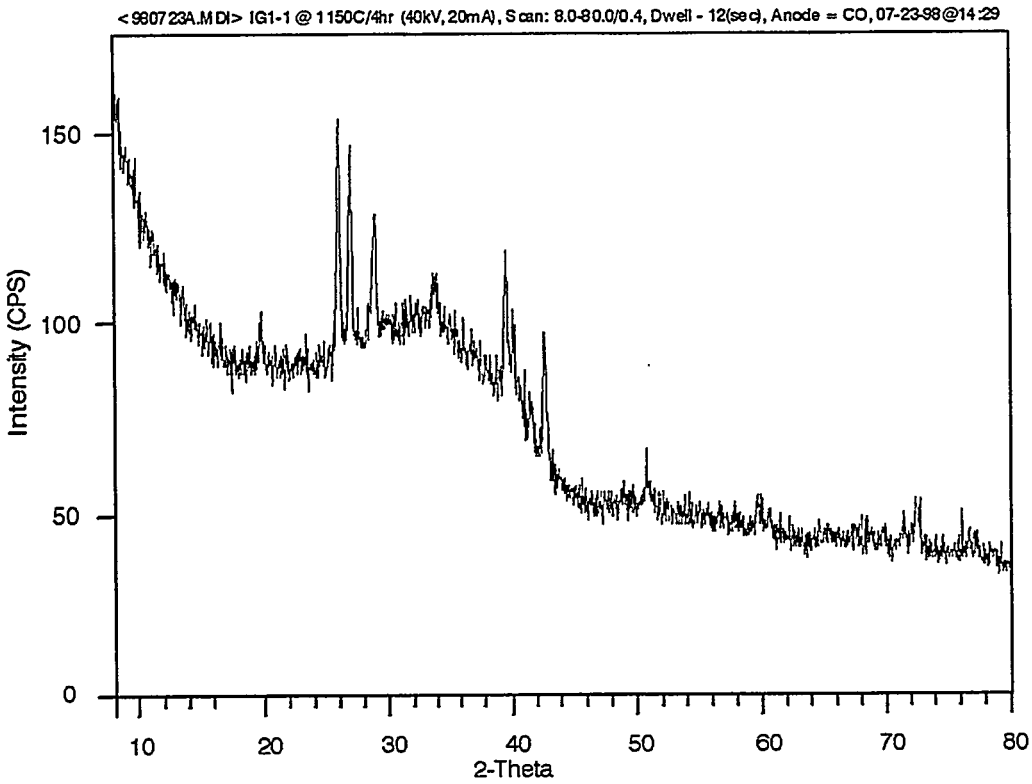

Figure A1-1. X-ray diffraction spectra of IG1-1 taken for 6 hours and showing the presence of lithium phosphate.

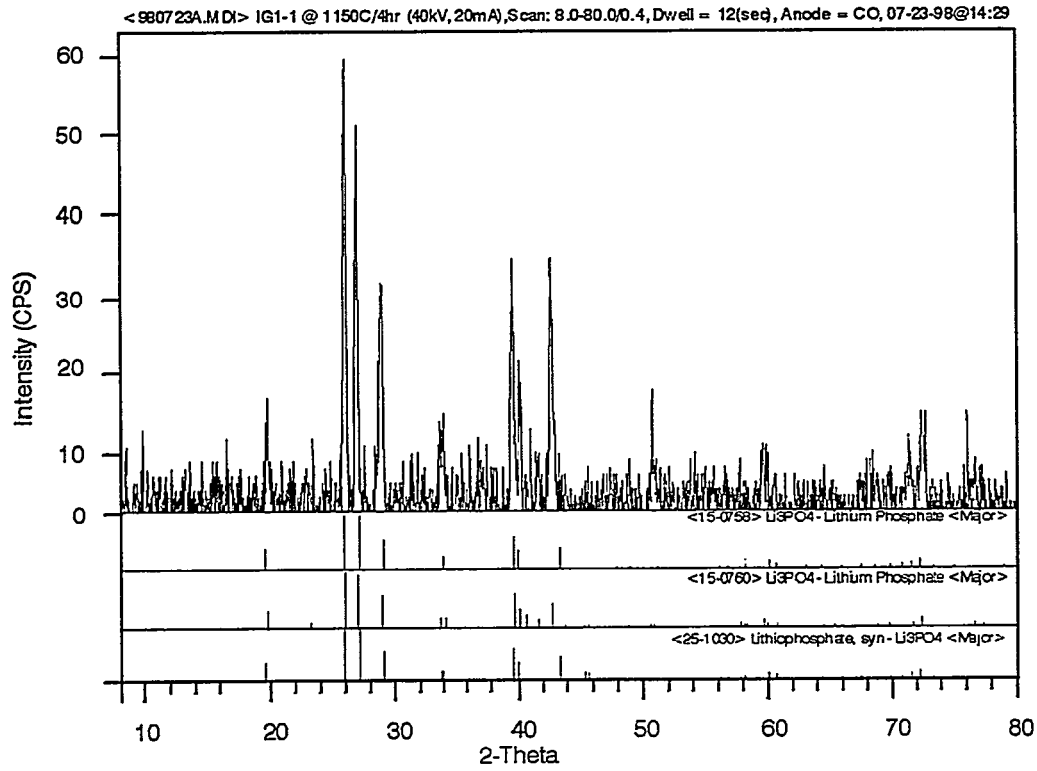

Figure A1-2. Reduced x-ray diffraction spectra of IG1-1 taken for 6 hours and showing the presence of lithium phosphate.

Gz99 0096

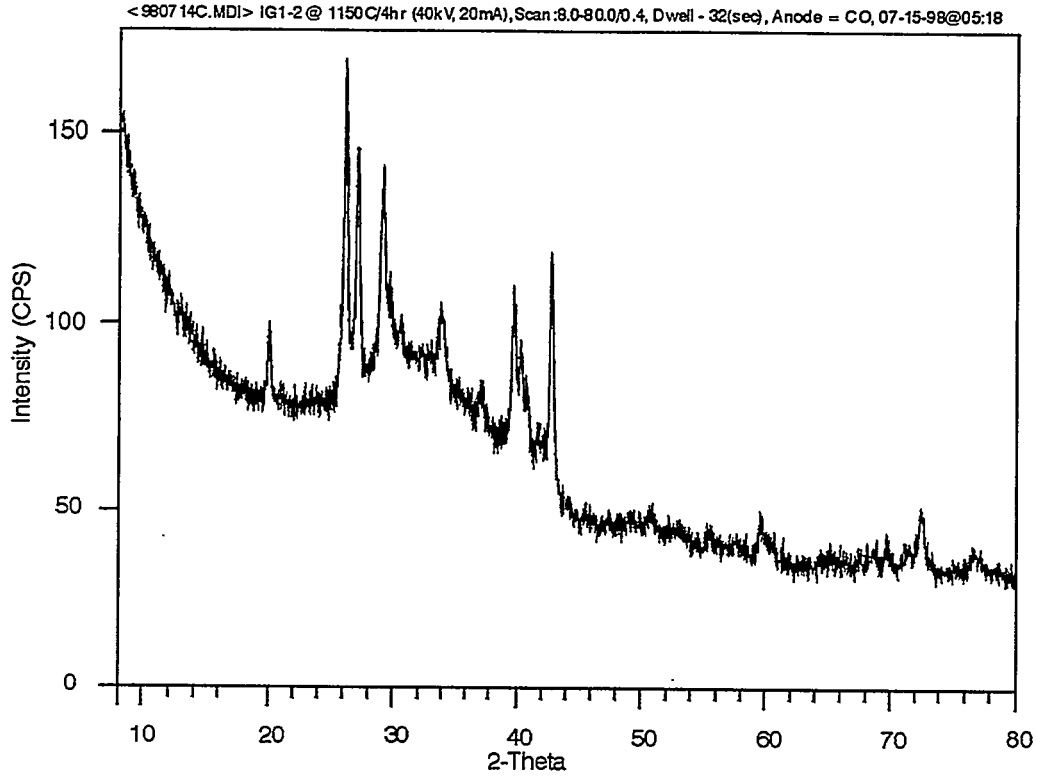

Figure A1-3. X-ray diffraction spectra of IG1-2 taken for 16 hours and showing the presence of lithium phosphate.

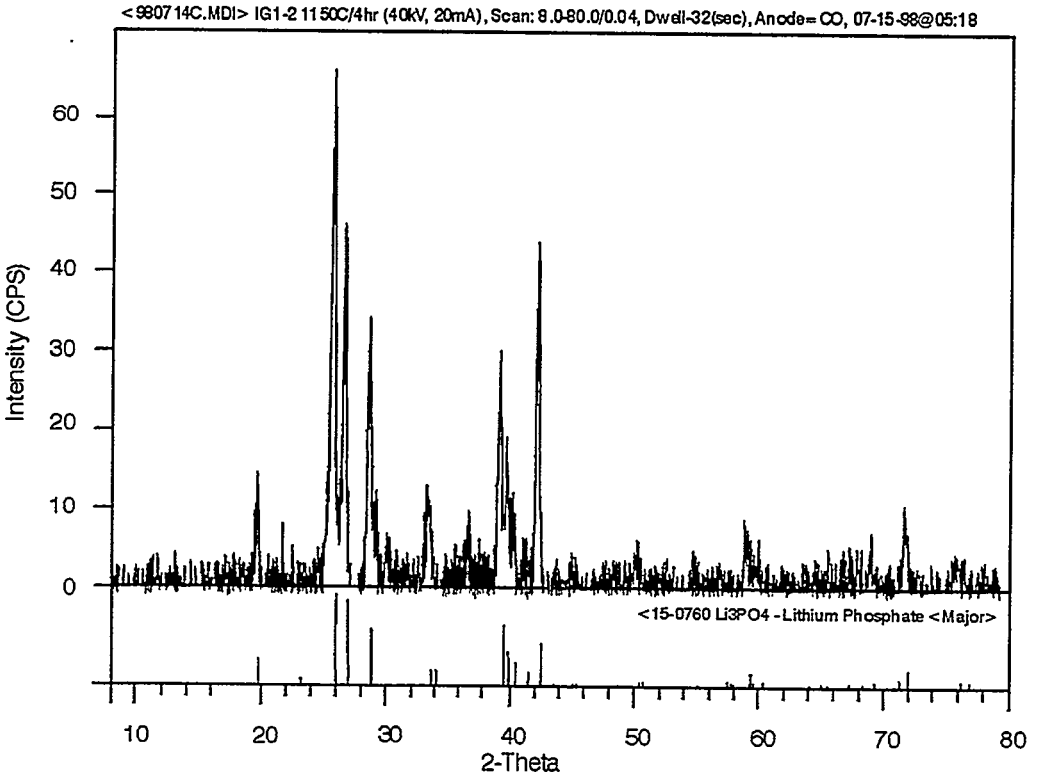

Figure A1-4. Reduced x-ray diffraction spectra of IG1-2 taken for 16 hours and showing the presence of lithium phosphate.

Gz99 0097

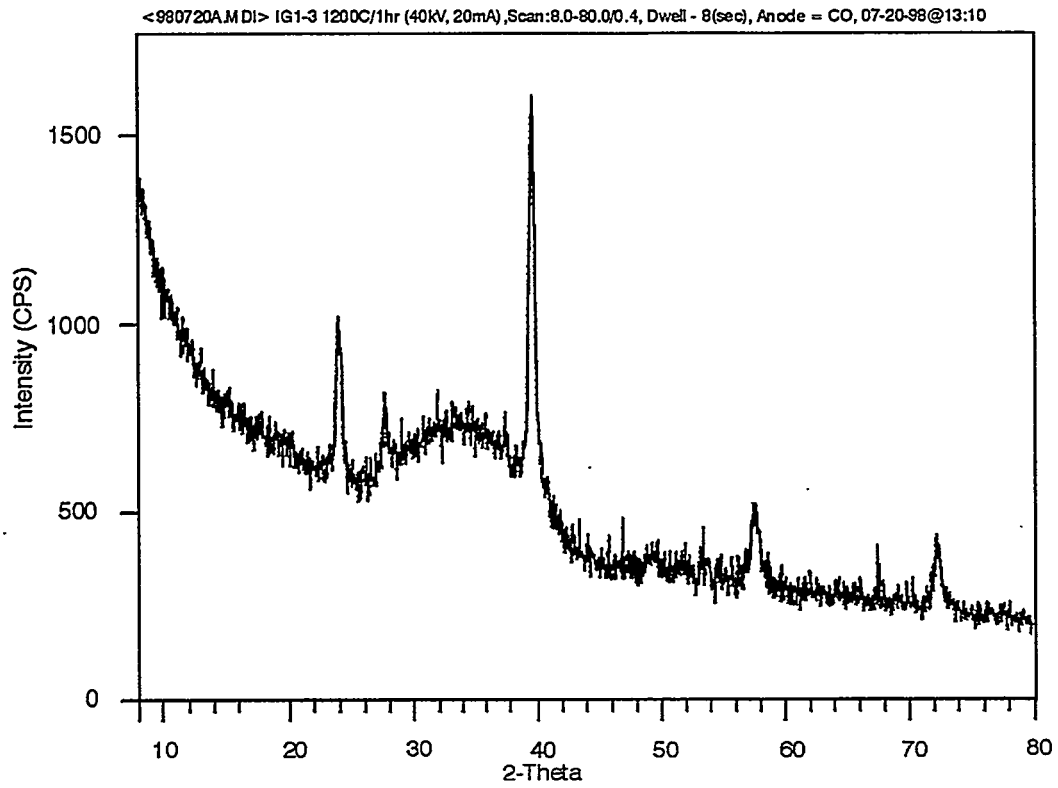

Figure A1-5. X-ray diffraction spectra of IG1-3 taken for 4 hours and showing the presence of sodium phosphate.

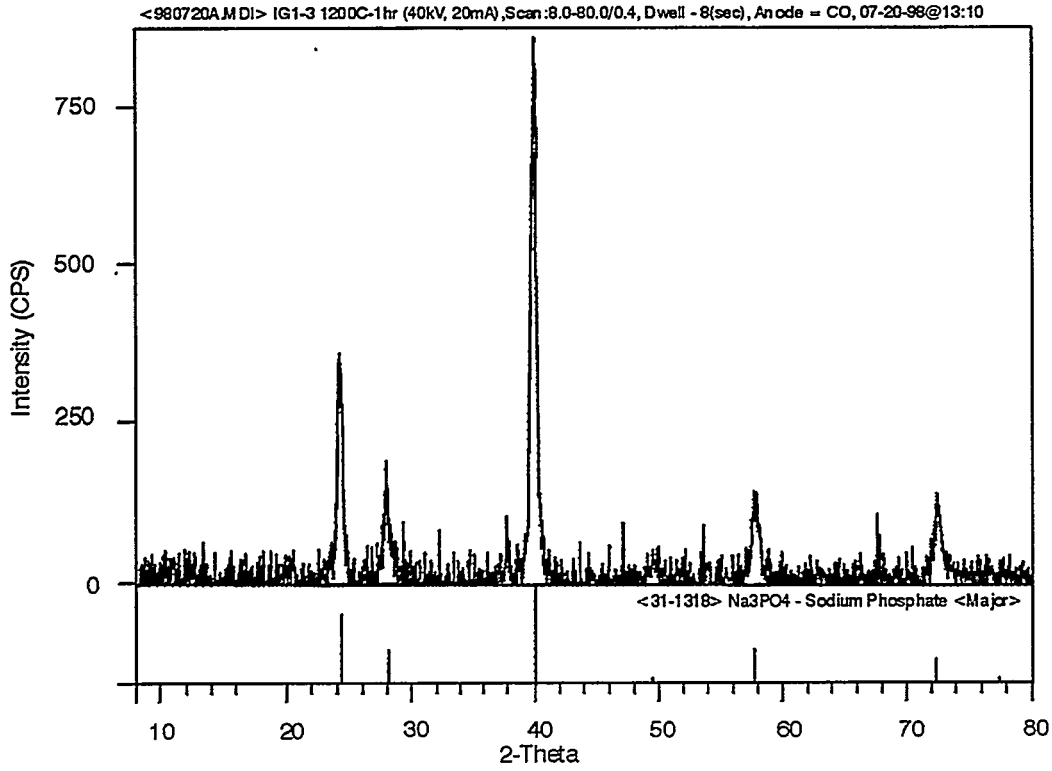

Figure A1-6. Reduced x-ray diffraction spectra of IG1-3 taken for 4 hours and showing the presence of sodium phosphate.

Gz99 0098

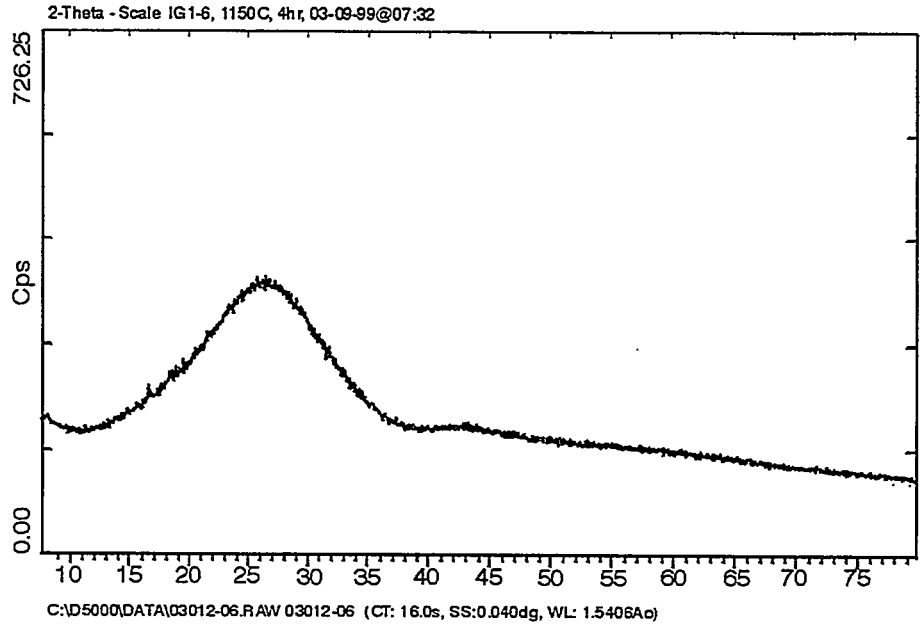

Figure A1-7. X-ray diffraction spectra of IG 1-6 taken for 8 hours without detection of crystallinity.

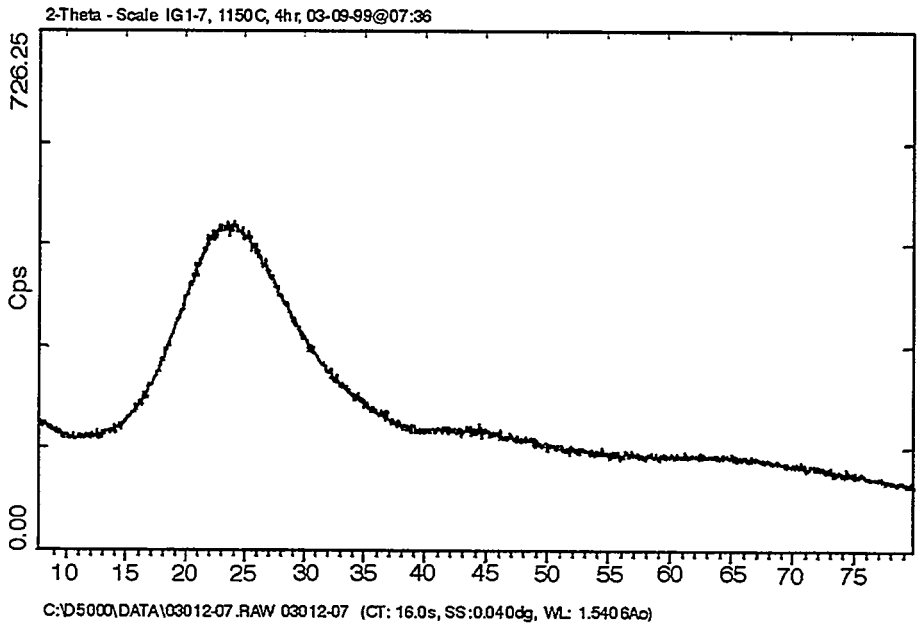

Figure A1-8. X-ray diffraction spectra of IG 1-7 taken for 8 hours without detection of crystallinity.

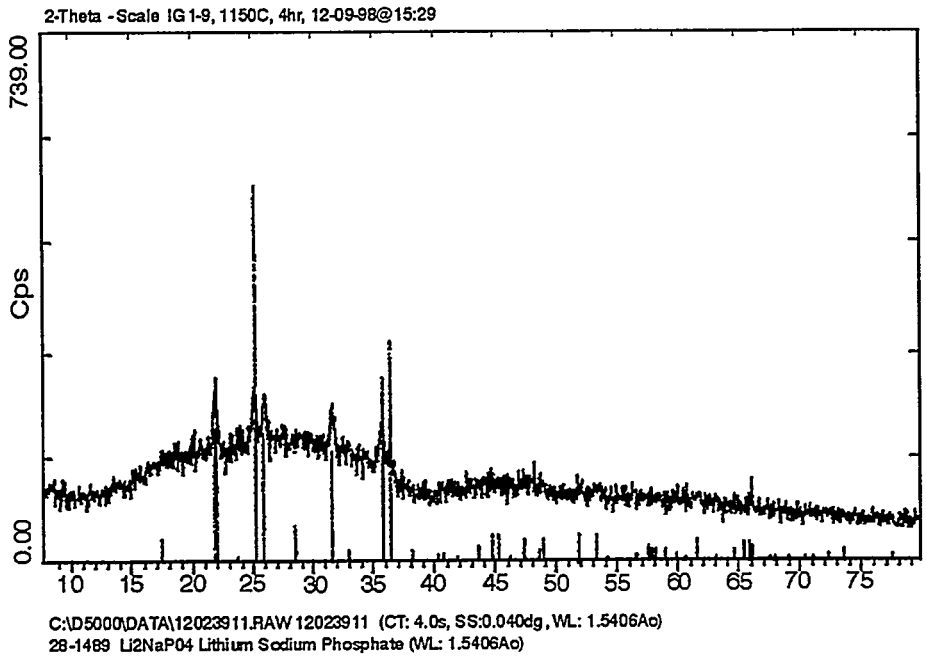

Figure A1-9. X-ray diffraction spectra of IG1-9 taken for 2 hours and showing the presence of lithium sodium phosphate.

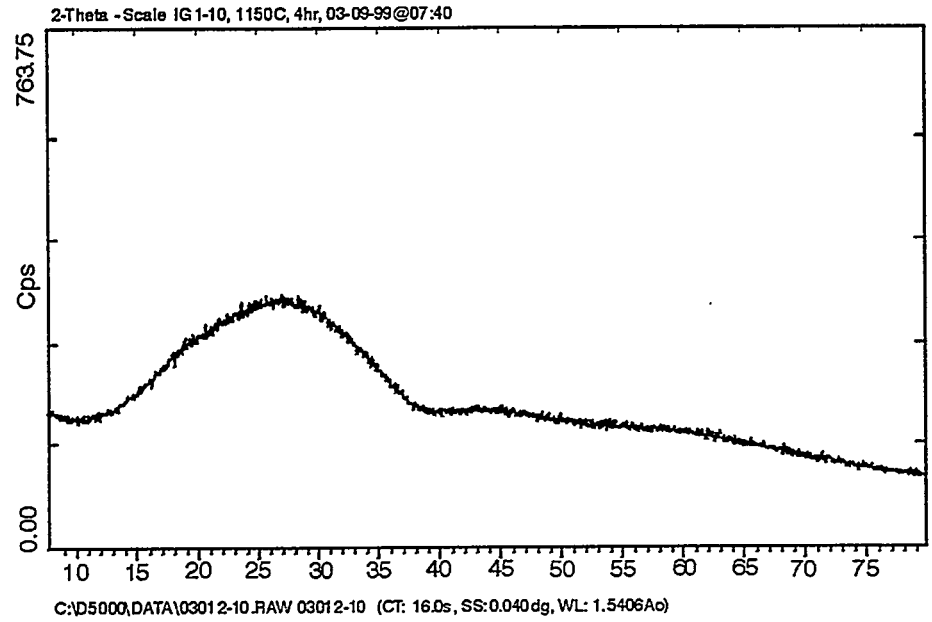

Figure A1-10. X-ray diffraction spectra of IG1-10 taken for 8 hours without detection of crystallinity.

Gz99 010C

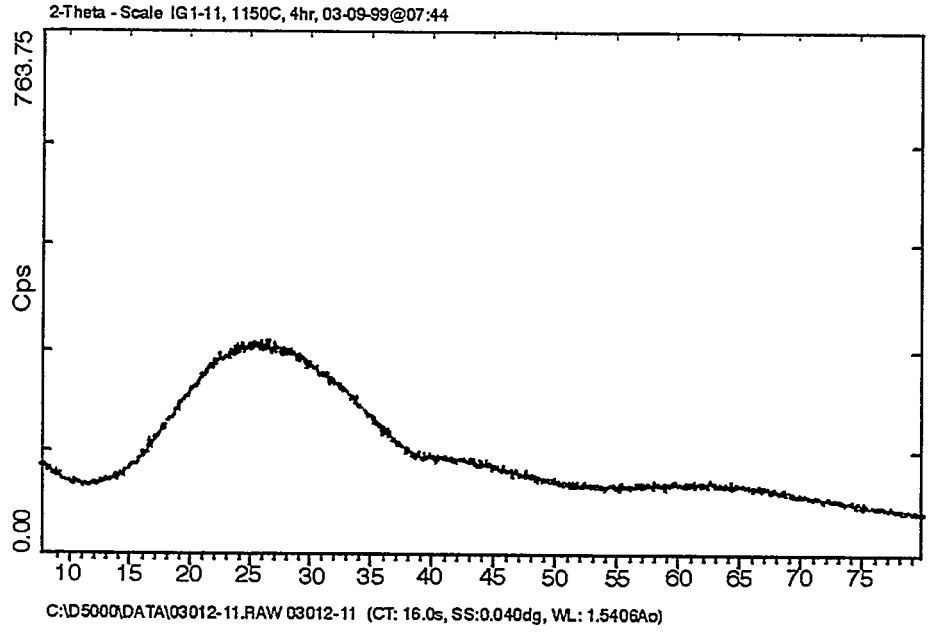

Figure A1-11. X-ray diffraction spectra of IG1-11 taken for 8 hours without detection of crystallinity.

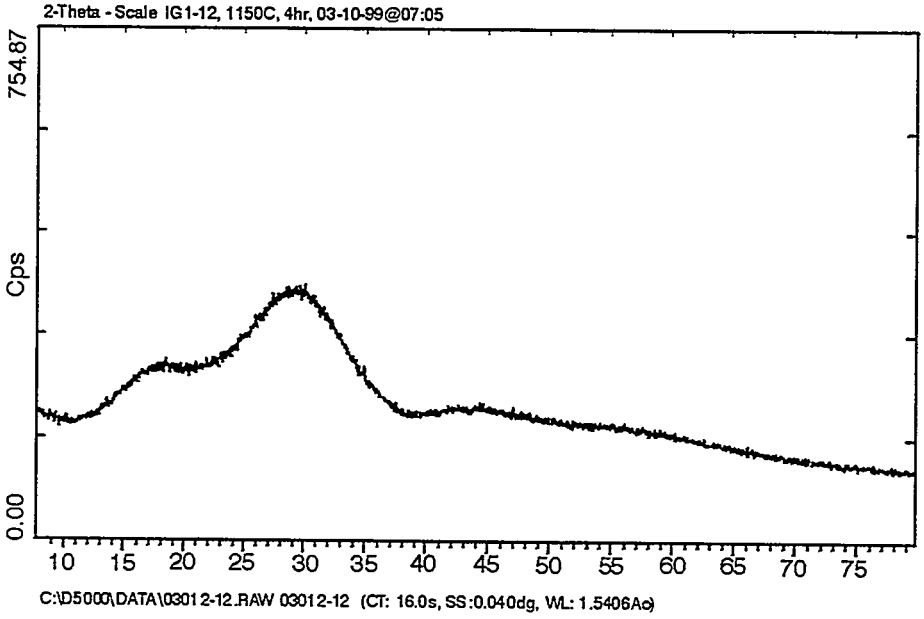

Figure A1-12. X-ray diffraction spectra of IG1-12 taken for 8 hours without detection of crystallinity.

Gz99 0101

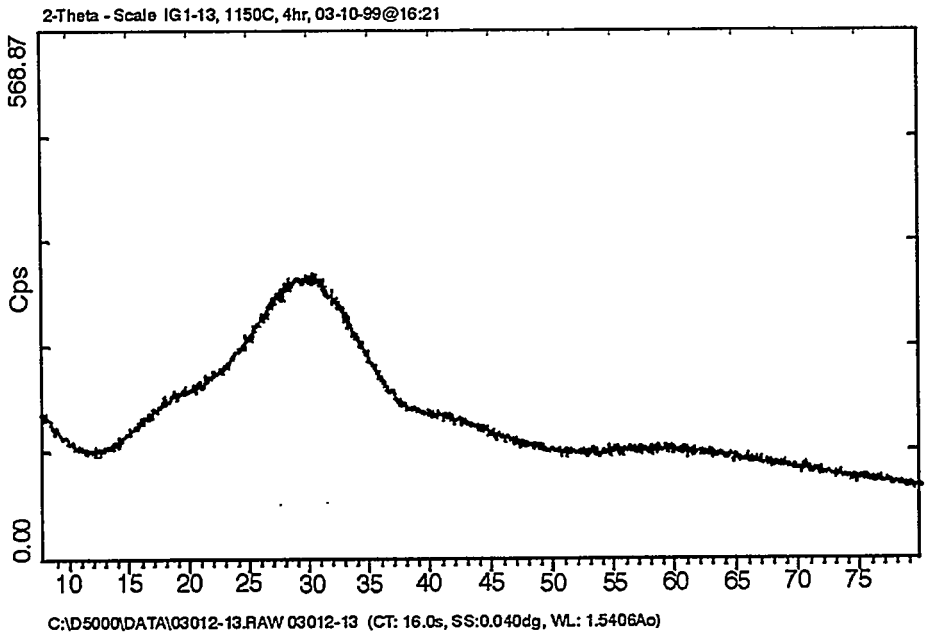

Figure A1-13. X-ray diffraction spectra of IG1-13 taken for 8 hours without detection of crystallinity.

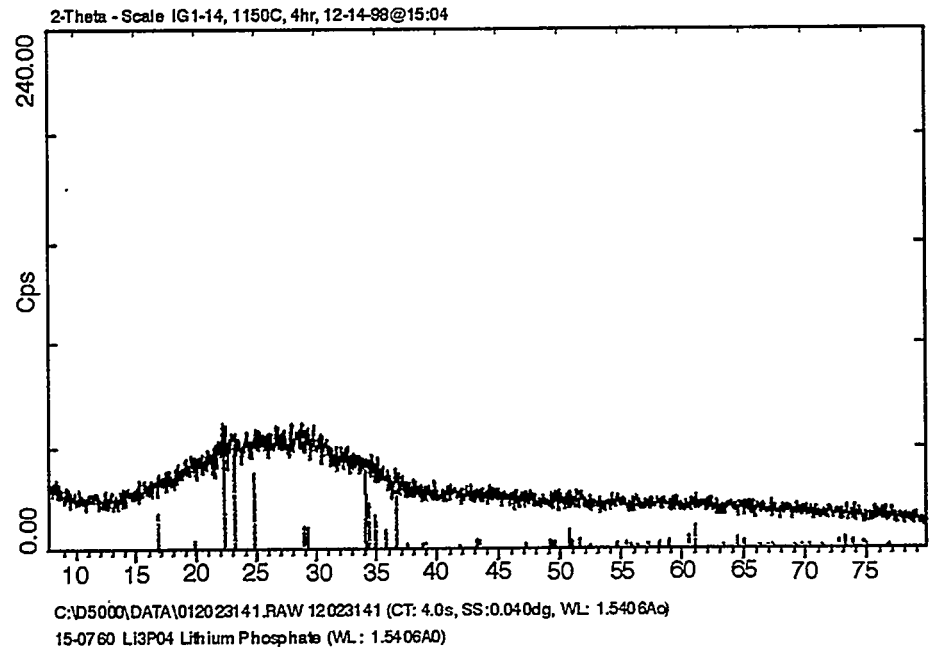

Figure A1-14. X-ray diffraction spectra of IG1-14 taken for 2 hours and showing the presence of lithium phosphate.

Gz99 0102

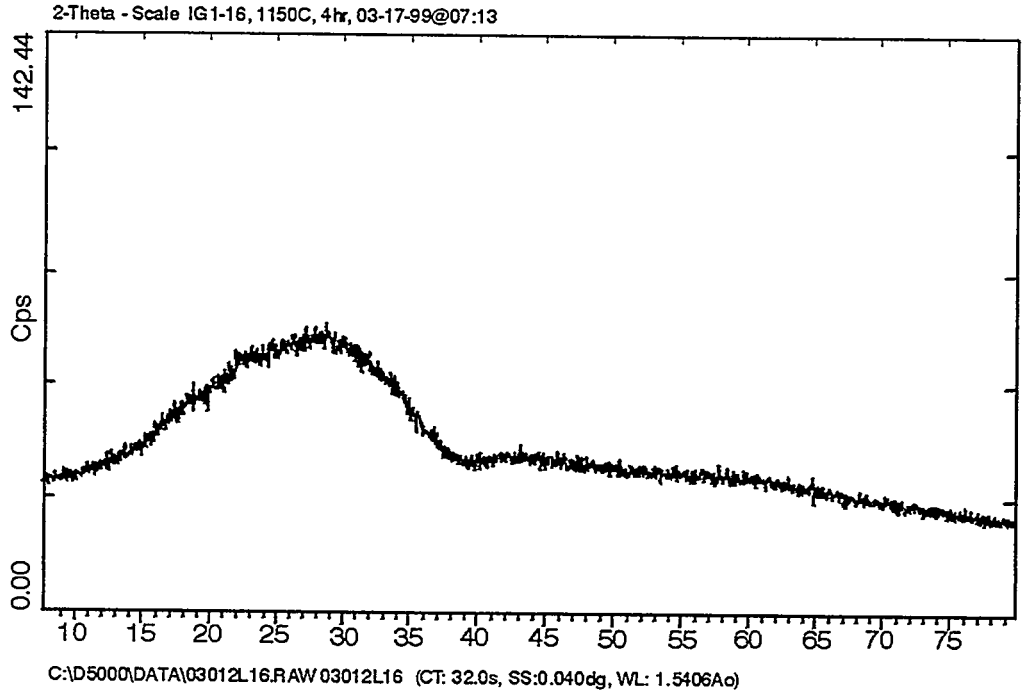

Figure A1-15. X-ray diffraction spectra of IG1-16 taken for 16 hours without detection crystallinity.

Gz990103

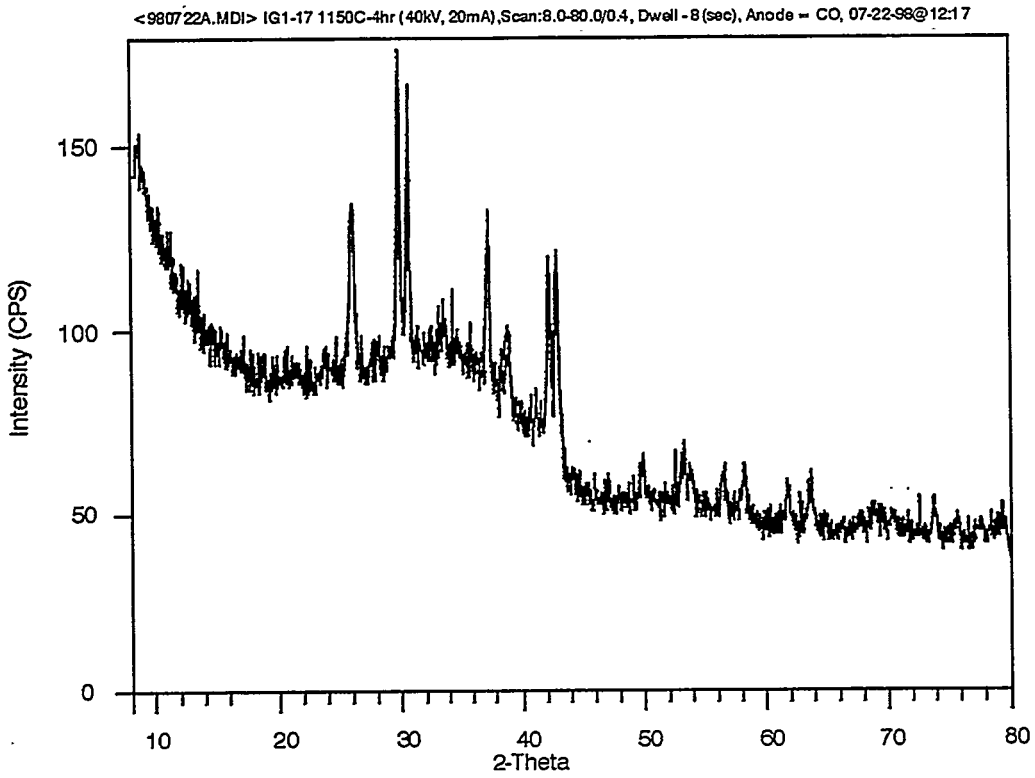

Figure A1-16. X-ray diffraction spectra of IG1-17 taken for 4 hours and showing the presence of lithium sodium phosphate.

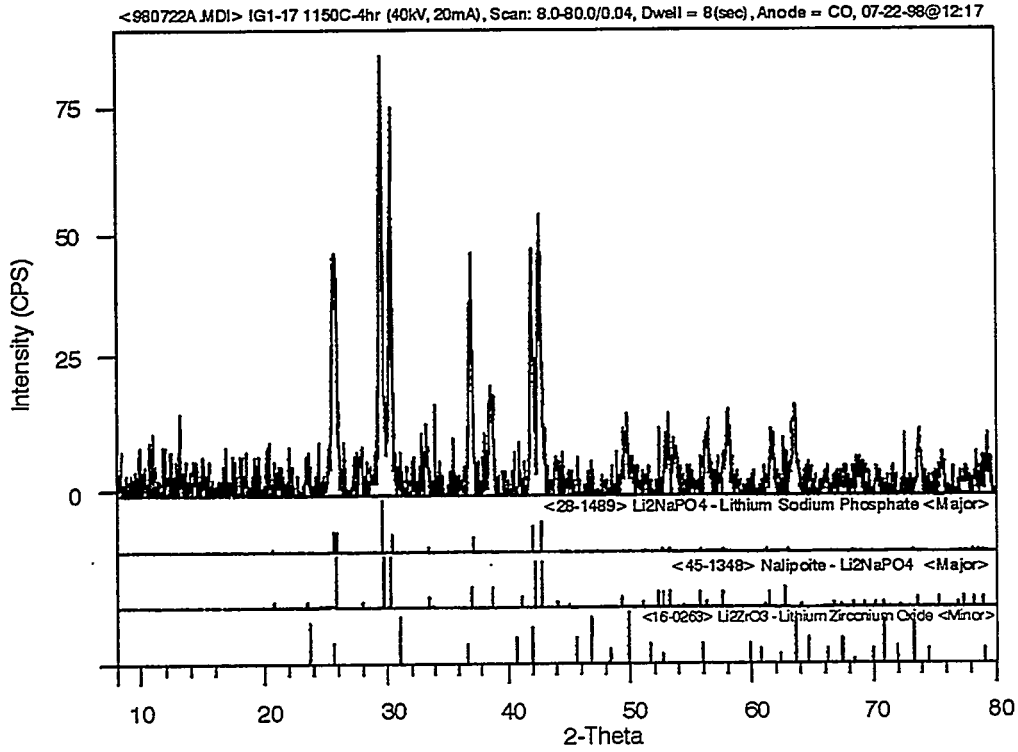

Figure A1-17. Reduced x-ray diffraction spectra of IG1-17 taken for 4 hours and showing the presence of lithium sodium phosphate.

Gz99 0104

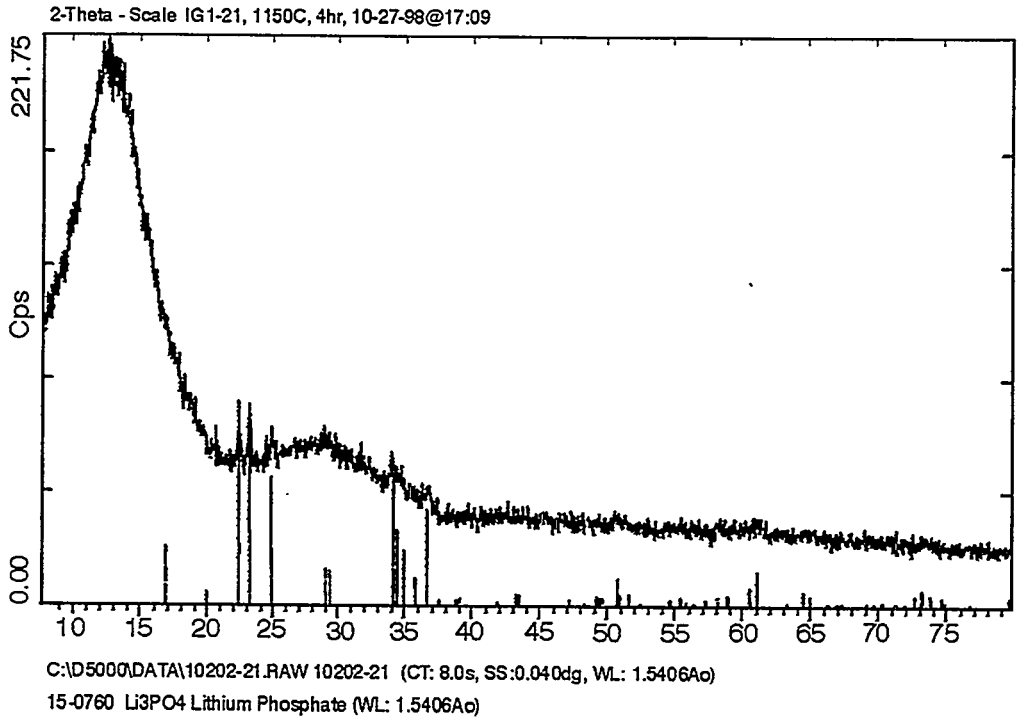

Figure A1-18. X-ray diffraction spectra of IG1-21 taken for 4 hours and showing the presence of lithium phosphate.

Gz990123

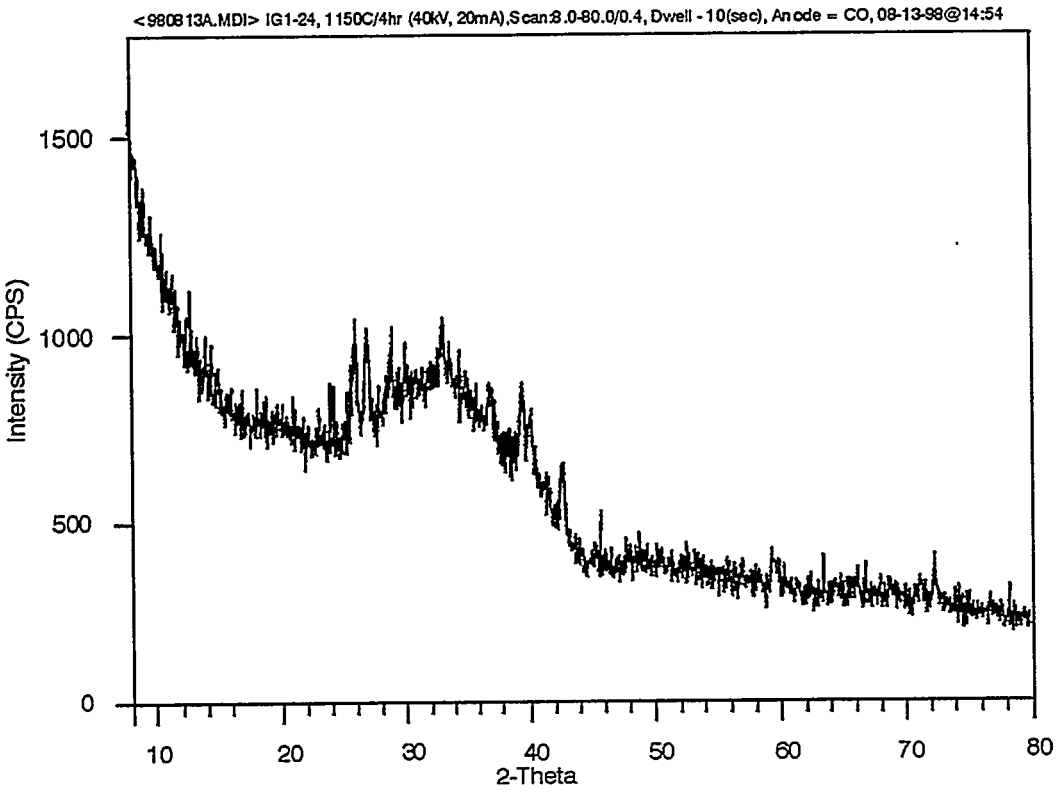

Figure A1-19. X-ray diffraction spectra of IG1-24 taken for 5 hours and showing the presence of lithium phosphate.

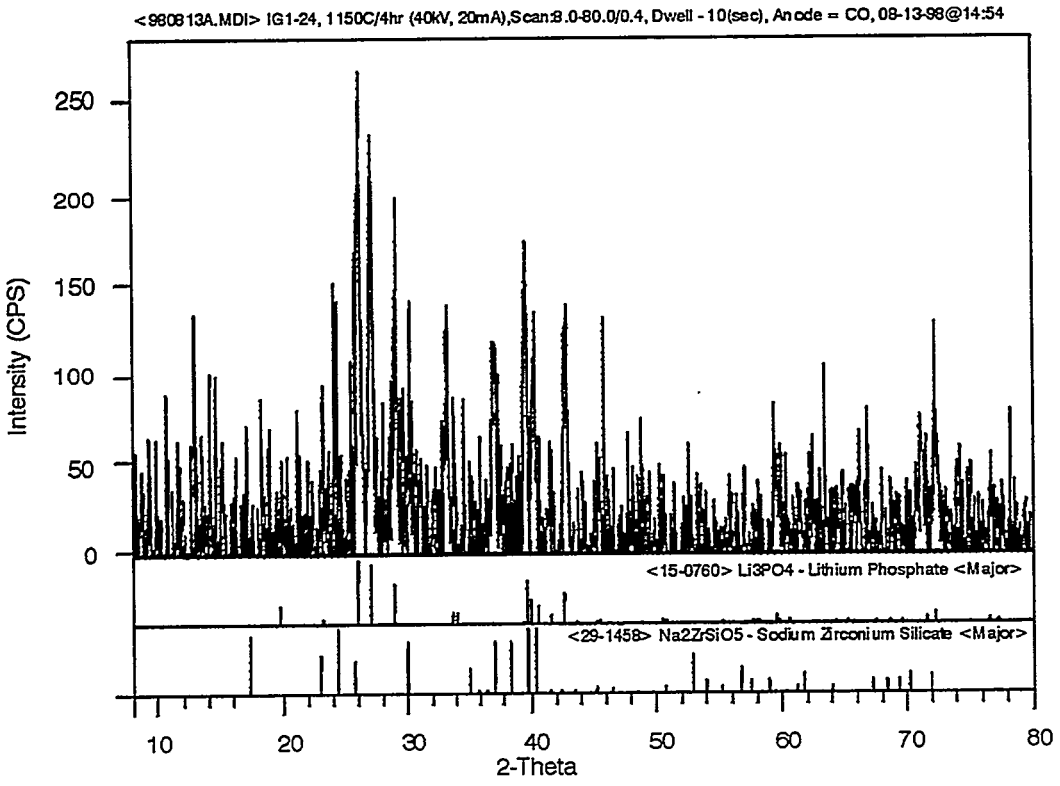

Figure A1-20. Reduced x-ray diffraction spectra of IG1-24 taken for 5 hours and showing the presence of lithium phosphate.

Gz99 00105

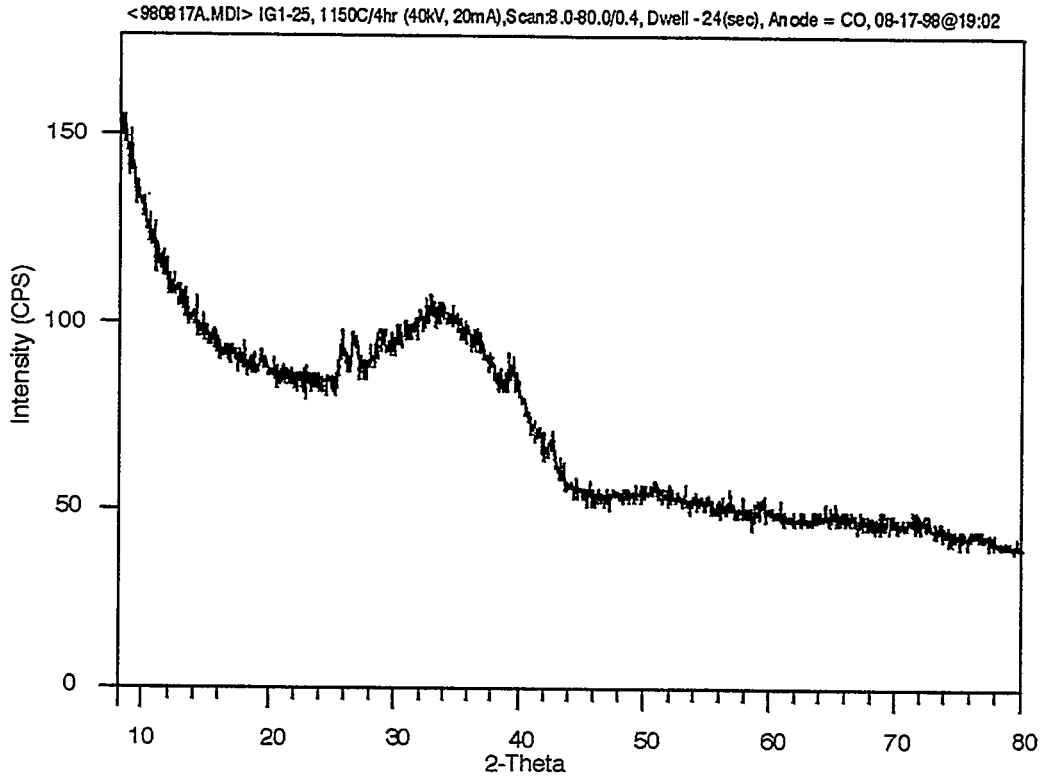

Figure A1-21. X-ray diffraction spectra of IG1-25 taken for 12 hours and showing the presence of lithium phosphate.

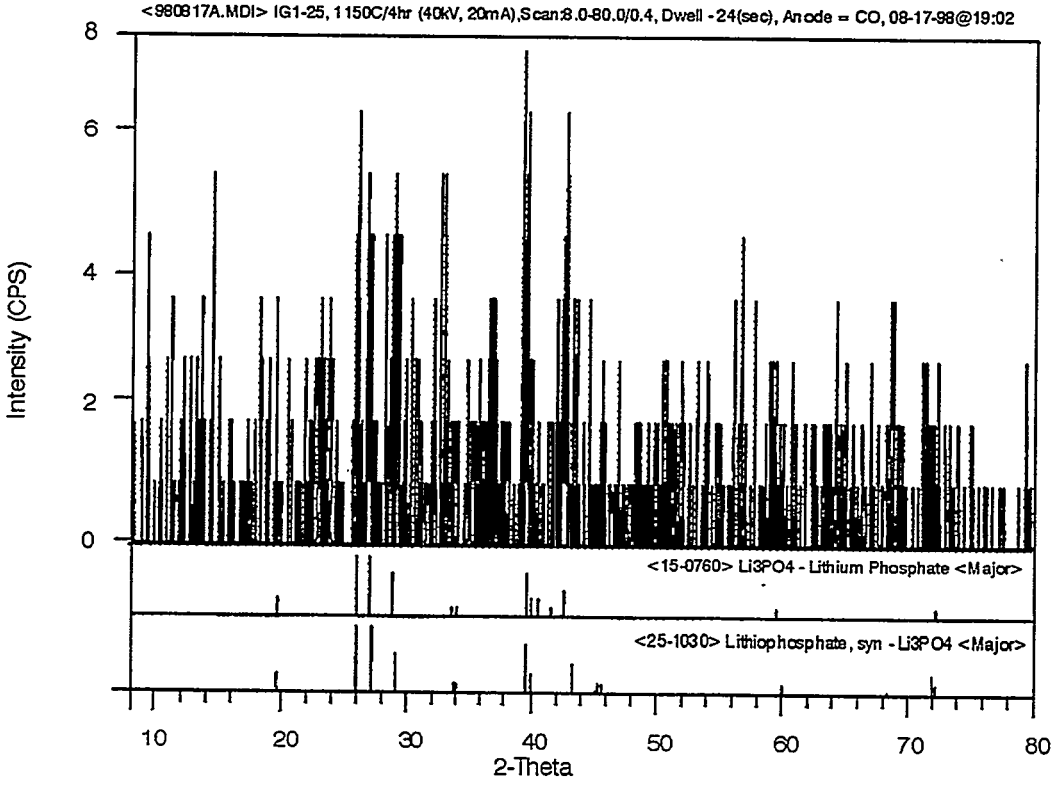

Figure A1-22. Reduced x-ray diffraction spectra of IG1-25 taken for 12 hours and showing the presence of lithium phosphate.

Gz99 00106

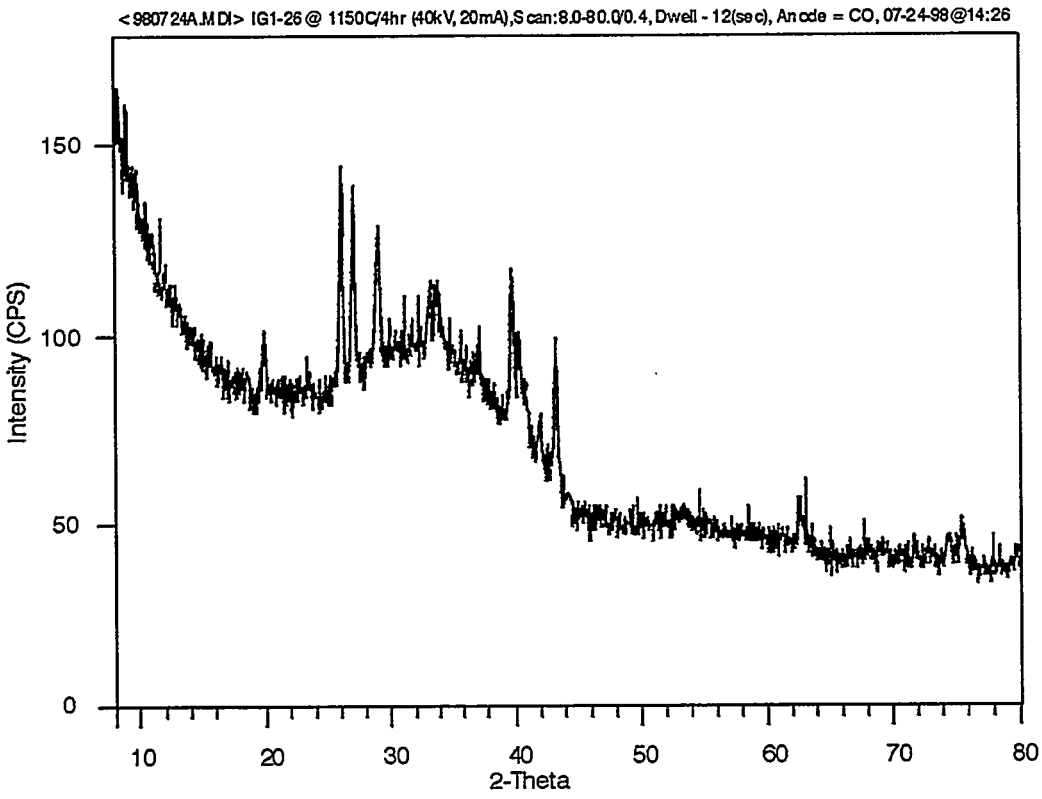

Figure A1-23. X-ray diffraction spectra of IG1-26 taken for 6 hours and showing the presence of lithium phosphate.

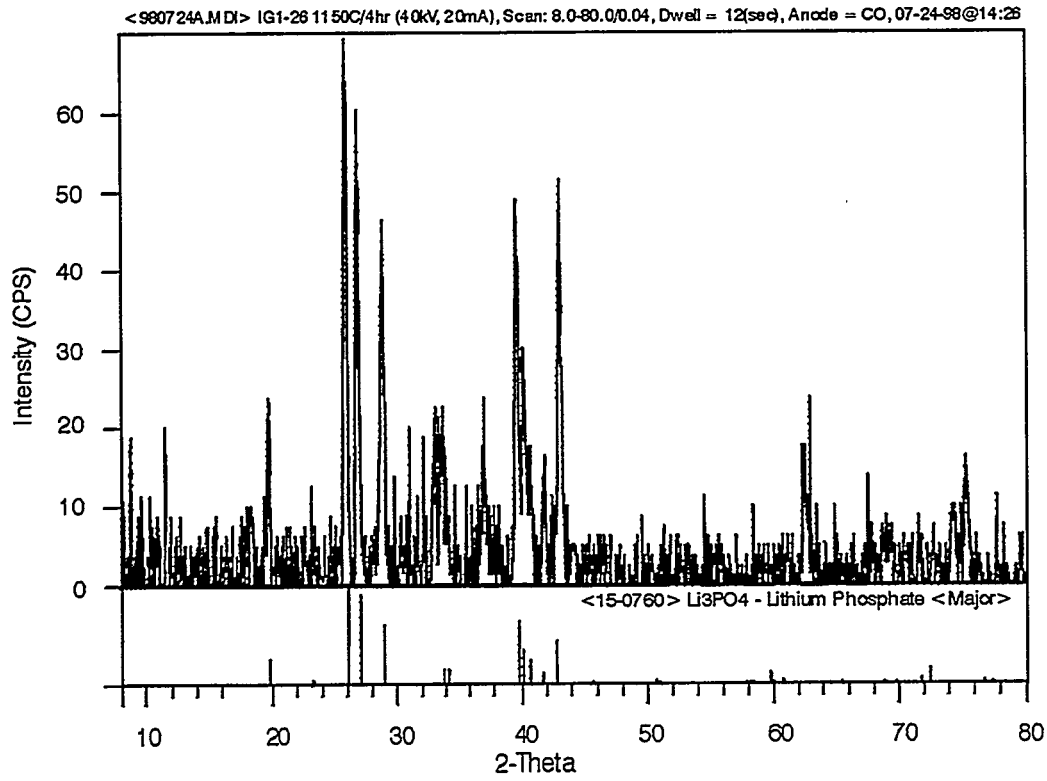

Figure A1-24. Reduced x-ray diffraction spectra of IG1-26 taken for 6 hours and showing the presence of lithium phosphate.

Gz99 0109

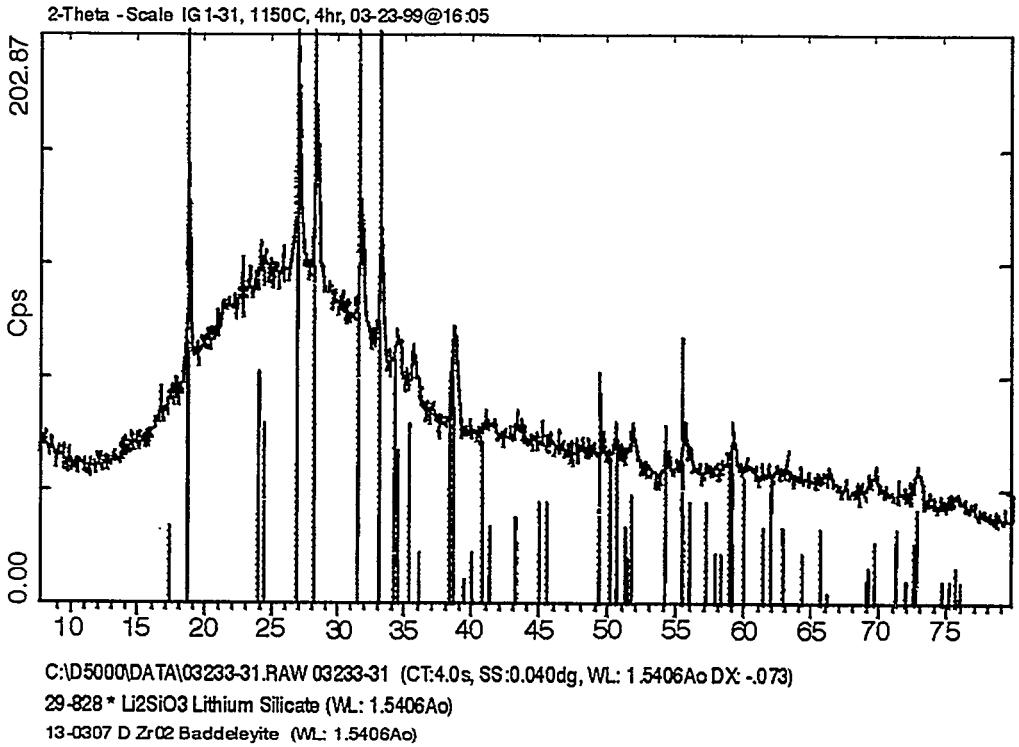

Figure A1-25. X-ray diffraction spectra of IG1-31 taken for 2 hours with detection of lithium silicate and zirconium oxide.

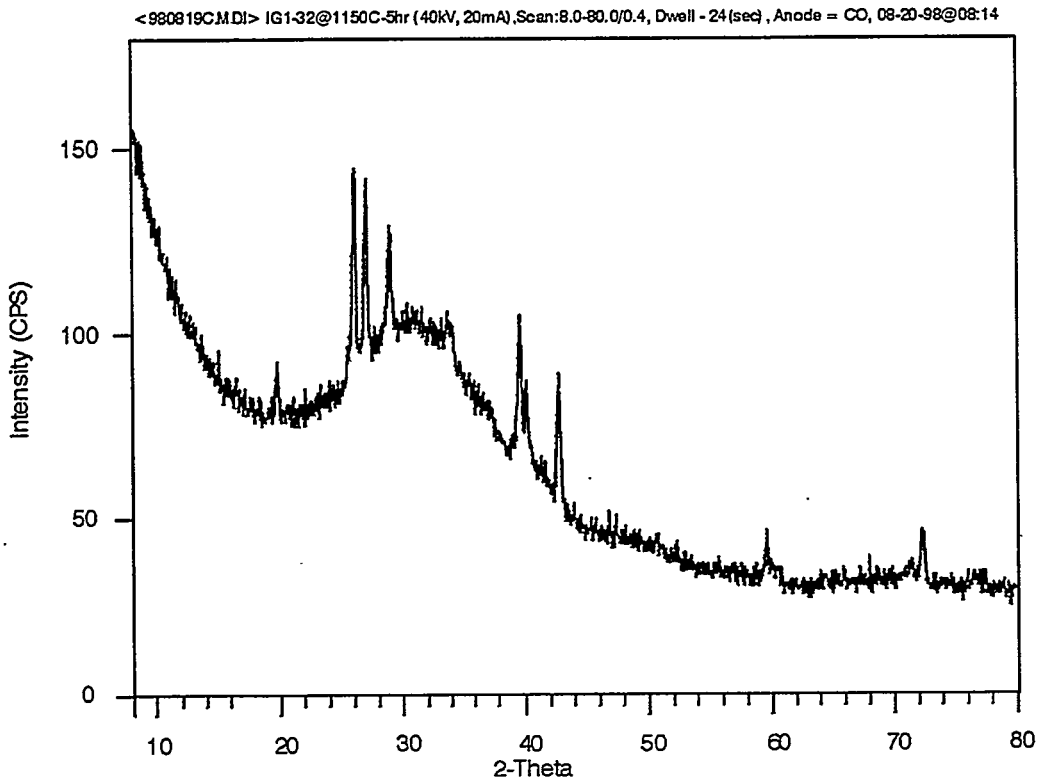

Figure A1-26. X-ray diffraction spectra of IG1-32 taken for 12 hours and showing the presence of lithium phosphate.

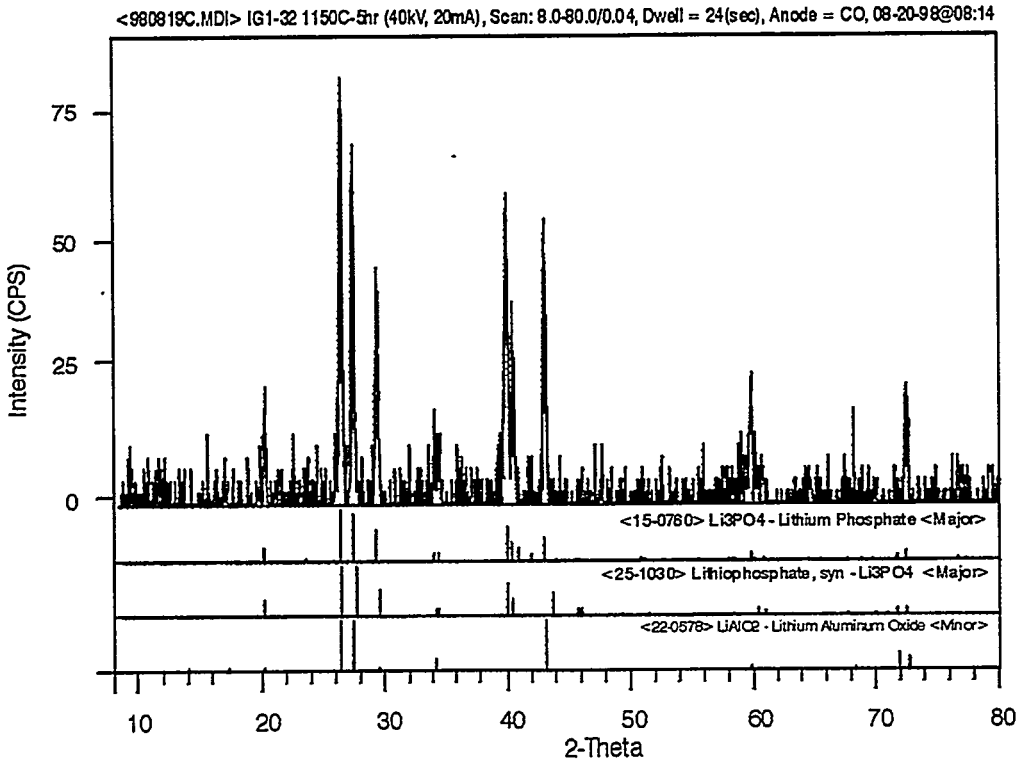

Figure A1-27. Reduced x-ray diffraction spectra of IG1-32 taken for 12 hours and showing the presence of lithium phosphate.

G799 0111

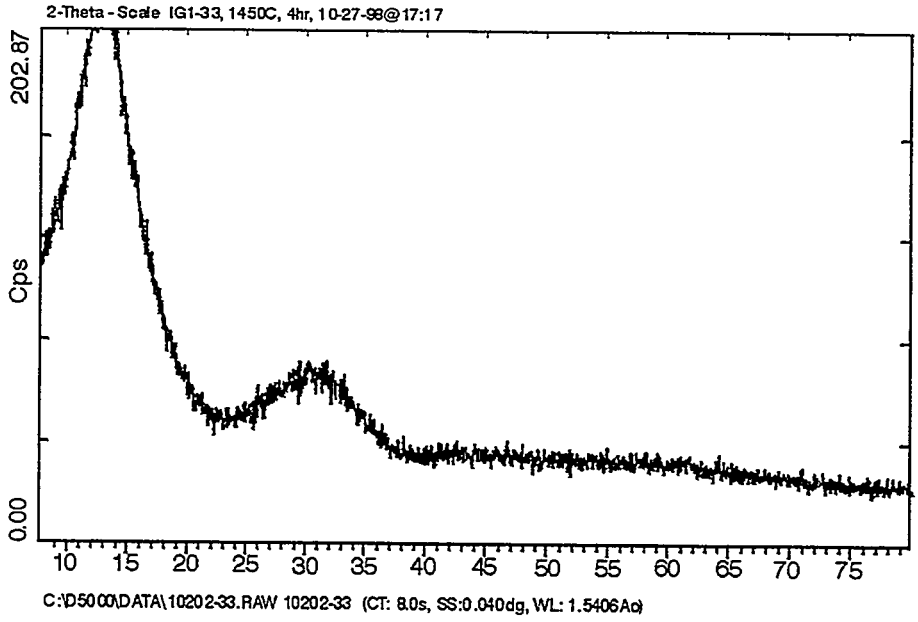

Figure A1-28. X-ray diffraction spectra of IG1-33 taken for 4 hours without detection of crystallinity.

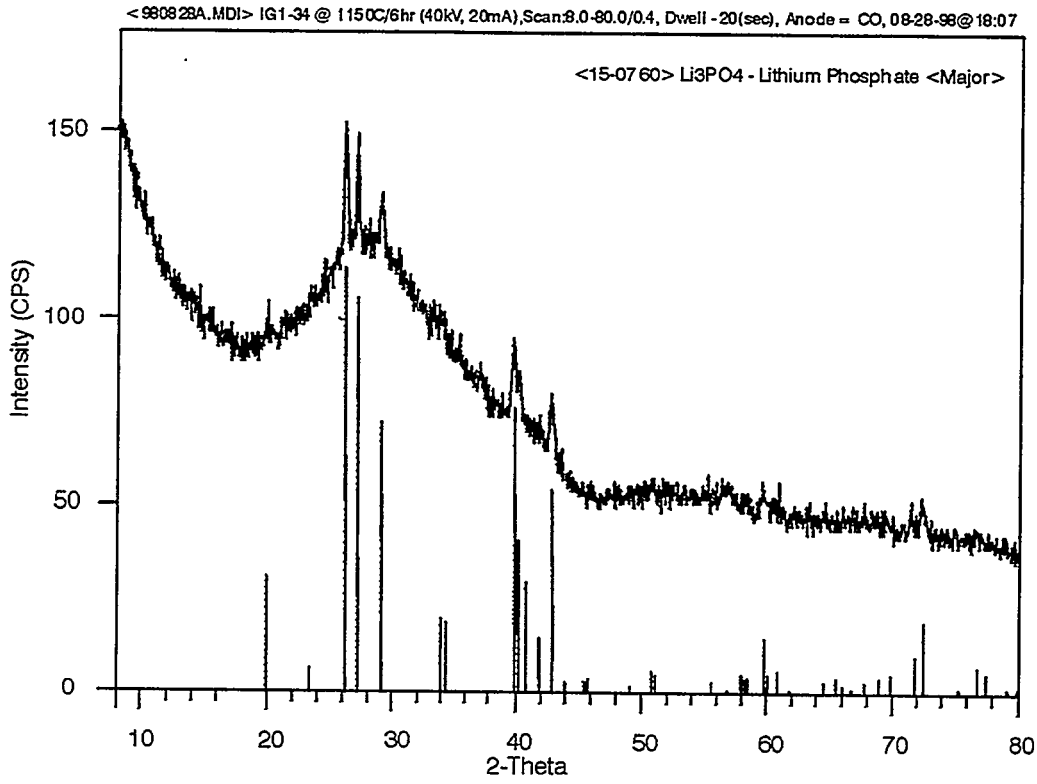

Figure A1-29. X-ray diffraction spectra of IG1-34 taken for 10 hours and showing the presence of lithium phosphate.

Gz990112

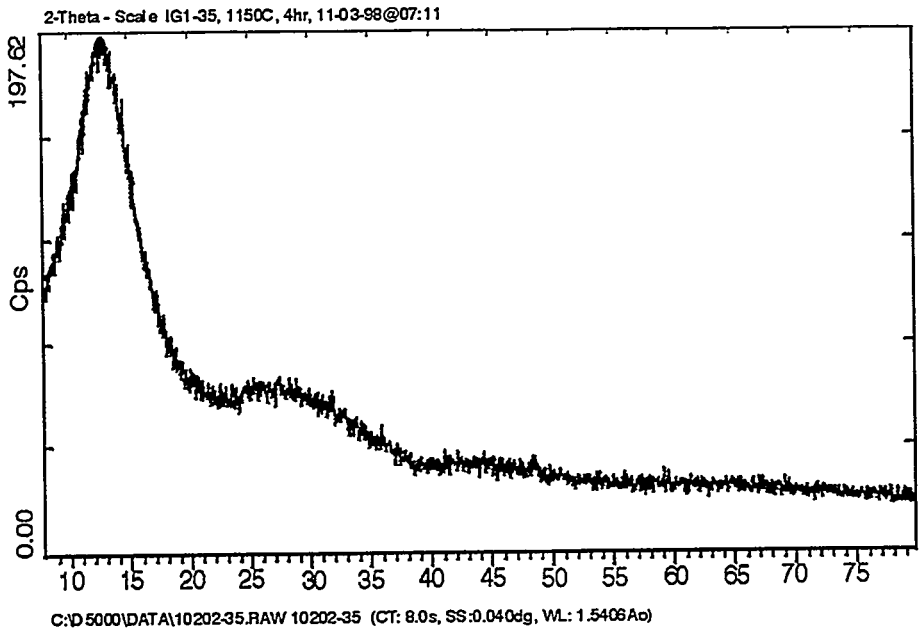

Figure A1-30. X-ray diffraction spectra of IG1-35 taken for 4 hours without detection of crystallinity.

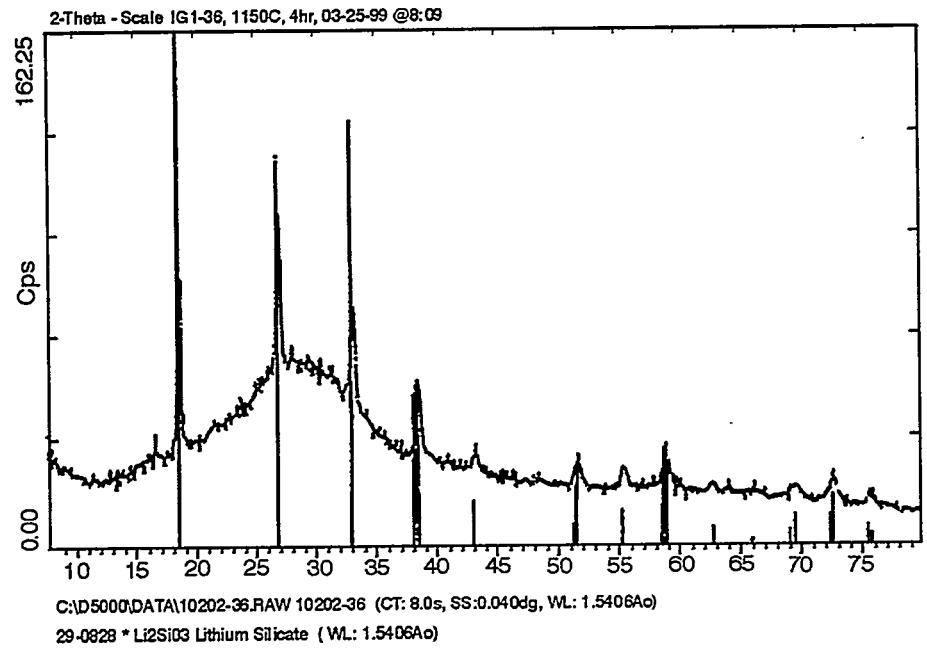

Figure A1-31. X-ray diffraction spectra of IG1-36 taken for 4 hours with detection of lithium silicate.

G799 0113

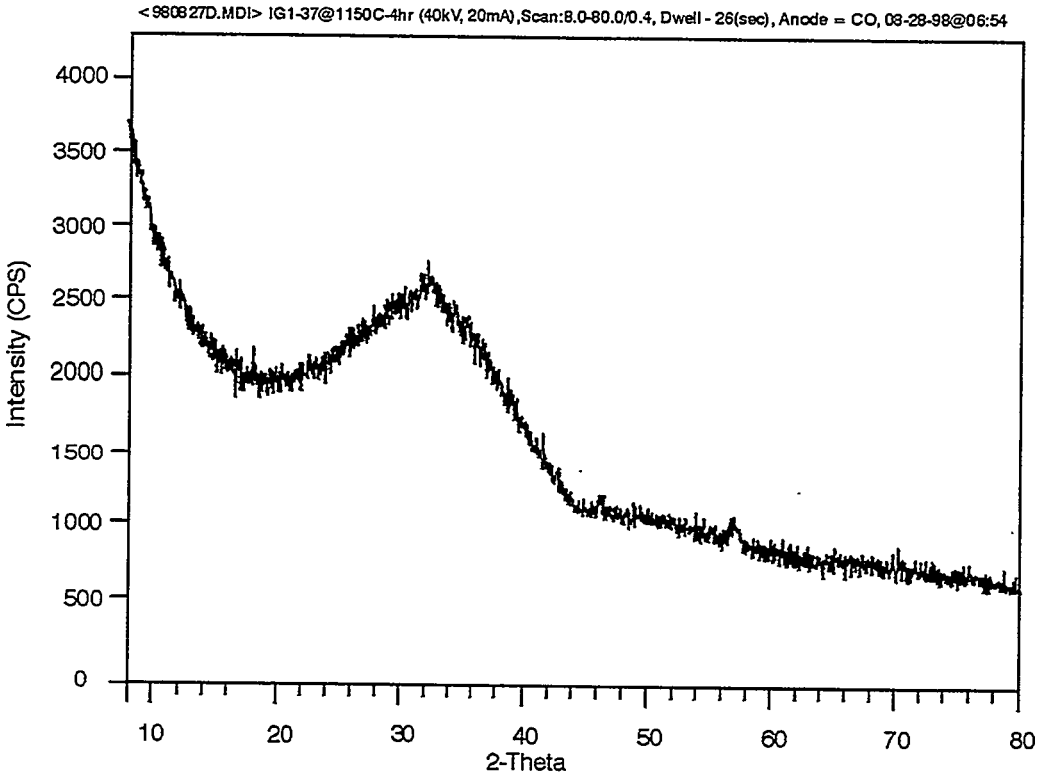

Figure A1-32. X-ray diffraction spectra of IG1-37 taken for 13 hours without detection of crystallinity.

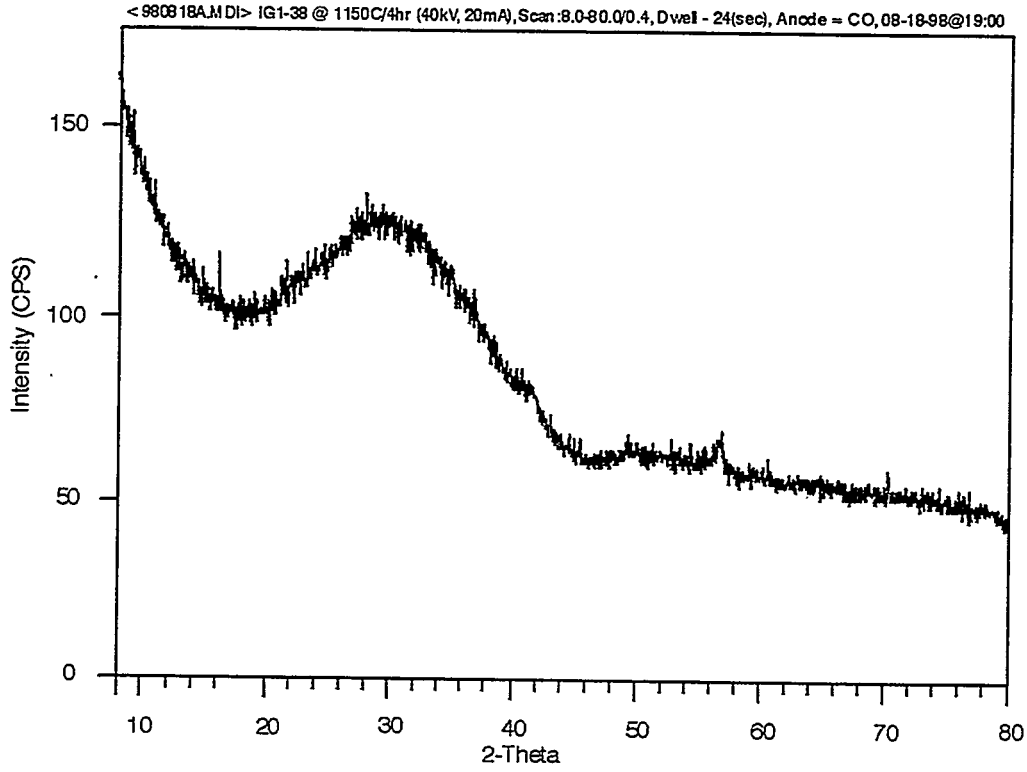

Figure A1-33. X-ray diffraction spectra of IG1-38 taken for 12 hours without detection of crystallinity.

Gz99 0114

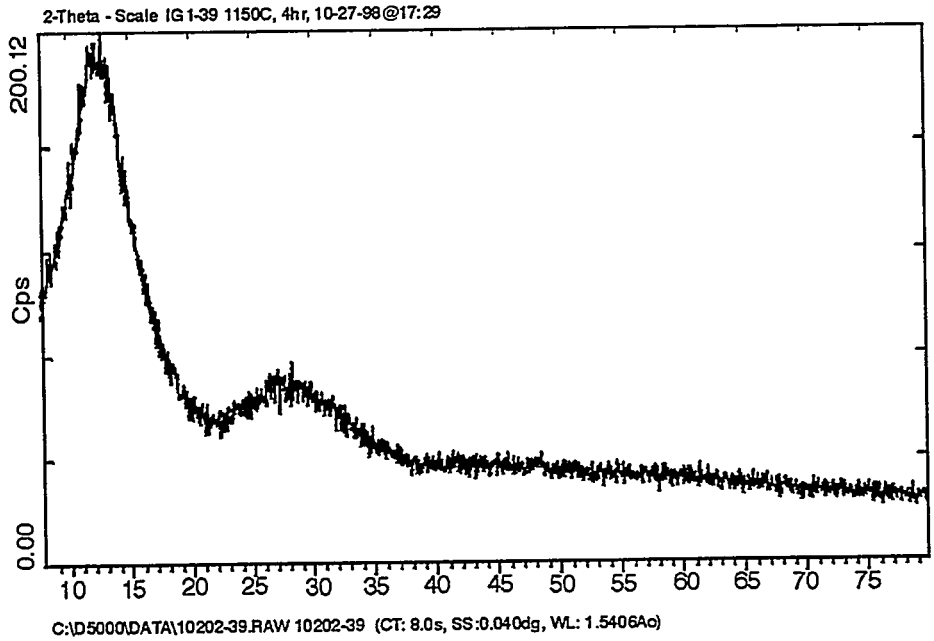

Figure A1-34. X-ray diffraction spectra of IG1-39 taken for 4 hours without detection of crystallinity.

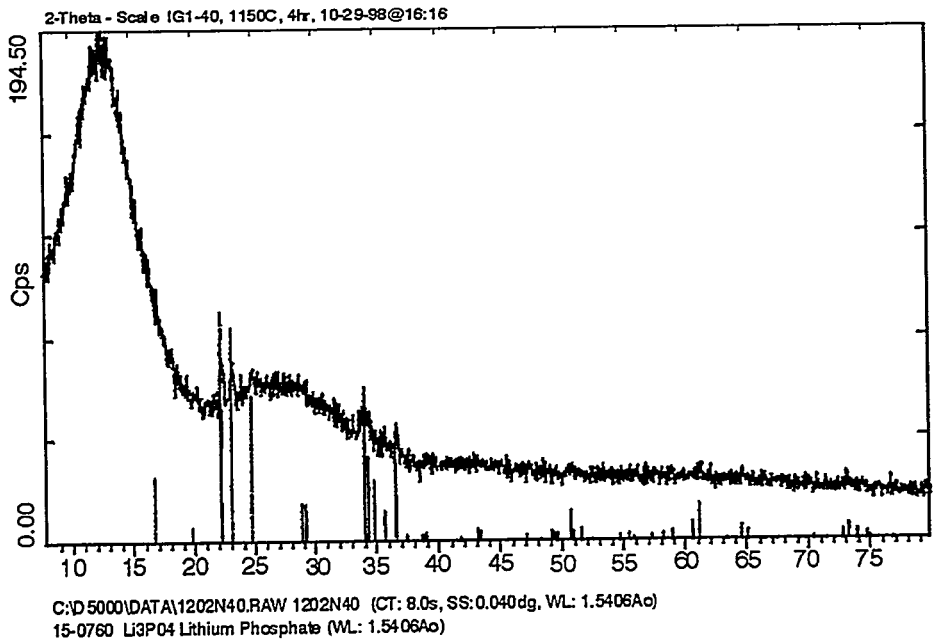

Figure A1-35. X-ray diffraction spectra of IG1-40 taken for 4 hours and showing the presence of lithium phosphate.

Gz99 0115

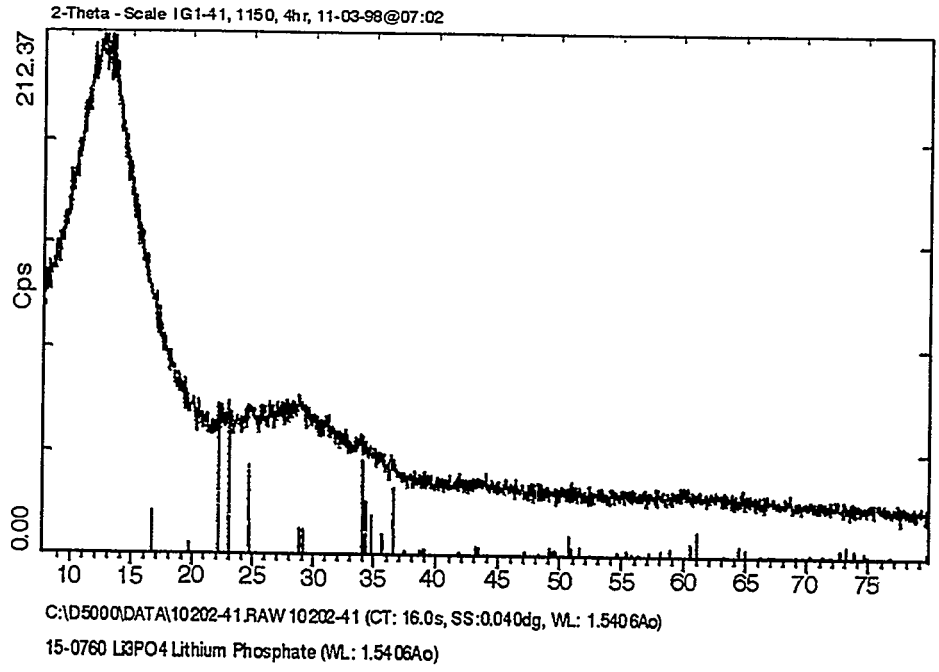

Figure A1-36. X-ray diffraction spectra of IG1-41 taken for 8 hours and showing the presence of lithium phosphate.

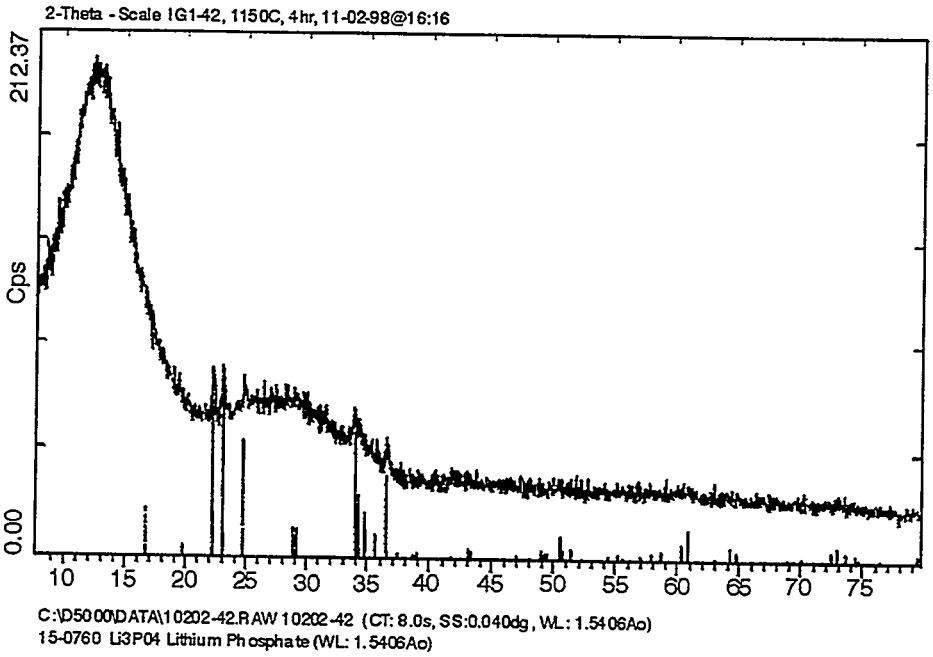

Figure A1-37. X-ray diffraction spectra of IG1-42 taken for 4 hours and showing the presence of lithium phosphate.

Gz99 0116

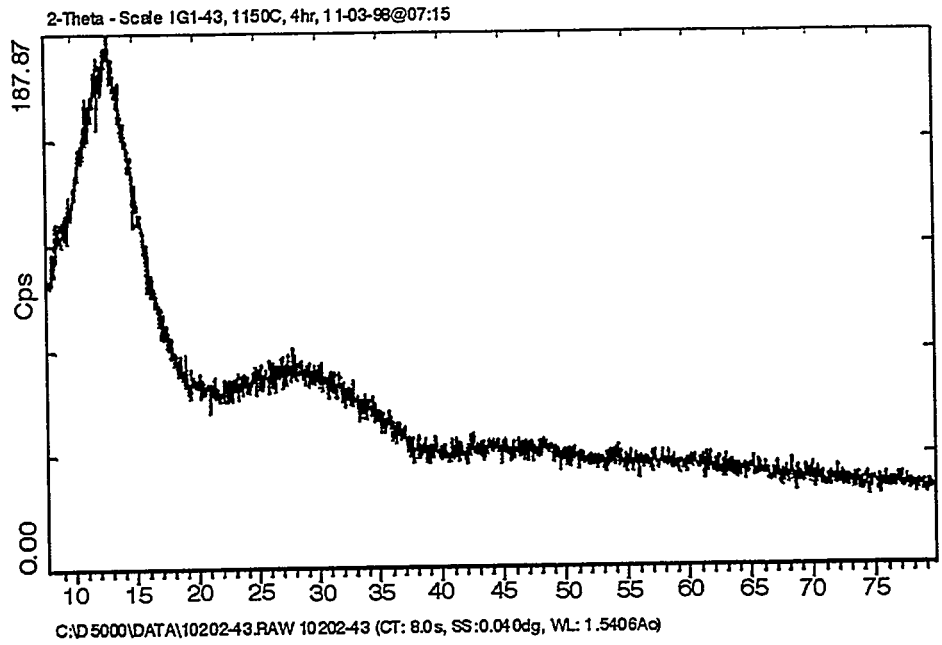

Figure A1-38. X-ray diffraction spectra of IG1-43 taken for 4 hours without detection of crystallinity.

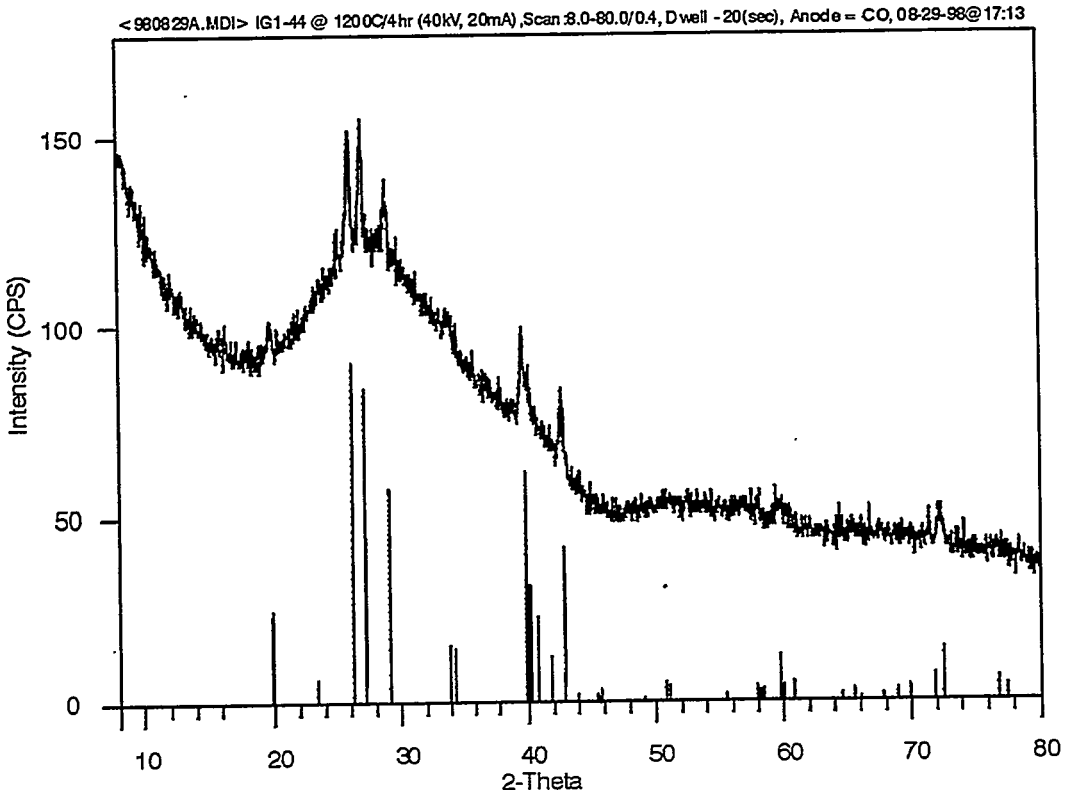

Figure A1-39. X-ray diffraction spectra of IG1-44 taken for 10 hours and showing the presence of lithium phosphate.

G799 0117

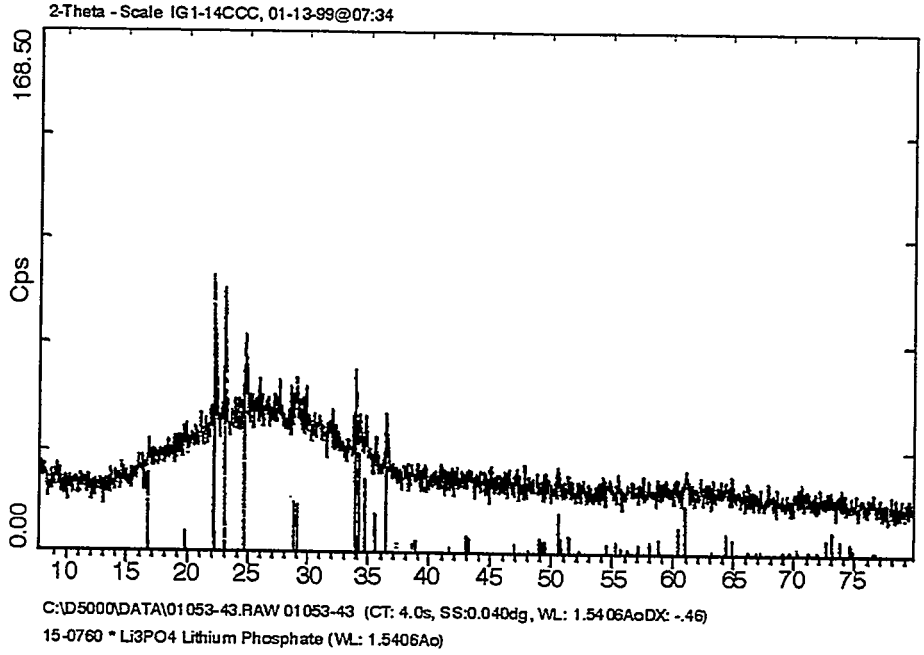

Figure A2-1. X-ray diffraction spectra of IG1-14CCC taken for 2 hours and showing the presence of lithium phosphate.

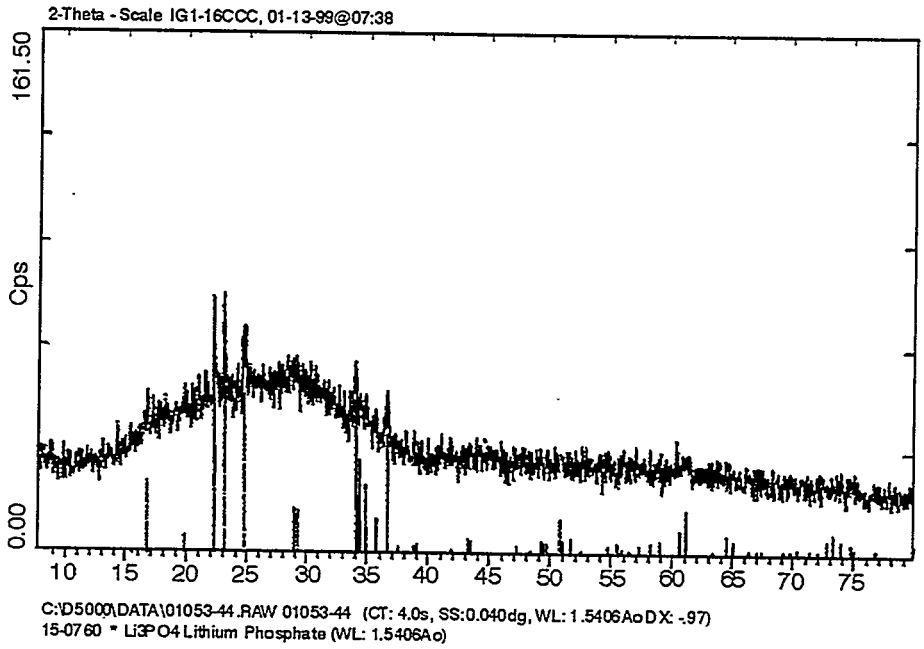

Figure A2-2. X-ray diffraction spectra of IG1-16CCC taken for 2 hours and showing the presence of lithium phosphate.

G799 0118

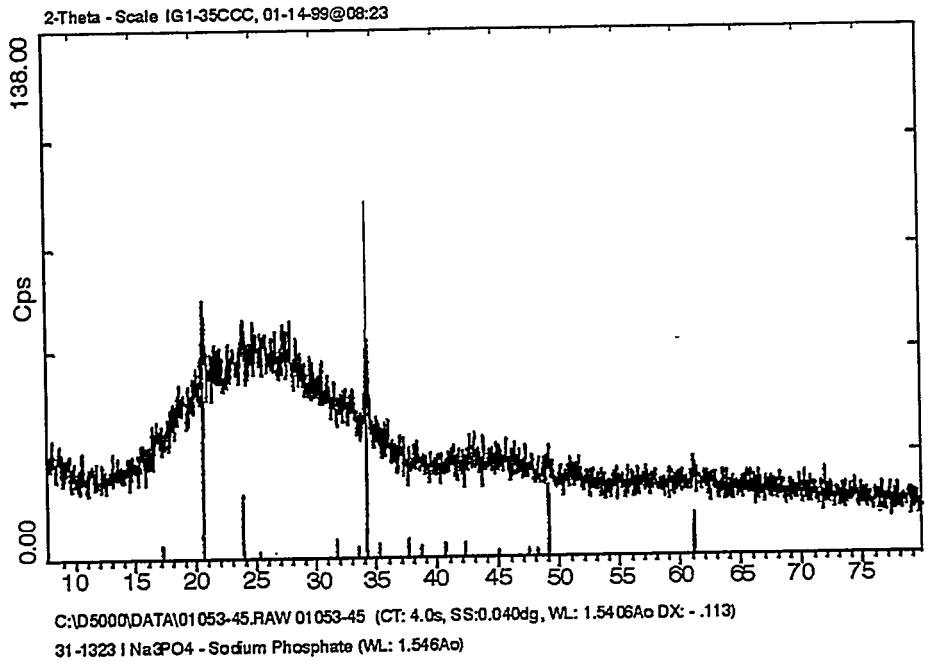

Figure A2-3. X-ray diffraction spectra of IG1-35CCC taken for 2 hours and showing the presence of sodium phosphate.

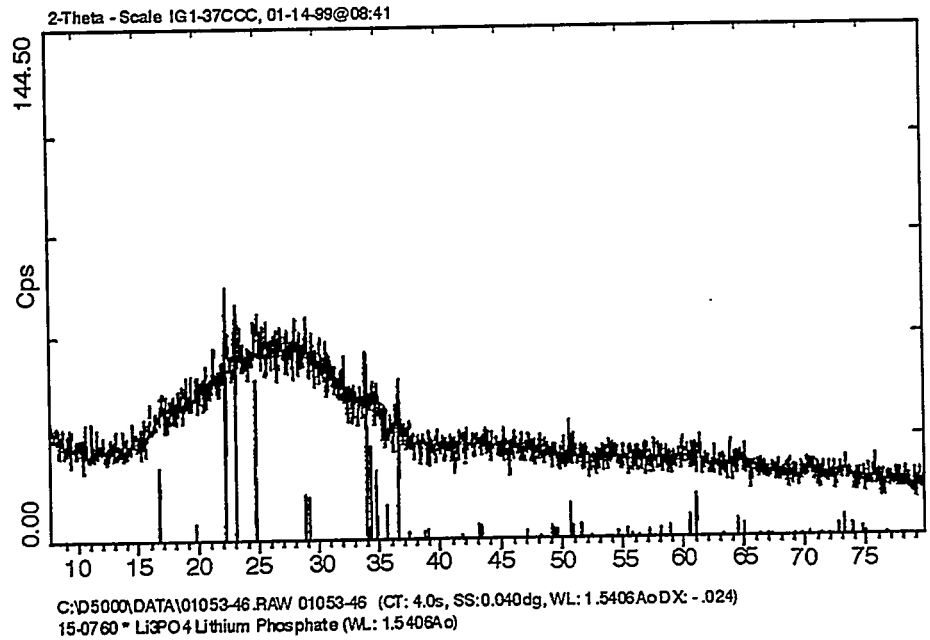

Figure A2-4. X-ray diffraction spectra of IG1-37CCC taken for 2 hours and showing the presence of lithium phosphate.

G:\99 01 19

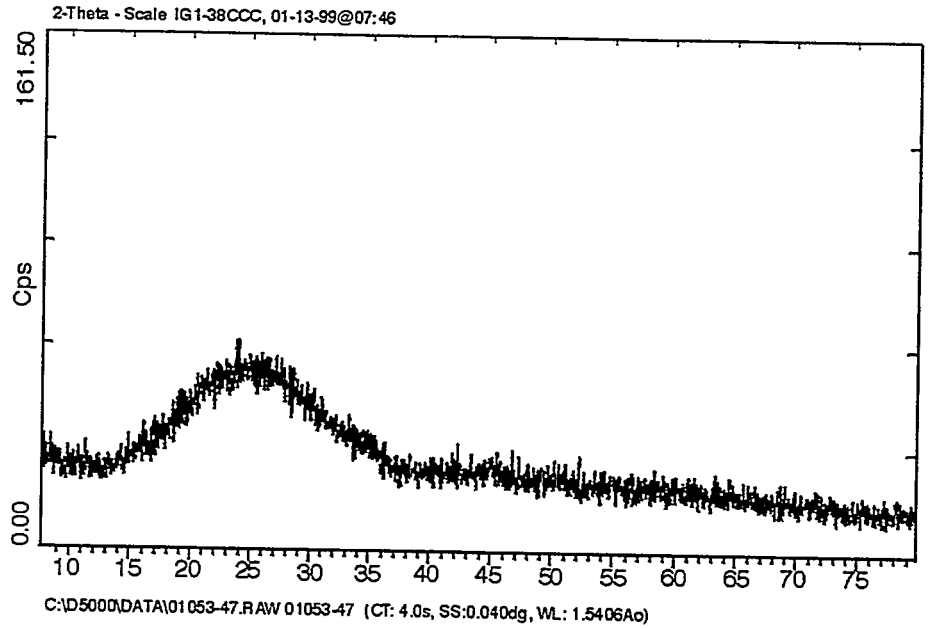

Figure A2-5. X-ray diffraction spectra of IG1-38CCC taken for 2 hours without detection of crystallinity.

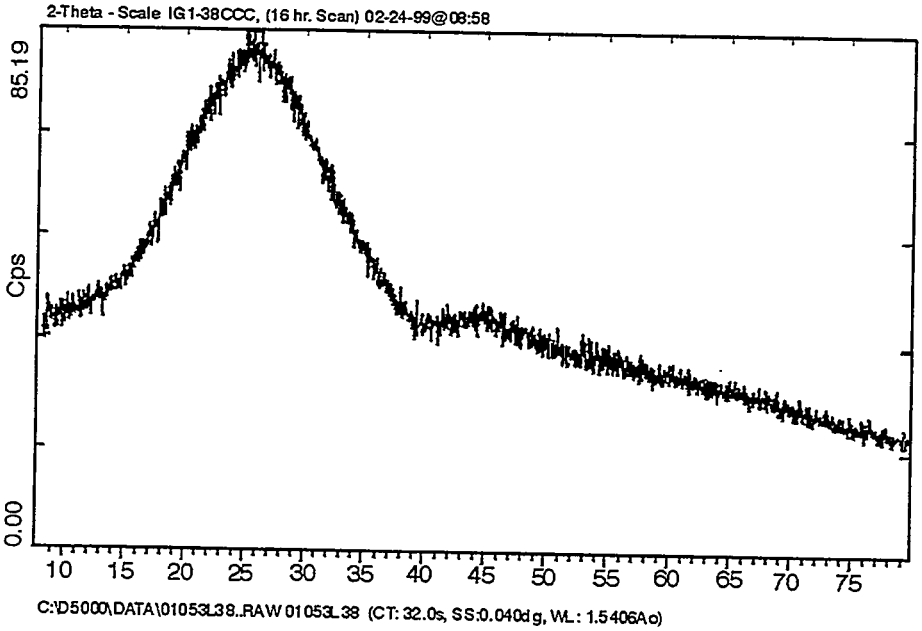

Figure A2-6. X-ray diffraction spectra of IG1-38CCC taken for 16 hours without detection of crystallinity..

G99 0120

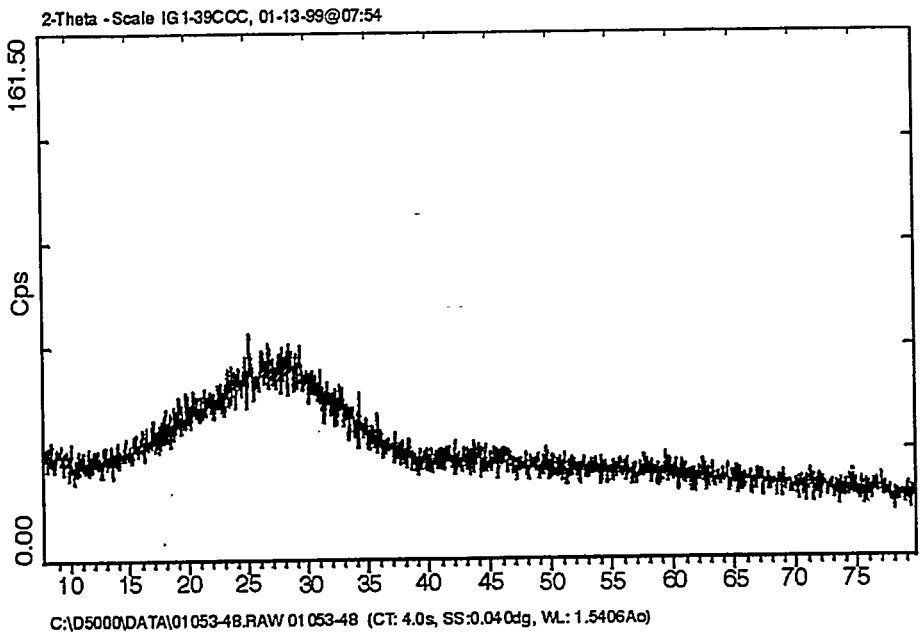

Figure A2-7. X-ray diffraction spectra of IG1-39CCC taken for 2 hours without detection of crystallinity.

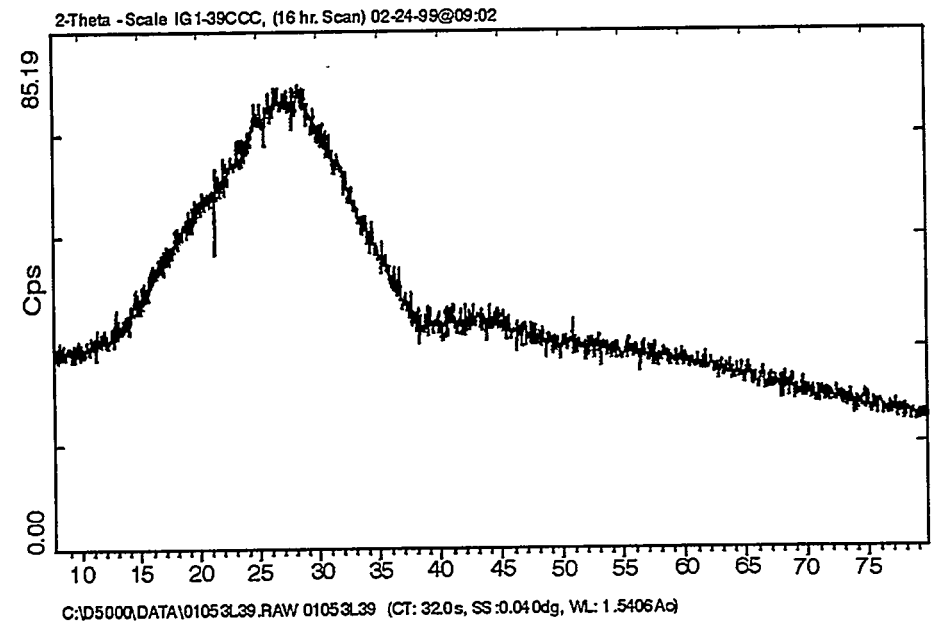

Figure A2-8. X-ray diffraction spectra of IG1-39CCC taken for 16 hours without detection of crystallinity.

G799 0121

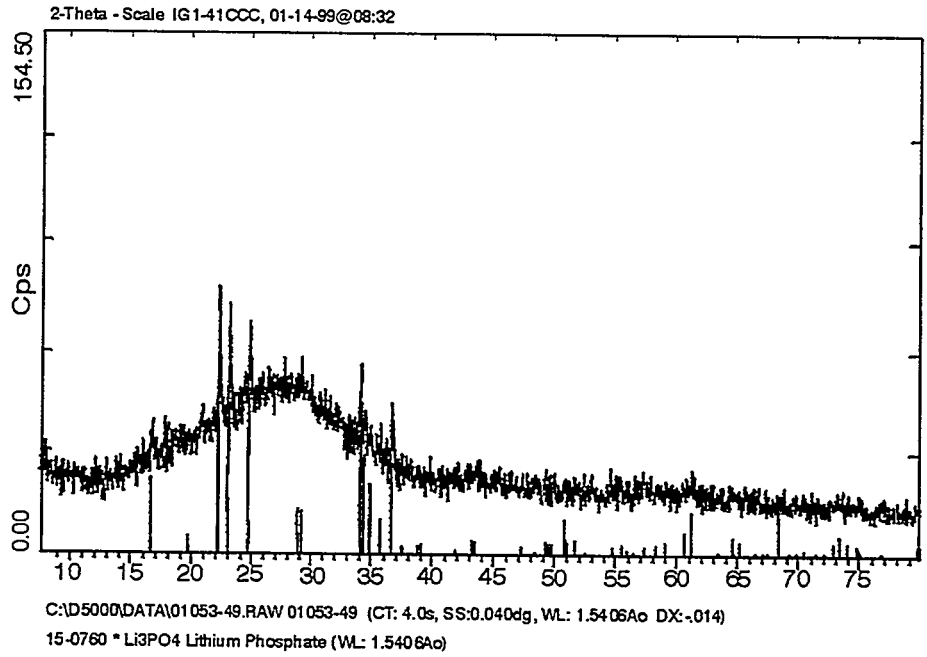

Figure A2-9. X-ray diffraction spectra of IG1-41CCC taken for 2 hours and showing the presence of lithium phosphate.

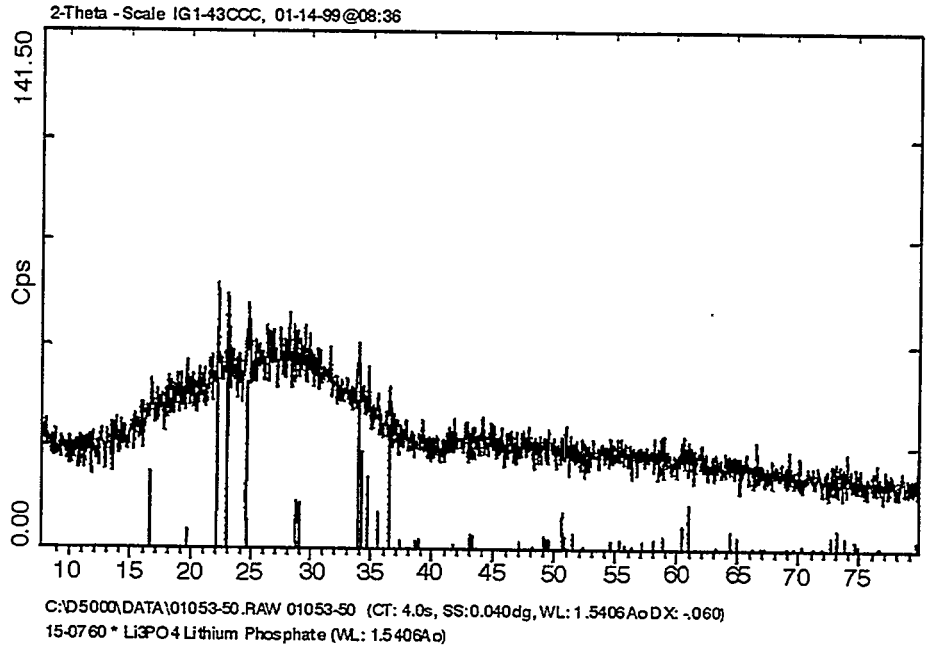

Figure A2-10. X-ray diffraction spectra of IG1-43CCC taken for 2 hours and showing the presence of lithium phosphate.

G:\99\0122

Appendix B

Raw Data from Application of PCT to INTEC CVS Glasses

Table B-1. Solution analyses (in ppm) for Phase 1a and Phase 1b glasses (ARM glass).

Phase	Batch ID	Test ID	Oven Level	Block	Al (ppm)	B (ppm)	Li (ppm)	Na (ppm)	P (ppm)	Si (ppm)	Zr (ppm)
1a	ARM-A	ARM-A-1	1	5	5.18	18.00	14.62	38.83	1.35	64.83	0.18
1a	ARM-A	ARM-A-2	2	6	5.23	18.50	14.23	37.50	1.58	61.67	0.15
1a	ARM-A	ARM-A-3	3	7	5.25	18.67	15.35	40.83	1.09	61.50	0.07
1a	ARM-B	ARM-B-1	1	1	4.83	23.00	14.32	37.83	1.45	71.33	0.07
1a	ARM-B	ARM-B-2	2	2	5.20	16.52	15.50	39.33	1.26	66.00	0.19
1a	ARM-B	ARM-B-3	3	3	4.85	20.33	13.93	39.17	1.32	66.17	0.07
1b	ARM	ARM-1	1	1	5.30	21.83	15.57	42.33	1.19	65.20	0.07
1b	ARM	ARM-2	2	2	5.55	21.00	15.77	42.00	0.53	73.67	0.07
1b	ARM	ARM-3	3	3	5.63	22.00	16.38	42.83	1.27	72.83	0.07
1b	ARMa	ARMa-1	1	4	4.62	20.83	18.00	48.17	1.24	72.00	0.07
1b	ARMa	ARMa-2	2	4	5.12	17.17	16.20	42.33	1.15	66.33	0.07
1b	ARMa	ARMa-3	3	4	4.92	17.00	15.40	43.17	1.07	66.33	0.07

Table B-2. Solution analyses (in ppm) for Phase 1a and Phase 1b glasses (blanks).

Phase	Batch ID	Test ID	Oven Level	Block	Al (ppm)	B (ppm)	Li (ppm)	Na (ppm)	P (ppm)	Si (ppm)	Zr (ppm)
1a	B	B-1	1	5	0.26	0.76	0.27	3.00	5.18	0.55	0.11
1a	B	B-2	2	6	0.10	0.39	0.08	0.61	0.70	0.27	0.08
1a	B	B-3	3	7	0.10	0.19	0.06	0.61	0.32	0.27	0.04
1b	B	B-1	1	1	0.10	1.01	0.01	0.27	0.32	0.23	0.04
1b	B	B-2	2	2	0.10	1.34	0.01	0.27	0.32	0.09	0.11
1b	B	B-3	3	3	0.10	1.21	0.01	0.54	0.32	0.09	0.04
1b	BB	BB-1	1	2	0.10	0.84	0.01	0.27	0.32	0.09	0.04
1b	BB	BB-2	2	2	0.10	0.42	0.01	0.27	0.32	0.09	0.04
1b	BB	BB-3	3	3	0.10	0.57	0.01	0.58	0.32	0.09	0.04

Table B-3. Solution analyses (in ppm) for Phase 1a and Phase 1b glasses (EA glass).

Phase	Batch ID	Test ID	Oven Level	Block	Al (ppm)	B (ppm)	Li (ppm)	Na (ppm)	P (ppm)	Si (ppm)	Zr (ppm)
1a	EA-A	EA-A-1	1	5	1.67	558.34	206.67	1783.37	5.33	1051.69	1.83
1a	EA-A	EA-A-2	2	6	1.67	571.68	191.67	1606.70	5.33	941.69	1.40
1a	EA-A	EA-A-3	3	7	3.68	535.01	176.67	1488.36	5.33	856.68	0.67
1a	EA-B	EA-B-1	1	1	1.67	720.01	213.34	1983.37	5.33	1056.69	0.67
1a	EA-B	EA-B-2	2	2	1.67	653.35	228.34	1850.04	5.33	986.69	0.67
1a	EA-B	EA-B-3	3	3	4.03	736.68	193.34	1733.37	5.33	990.02	0.67
1b	EA1	EA-1	1	1	1.67	581.68	185.00	1666.70	5.33	945.02	0.67
1b	EA1	EA-2	2	2	3.88	318.34	119.50	933.35	5.33	616.68	0.67
1b	EA1	EA-3	3	3	3.57	483.34	143.34	1300.03	5.33	818.35	0.67
1b	EA2	EA2-1	1	4	1.67	513.34	190.00	1588.37	5.33	846.68	0.67
1b	EA2	EA2-2	2	4	1.67	526.68	178.34	1623.37	5.33	875.02	0.67
1b	EA2	EA2-3	3	4	1.67	545.01	195.00	1716.70	5.33	880.02	0.67

Table B-4. Solution analyses (in ppm) for Phase 1a and Phase 1b glasses (multi-element standard).

Phase	Batch ID	Test ID	Oven Level	Block	Al (ppm)	B (ppm)	Li (ppm)	Na (ppm)	P (ppm)	Si (ppm)	Zr (ppm)
1a	std	—	—	1	4.23	21.90	9.89	85.20	0.32	54.10	0.04
1a	std	—	—	1	4.07	22.90	9.71	75.90	0.32	52.50	0.04
1a	std	—	—	1	4.00	23.90	9.14	80.40	0.32	57.30	0.04
1a	std	—	—	2	3.88	19.10	11.20	94.70	0.32	51.40	0.11
1a	std	—	—	2	4.10	18.50	10.60	88.70	0.32	51.00	0.11
1a	std	—	—	2	4.38	21.30	11.30	87.80	0.32	55.00	0.11
1a	std	—	—	3	4.26	23.40	10.30	93.10	0.32	52.30	0.04
1a	std	—	—	3	3.89	21.60	9.36	83.30	0.32	49.70	0.04
1a	std	—	—	3	3.64	23.00	11.00	96.90	0.32	53.40	0.04
1a	std	—	—	4	4.24	19.30	9.86	83.50	0.32	53.10	0.04
1a	std	—	—	4	3.99	18.40	9.56	85.70	0.32	51.20	0.04
1a	std	—	—	4	3.89	18.60	10.10	87.00	0.32	47.70	0.18
1a	std	—	—	5	4.20	18.20	10.60	86.30	0.32	53.30	0.11
1a	std	—	—	5	3.82	19.80	9.86	84.10	0.32	53.20	0.10
1a	std	—	—	5	3.75	20.80	9.84	80.60	0.32	52.00	0.11
1a	std	—	—	6	4.22	21.80	10.30	87.10	0.32	52.20	0.09
1a	std	—	—	6	4.34	21.50	10.20	86.30	0.32	53.20	0.09
1a	std	—	—	6	4.06	20.70	10.10	84.20	0.32	54.20	0.09
1a	std	—	—	7	3.83	19.40	10.50	86.30	0.32	50.30	0.04
1	std	—	—	7	3.63	19.70	10.20	82.70	0.32	47.70	0.04
1a	std	—	—	7	3.62	21.40	10.20	80.90	0.32	47.40	0.04
1b	std	—	—	1	4.09	20.40	9.92	84.00	0.32	51.80	0.04
1b	std	—	—	1	4.01	21.40	10.00	83.50	0.32	50.40	0.04
1b	std	—	—	1	3.94	21.00	9.75	81.40	0.32	50.50	0.04
1b	std	—	—	2	4.05	20.70	9.91	80.00	0.32	52.80	0.04
1b	std	—	—	2	4.08	21.70	9.68	77.70	0.32	50.50	0.04
1b	std	—	—	2	4.08	22.20	9.98	79.80	0.32	52.00	0.04
1b	std	—	—	3	4.10	21.30	10.40	83.40	0.32	52.70	0.04
1b	std	—	—	3	3.89	22.90	10.50	82.00	0.32	51.80	0.04
1b	std	—	—	3	3.79	21.00	9.81	83.50	0.32	53.60	0.04
1b	std	—	—	4	3.95	19.50	9.90	86.70	0.32	51.80	0.04
1b	std	—	—	4	3.97	18.70	10.00	86.10	0.32	50.40	0.04
1b	std	—	—	4	3.87	20.20	10.00	85.60	0.32	51.60	0.04

Table B-5. Solution analyses (in ppm) for Phase 1a glasses (IG1-1 through IG1-10).

Phase	Batch ID	Test ID	Oven Level	Block	Al (ppm)	B (ppm)	Li (ppm)	Na (ppm)	P (ppm)	Si (ppm)	Zr (ppm)
1a	IG1-1	IG1-1-1	1	1	1.67	175.00	83.67	465.01	95.34	308.34	0.67
1a	IG1-1	IG1-1-2	2	2	1.67	129.84	81.00	465.01	91.67	265.01	0.67
1a	IG1-1	IG1-1-3	3	3	1.67	188.34	84.67	525.01	110.84	313.34	0.67
1a	IG1-2	IG1-2-1	1	5	1.67	231.67	55.00	350.01	91.50	170.00	1.82
1a	IG1-2	IG1-2-2	2	6	1.67	298.34	61.17	376.67	116.50	170.00	4.38
1a	IG1-2	IG1-2-3	3	7	1.67	338.34	58.50	363.34	97.50	166.67	0.67
1a	IG1-3	IG1-3-2	2	4	1.67	560.01	6.18	5450.11	2266.71	915.02	0.67
1a	IG1-3	IG1-3-3	3	4	1.67	596.68	5.27	5350.11	2500.05	1003.35	0.67
1a	IG1-3	IG1-3-1	1	4	1.67	591.68	5.48	4866.76	2566.72	945.02	0.67
1a	IG1-4	IG1-4-1	1	1	0.17	11.92	300.01	80.67	66.83	98.34	0.07
1a	IG1-4	IG1-4-2	2	2	0.17	8.08	37.33	87.67	68.00	97.50	0.48
1a	IG1-4	IG1-4-3	3	3	0.17	11.33	33.33	85.84	71.00	98.34	0.52
1a	IG1-5	IG1-5-2	2	4	1.67	328.34	0.17	465.01	144.50	165.34	0.67
1a	IG1-5	IG1-5-1	1	4	1.67	346.67	0.17	931.69	166.67	180.00	0.67
1a	IG1-5	IG1-5-3	3	4	1.67	320.01	0.17	816.68	149.00	165.34	0.67
1a	IG1-6	IG1-6-1	1	5	1.67	798.35	411.67	643.35	5.33	903.35	1.77
1a	IG1-6	IG1-6-2	2	6	1.67	921.69	431.68	670.01	5.33	831.68	1.53
1a	IG1-6	IG1-6-3	3	7	1.67	978.35	438.34	676.68	5.33	808.35	0.67
1a	IG1-7	IG1-7-1	1	4	38.33	25.17	24.67	2.48	0.53	122.84	10.00
1a	IG1-7	IG1-7-3	3	4	43.00	27.33	31.17	4.35	0.53	136.17	11.90
1a	IG1-7	IG1-7-2	2	4	40.50	26.33	29.50	7.20	0.53	124.50	9.53
1a	IG1-8	IG1-8-1	1	1	16.27	6.45	18.67	37.83	38.83	50.33	1.02
1a	IG1-8	IG1-8-2	2	2	16.03	3.40	20.67	42.50	38.50	47.00	0.20
1a	IG1-8	IG1-8-3	3	3	15.62	5.07	17.67	43.50	41.33	52.33	0.07
1a	IG1-9	IG1-9-1	1	5	4.97	231.67	38.17	731.68	213.34	78.00	1.78
1a	IG1-9	IG1-9-2	2	6	4.55	253.34	33.17	696.68	186.67	78.33	1.45
1a	IG1-9	IG1-9-3	3	7	5.97	216.67	32.17	635.01	150.50	82.33	0.67
1a	IG1-10	IG1-10-1	1	1	1.67	601.68	836.68	2050.04	1.20	2850.06	0.67
1a	IG1-10	IG1-10-2	2	2	1.67	585.01	991.69	2183.38	1.75	2933.39	0.67
1a	IG1-10	IG1-10-3	3	3	1.67	601.68	853.35	2383.38	5.33	2816.72	0.67

Table B-6. Solution analyses (in ppm) for Phase 1a glasses (IG1-11 through IG1-20).

Phase	Batch ID	Test ID	Oven Level	Block	Al (ppm)	B (ppm)	Li (ppm)	Na (ppm)	P (ppm)	Si (ppm)	Zr (ppm)
1a	IG1-11	IG1-11-3	3	4	45.33	10.47	19.33	306.67	0.53	157.50	0.07
1a	IG1-11	IG1-11-1	1	4	37.33	8.58	18.17	275.01	0.53	139.84	0.07
1a	IG1-11	IG1-11-2	2	4	38.50	8.13	16.67	255.01	0.53	138.00	0.07
1a	IG1-12	IG1-12-1	1	5	1.67	396.67	0.17	925.02	5.33	65.67	1.85
1a	IG1-12	IG1-12-2	2	6	1.67	440.01	0.17	895.02	5.33	58.50	1.45
1a	IG1-12	IG1-12-3	3	7	1.67	453.34	0.17	908.35	5.33	59.17	0.67
1a	IG1-13	IG1-13-1	1	4	24.33	795.02	1716.70	8066.83	5.33	10423.54	0.67
1a	IG1-13	IG1-13-2	2	4	23.33	861.68	1288.36	6116.79	5.33	8166.83	0.67
1a	IG1-13	IG1-13-3	3	4	39.67	1151.69	1623.37	8516.84	10.97	11335.23	0.67
1a	IG1-14	IG1-14-1	1	1	21.17	24.67	11.88	156.00	3.63	92.50	0.07
1a	IG1-14	IG1-14-2	2	2	21.17	19.83	14.42	162.50	3.70	86.17	1.09
1a	IG1-14	IG1-14-3	3	3	19.83	22.83	14.03	166.67	3.58	95.67	0.40
1a	IG1-15	IG1-15-1	1	5	4.12	18.50	21.50	89.00	36.67	84.84	0.21
1a	IG1-15	IG1-15-2	2	6	5.27	21.33	21.83	96.50	37.33	98.84	0.33
1a	IG1-15	IG1-15-3	3	7	4.87	22.50	22.83	96.84	37.17	98.67	0.31
1a	IG1-16	IG1-16-1	1	1	11.28	16.83	8.60	144.84	6.28	71.83	0.47
1a	IG1-16	IG1-16-2	2	2	11.02	15.10	9.70	154.67	6.90	70.33	0.66
1a	IG1-16	IG1-16-3	3	3	10.68	15.73	9.63	143.84	6.77	66.67	0.07
1a	IG1-17	IG1-17-1	1	5	7.72	8.22	2.27	85.17	13.40	46.17	0.84
1a	IG1-17	IG1-17-2	2	6	8.47	9.07	2.43	89.50	13.53	48.83	0.87
1a	IG1-17	IG1-17-3	3	7	7.57	8.27	2.33	88.17	13.33	46.83	0.07
1a	IG1-18	IG1-18-1	1	1	7.65	22.33	13.13	51.50	26.00	64.00	0.35
1	IG1-18	IG1-18-2	2	2	7.83	18.50	18.17	56.50	29.00	60.67	2.87
1a	IG1-18	IG1-18-3	3	3	7.82	26.17	14.15	63.00	28.33	63.17	0.07
1a	IG1-19	IG1-19-1	1	5	7.20	18.33	13.00	51.17	24.83	58.17	0.31
1a	IG1-19	IG1-19-2	2	6	7.63	20.83	13.18	53.00	27.33	60.00	2.75
1a	IG1-19	IG1-19-3	3	7	8.05	19.50	13.23	52.00	25.17	54.83	0.33
1a	IG1-20	IG1-20-1	1	1	4.68	19.83	10.53	43.50	21.00	48.33	0.16
1a	IG1-20	IG1-20-2	2	2	5.07	14.37	10.97	44.50	22.00	45.83	0.89
1a	IG1-20	IG1-20-3	3	3	4.43	19.33	10.83	48.33	24.00	46.50	0.37

Table B-7. Solution analyses (in ppm) for Phase 1a glasses (IG1-21 through IG1-30).

Phase	Batch ID	Test ID	Oven Level	Block	Al (ppm)	B (ppm)	Li (ppm)	Na (ppm)	P (ppm)	Si (ppm)	Zr (ppm)
1a	IG1-21	IG1-21-1	1	5	13.93	49.33	41.50	101.00	5.33	47.83	2.30
1a	IG1-21	IG1-21-2	2	6	13.62	77.83	46.00	108.17	8.00	54.50	0.93
1a	IG1-21	IG1-21-3	3	7	13.15	76.67	46.50	103.34	6.80	55.33	0.07
1a	IG1-22	IG1-22-1	1	1	12.63	26.33	11.63	72.33	21.83	48.00	0.26
1a	IG1-22	IG1-22-2	2	2	14.25	24.17	13.70	74.67	21.33	46.33	3.02
1a	IG1-22	IG1-22-3	3	3	12.80	32.17	12.57	85.34	24.33	51.83	2.10
1a	IG1-23	IG1-23-1	1	5	9.75	6.60	11.37	51.00	25.17	44.17	0.94
1a	IG1-23	IG1-23-2	2	6	11.23	7.15	12.12	53.00	25.00	44.83	1.01
1a	IG1-23	IG1-23-3	3	7	11.77	8.47	11.70	54.67	22.00	45.83	1.29
1a	IG1-24	IG1-24-1	1	1	12.53	81.00	38.50	100.17	7.87	53.17	0.80
1a	IG1-24	IG1-24-2	2	2	11.53	70.17	46.17	111.17	8.40	51.33	0.42
1a	IG1-24	IG1-24-3	3	3	11.70	83.50	47.17	113.34	8.93	56.00	0.52
1a	IG1-25	IG1-25-1	1	5	9.57	18.00	16.83	114.17	6.15	60.83	0.65
1a	IG1-25	IG1-25-2	2	6	11.67	21.50	18.50	127.84	7.20	62.83	0.31
1a	IG1-25	IG1-25-3	3	7	11.58	21.33	19.83	133.84	6.72	62.00	0.07
1a	IG1-26	IG1-26-1	1	1	1.67	211.67	89.17	488.34	104.84	316.67	0.67
1a	IG1-26	IG1-26-2	2	2	1.67	149.00	95.67	521.68	106.84	311.67	0.67
1a	IG1-26	IG1-26-3	3	3	3.43	195.00	91.34	583.35	116.50	320.01	0.67
1a	IG1-27	IG1-27-1	1	5	14.87	3.72	19.00	40.67	39.17	48.33	0.53
1a	IG1-27	IG1-27-2	2	6	16.48	4.30	19.83	39.83	40.50	46.50	2.07
1a	IG1-27	IG1-27-3	3	7	15.50	4.28	20.17	42.33	35.67	45.00	0.83
1a	IG1-28	IG1-28-1	1	1	15.37	5.15	18.33	40.00	40.33	49.00	0.07
1a	IG1-28	IG1-28-2	2	2	17.00	3.58	23.00	44.17	43.17	52.33	0.32
1a	IG1-28	IG1-28-3	3	3	14.98	6.02	22.17	46.00	48.00	51.83	0.02
1a	IG1-29	IG1-29-1	1	5	30.17	9.97	21.33	25.33	0.53	101.84	0.20
1a	IG1-29	IG1-29-2	2	6	34.50	12.43	24.33	28.50	1.27	117.17	0.15
1a	IG1-29	IG1-29-3	3	7	30.67	13.17	24.00	28.83	0.53	109.00	0.07
1a	IG1-30	IG1-30-1	1	1	2.58	483.34	538.34	2233.38	12.80	1496.70	0.67
1a	IG1-30	IG1-30-2	2	2	4.45	426.68	570.01	2533.38	11.68	1481.70	0.67
1a	IG1-30	IG1-30-3	3	3	4.67	465.01	501.68	2566.72	15.52	1441.70	0.67

Table B-8. Solution analyses (in ppm) for Phase 1b glasses (IG1-31 through IG1-39).

Phase	Batch ID	Test ID	Oven Level	Block	Al (ppm)	B (ppm)	Li (ppm)	Na (ppm)	P (ppm)	Si (ppm)	Zr (ppm)
1b	IG1-31	IG1-31-1	1	1	39.83	138.67	103.00	138.34	0.53	108.84	8.83
1b	IG1-31	IG1-31-2	2	2	40.83	146.17	108.00	139.00	0.53	118.00	9.42
1b	IG1-31	IG1-31-3	3	3	41.17	138.34	108.17	137.00	0.53	112.17	9.53
1b	IG1-32	IG1-32-1	1	1	23.17	5.82	21.00	19.67	13.43	67.67	0.07
1b	IG1-32	IG1-32-2	2	2	23.67	6.07	24.17	20.50	14.53	75.67	0.07
1b	IG1-32	IG1-32-3	3	3	21.33	6.15	22.17	19.50	13.78	72.17	0.07
1b	IG1-33	IG1-33-1	1	4	1.67	185.00	104.17	3100.06	5.33	1966.71	0.67
1b	IG1-33	IG1-33-2	2	4	1.67	181.67	104.17	3066.73	5.33	1950.04	0.67
1b	IG1-33	IG1-33-3	3	4	1.67	176.67	104.50	3300.07	5.33	2016.71	0.67
1b	IG1-34	IG1-34-1	1	1	0.17	21.17	43.50	8.47	17.50	138.50	0.74
1b	IG1-34	IG1-34-2	2	2	0.37	25.83	46.00	8.90	18.50	146.00	0.07
1b	IG1-34	IG1-34-3	3	3	0.17	24.00	46.50	9.10	24.67	144.34	0.25
1b	IG1-35	IG1-35-1	1	1	11.53	36.00	25.33	100.00	4.00	68.83	0.48
1b	IG1-35	IG1-35-2	2	2	11.45	40.67	26.50	98.84	3.85	73.17	0.07
1b	IG1-35	IG1-35-3	3	3	11.60	46.50	30.50	119.84	4.35	78.83	0.07
1b	IG1-36	IG1-36-1	1	1	12.78	260.01	736.68	1576.70	5.33	2400.05	0.67
1b	IG1-36	IG1-36-2	2	2	15.43	270.01	765.02	1521.70	5.33	2483.38	0.67
1b	IG1-36	IG1-36-3	3	3	14.00	296.67	753.35	1573.37	5.33	2433.38	0.67
1b	IG1-37	IG1-37-1	1	1	1.67	513.34	4.27	1185.02	85.50	213.34	0.67
1b	IG1-37	IG1-37-2	2	2	3.43	480.01	1.63	1093.36	85.50	221.67	0.67
1b	IG1-37	IG1-37-3	3	3	3.03	480.01	3.05	1098.36	86.34	230.00	0.67
1b	IG1-38	IG1-38-1	1	1	0.53	86.84	62.17	93.84	12.77	150.67	0.07
1b	IG1-38	IG1-38-2	2	2	0.73	97.67	67.00	93.84	12.67	159.34	0.07
1b	IG1-38	IG1-38-3	3	3	0.77	101.17	66.00	99.84	12.63	166.67	0.07
1b	IG1-39	IG1-39-1	1	1	12.40	128.17	82.17	133.50	2.17	65.33	0.34
1b	IG1-39	IG1-39-2	2	2	13.33	133.67	90.67	140.50	2.13	72.67	0.20
1b	IG1-39	IG1-39-3	3	3	13.27	133.34	90.34	151.00	2.30	75.00	0.07

Table B-9. Solution analyses (in ppm) for Phase 1b glasses (IG1-40 through IG1-44).

Phase	Batch ID	Test ID	Oven Level	Block	Al (ppm)	B (ppm)	Li (ppm)	Na (ppm)	P (ppm)	Si (ppm)	Zr (ppm)
1b	IG1-40	IG1-40-1	1	1	1.67	258.34	149.84	485.01	53.83	556.68	0.67
1b	IG1-40	IG1-40-2	2	2	1.67	260.01	147.00	461.68	1.17	555.01	0.67
1b	IG1-40	IG1-40-3	3	3	1.67	266.67	145.67	466.68	54.17	540.01	0.67
1b	IG1-41	IG1-41-1	1	1	1.67	901.68	356.67	3266.73	91.34	3116.73	0.67
1b	IG1-41	IG1-41-2	2	2	1.67	945.02	348.34	2966.73	90.17	3300.07	0.67
1b	IG1-41	IG1-41-3	3	3	1.67	978.35	370.01	3266.73	82.50	3316.73	0.67
1b	IG1-42	IG1-42-1	1	1	14.12	8.87	16.05	39.83	7.03	55.17	0.55
1b	IG1-42	IG1-42-2	2	2	14.48	8.78	15.83	36.50	6.63	53.00	1.09
1b	IG1-42	IG1-42-3	3	3	15.07	10.58	17.83	43.33	6.93	59.67	0.07
1b	IG1-43	IG1-43-1	1	1	8.35	52.67	7.63	128.00	4.93	49.17	0.28
1b	IG1-43	IG1-43-2	2	2	8.70	63.00	9.02	143.67	5.32	51.83	0.14
1b	IG1-43	IG1-43-3	3	3	8.07	53.50	8.00	128.34	5.15	48.17	0.07
1b	IG1-44	IG1-44-1	1	1	0.17	24.50	44.67	8.90	19.17	143.50	0.55
1b	IG1-44	IG1-44-2	2	2	0.17	24.83	51.67	9.45	21.67	161.50	0.07
1b	IG1-44	IG1-44-3	3	3	0.17	26.50	47.50	9.57	21.50	153.34	1.92